„Dunărea de Jos" University of Galați
Doctoral School of Mechanical and Industrial Engineering

Extended Abstract of
PhD Thesis

TRIBOLOGICAL CHARACTERIZATION OF SOYBEAN OIL ADDITIVATED WITH NANO MATERIALS BASED ON CARBON (BLACK CARBON, GRAPHITE AND GRAPHENE)

PhD Student
eng. George Cătălin Cristea

Scientific coordinator
prof. eng. Lorena Deleanu, PhD

Series I6: Mechanical Engineering No. 39
GALAȚI
2017

ROMÂNIA
MINISTERUL EDUCAȚIEI NAȚIONALE
UNIVERSITATEA „DUNĂREA DE JOS" DIN GALAȚI

UNIVERSITAS GALATIENSIS

DECIZIA

nr. 3096/22/11/2017

Conform modificărilor aduse Codului studiilor universitare de doctorat prin Hotărârea Guvernului României nr. 134/2016 şi de Regulamentul de organizare şi funcţionare al CNATDCU aprobat prin Ordinul Ministrului Educaţiei Naţionale şi Cercetării Ştiinţifice nr. 3482/24.03.2016 – Anexa 1 – Metodologia de evaluare a tezelor de doctorat;

având în vedere referatul conducătorului ştiinţific Prof.dr.ing. Lorena DELEANU cu numărul 29924/21.11.2017, privind propunerea comisiei de susţinere publică a tezei de doctorat;

conform aprobării Consiliului pentru studiile universitare de doctorat în data de 22.11.2017;

în baza Ordinului Ministrului Educaţiei Naţionale şi Cercetarii Ştiinţifice nr. 3174/18.02.2016 privind numirea rectorului;

Rectorul universităţii decide:

Art. 1. Se numeşte comisia pentru evaluarea şi susţinerea publică a tezei de doctorat de către doctorand/a/ul **ing. CRISTEA R. GEORGE-CĂTĂLIN**, domeniul **Inginerie mecanică,** în următoarea componenţă:

1. Preşedinte	**Prof.dr.ing. Eugen-Victor-Cristian RUSU** Director CSUD - Universitatea „Dunărea de Jos" din Galaţi
2. Conducător de doctorat	**Prof.dr.ing. Lorena DELEANU** Universitatea „Dunărea de Jos" din Galaţi
3. Referent oficial	**Prof.dr.ing. Alexandru RĂDULESCU** Universitatea POLITEHNICA din Bucureşti
4. Referent oficial	**Prof.dr.ing. Ilie MUSCĂ** Universitatea „Ştefan cel Mare" din Suceava
5. Referent oficial	**Conf.dr.ing. Constantin GEORGESCU** Universitatea „Dunărea de Jos" din Galaţi

Art. 2. Şcoala doctorală de Inginerie mecanică şi industrială, Secretariatul doctorat, Compartimentul salarizare şi Serviciul financiar vor duce la îndeplinire prevederile prezentei decizii.

ROMÂNIA Rectorat

RECTOR,
Prof. dr. ing. Iulian Gabriel BÎRSAN

Acknowledgement

At the end of this phase of my professional life, I want to thank those who have given me the support and have guided me throughout this PhD thesis.

First of all, with great respect and consideration, I would like to return thanks to Professor Engineer Lorena Deleanu, who, as a scientific leader, has given me permanent guidance, support and encouragement during the doctoral study and elaboration period of the thesis.

I would like to express my sincere thanks to the commission for the guidance and evaluation of this paper, composed of professor eng. Gabriel Andrei PhD, lecturer chemist Dima Dumitru, PhD, and ass. professor eng. Constantin Georgescu, PhD, especially for the help offered, but also for the competent guidance and recommendations with a high degree of professionalism.

This PhD thesis would not have been complete without the help of professor Eng. Alexandru Valentin Rădulescu, PhD, from the "Politehnica" University of Bucharest, and eng. Cornel-Camil Suciu, PhD., from "Ştefan cel Mare" University of Suceava.

I also want to thank to Eng. Alexandru Petrică, PhD, for the support given in using microscopes and eng. Răzvan Şolea, PhD, for helping me with the calibration of the testing equipment.

I would like to thank Mr. Constantin Uzuneanu and Mrs. Mirela Antache from Prutul SA for providing the basic material of this thesis.

With great gratitude and love, I render thanks to my parents and my friend, Alina, who encouraged me, surrounded me with their affection and patience, and who supported me from all points of view during this period.

George Cătălin Cristea

Table of content

Chapter 1
Vegetal lubricants and nano additives to improve the tribological behavior

1.1. Lubricants based on vegetal oils

The OECD presented a report on the lubricants and additives in 2014 [OECD, 2014] stating that vegetable oils have an upward trend in their use as lubricants, especially for areas with a stronger impact on the environment.

Worldwide, 40 million tons of lubricants are consumed annually, while petroleum-based lubricants are still dominant. They begin to be challenged and replaced by synthetic oils and even by vegetable oils.

In 2016, Romania was the third largest producer of industrial seeds in the EU (rapeseed, soybean and sunflower). Nowadays research on soybean oil to replace mineral oil is of particular importance.

Vegetable oils can act as anti-wear additives and friction modifiers, due to the strong interactions that form with the surfaces they come into contact with, especially metallic surfaces. The long molecular chains of fatty acids and the presence of polar groups in the vegetable oil structure give them the ability to adhere and maintain their surfaces in contact, even with relatively severe regimes [Adhvaryu, 2004]. This would be the explanation of the very particular behavior of vegetable oils under the conditions of fluid lubrication and full film. Hence the need to control the fatty acid composition of vegetable oils [Biresaw, 2008]. The composition in fatty acids also varies with the nature of the soil, the climate and human intervention on the seeds, and even for the same place and the same type of seed, the annual conditions can influence the quality of the vegetal oil.

Quinchia et al. [Quinchia, 2009] revealed by experimental results that for vegetable oils, the fatty acid composition contributes to better lubricity and has efficacy in reducing wear as compared to mineral and synthetic oils.

Addition of additives to vegetable oils (such as ethylene-vinyl acetate and ethyl cellulose copolymer) improved the friction behavior of sunflower, soybean and castor oil by favoring the formation of a bounding lubrication film.

1.2. SWOT analysis of the use of vegetal lubricants

A SWOT analysis (Fig. 1.1) for the introduction of vegetable oils as lubricants showed that a set of properties should be considered when the designer decides this lubrication solution [Cermak, 2005], [Erhan, 2005].

Strengths	**Weak points**
• biodegradability [Murilo, 2011], • environmental (non-polluting or environmental friendly), • extraction from renewable resources (even with a reference to 100 years) or the possibility of recycling or re-use of the lubricant, • high viscosity index, • better flamability characteristics, auto ignition points, and higher ignition temperature on hot surfaces.	• lower viscosity as compared to mineral and synthetic oils [Paredes, 2014.], [Biresaw G, 2008], [Liu Z., 2015], • oxidation [Erhan, 2005], [Solea, 2013], [Wang M., 2014], • temperature range lower than that of mineral and synthetic oils [Fox, 2007], • many of the properties are more time-dependent than those of mineral and synthetic oils, • low temperature properties are lower for vegetal oils than other lubricants.
Oportunity	**Threats**
• complying with more stringent environmental protection requirements will minimize health and pollution risks. The new market shares for organic lubricants (obtained from renewable resources, especially plants) and biodegradable have increased for areas such as hydraulic fluids, chain lubricants, mold lubricants, two-stroke engines, turbine fluids, etc. [Norbby, 2003].	• the need to redesign systems using bioliquids, a solution that is possibly more costly, • accepting lowering some system operating parameters (especially load and maintenance, but not limited to) [Nagendramma, 2012]. • the price still high (but not forgetting that, for example, synthetic oils in the 1990s were almost 10 times more expensive than mineral ones, today the ratio being only 3 to 1), market and users inertia, the diversity of environmental and safety specifications and a global policy that has not yet been clearly addressed on environmental issues.

Fig. 1.1. SWOT analysis of the use of vegetal lubricants

1.3. Research in the field of vegetal oils

The use of vegetal oils as lubricants implies a research on the set of tribological features, including those that can be highlighted on the four-ball tribotester [Jayadasa, 2007], [Syahrullai, 1996]. Thus, it is necessary to know the influences caused by the nature of the lubricant, chemical and rheological changes can be determined after a certain expertation time for certain load and speed conditions, the influence of additives, etc. [Campanella, 2010.], [Mobarak, 2014], [Ji X., 2012].

In the literature, there are reported tests on the four-ball tribotest for vegetal oil [Ilie F., 2016], [Cristea, 2017], [Padgurskas, 2013], but the data are far from being comparable and useful for industrial scale applications. Thus, the knowledge of the behavior of these oils on the four-ball machine is of interest because it is possible to compare the vegetal oils, whether they are additivated or not, with those already in use, mineral or synthetic ones.

Cermak [Cermak, 2005] tested vegetable oils on the four-ball tester in accordance with the American Standard ASTM D4172 and obtained good values for friction coefficient and diameters of wear scar of 0.53 mm for Cuphea oil and 0.89 mm for Lesquerella crude oil. It is interesting to note that soybean oil had a wear scar diameter higher (0.70 mm) than other oils tested in this study (grasshopper oil - 0.629 mm, cress oil - 0.59 mm).

1.4. Soybean oil as lubricant

In the US, Northern Iowa has an Ag-Based Industrial Lubricants Research Center (UNI-NABL), which patented 30 genetically modified soybean lubricants (oils and greases), including a hydraulic fluid for tractor, hydraulic oils for manufactering processes and transmissions, metalworking fluids and cooling fluids, chain oils, gear oils, fluids for the food industry, compressor oils, transformer oils, grease for cars, trains, etc. [James, 2006]. The North American market for soy-based lubricants was estimated at USD 191.5 million in 2016.

The soybean oil has a better lubricity, low volatility and a high viscosity index. Flammability characteristics are similar to those of the rapeseed oil [Șolea, 2013], [Cristea, 2017]. Moreover, this oil has a good solubility for contaminants, additives and polar deposits as compared to mineral oils. The user should expect this oil to change its viscosity, oxidation and polymerization during use in a more intense way than other lubricants. Chemical modification of soybean oil and/or the use of antioxidants can have a positive effect, but will increase the cost of lubricant formulation.

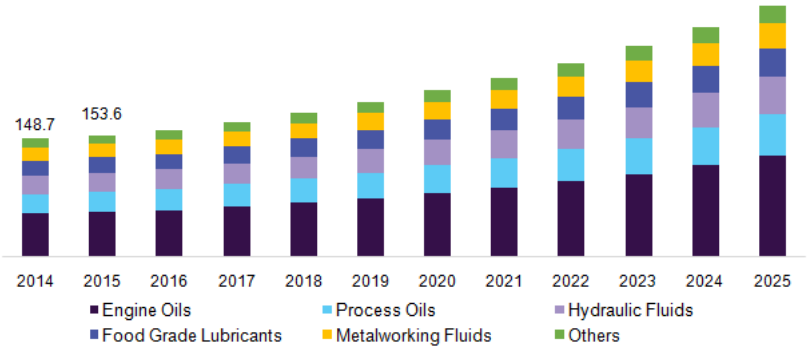

Fig. 1.2. Soybean lubricant market in the USA, depending on the application, 2014-2025 (million USD) [http://www.grandviewresearch.com/industry-analysis/north-america-soybean-oil-based-lubricants-market]

1.5. Anti-wear additives and friction modifiers

Anti-wear additives and friction additives are used for medium stresses and the protective film relies heavily on adsorption processes and on the regeneration of the protective film even though it partially deteriorates during the exploration.

Friction modifiers are adsorbed or fixed to the surface and form a film or a powdery intermediate layer that reduces friction. They can be classified into two distinct groups depending on the friction reduction mechanism:

- through the adsorbed film,
- by friction with the third body.

The first is generally due to polar molecules having a polar functional radical (alcohols, aldehydes, ketones, esters and carboxylic acids) and a nonpolar terminal group. The polar group of the molecule adheres to the surface with long chains exposed to moving surfaces, reducing friction. They may also have polar elements that can chemically react with the surface to form a protective film. Vegetal oils and animal fats have such molecular structures and, therefore, they have good results in reducing friction.

In addition to organic friction modifiers, some solid lubricants are added to oils with the same purpose of reducing friction. This group of friction modifiers includes carbon materials (fulerene, nanotubes, graphite, graphene, etc.), but also molybdenum and wolfram sulphides, fluorinated polymers, such as PTFE and perfluoropolyalkylethers (PFPAE). These can also be added in greases and composites that will function in dry conditions [Friedrich, 2008].

Solid lubricants (micro or nano) also help in situations where sliding surfaces have a more rough texture, "leveling" the profile of both surfaces. They are also recommended for reciprocal movements (in the case of the piston ring), which also produces a reduction in wear. It is added to lubricants that come into contact with surfaces with which EP additives can not chemically react, such as polymers and ceramics and some of their composites [Rudnick, 2009].

Modifying friction additives can be grouped into solid lubricants and organic modifiers. The first group consists of carbon materials (graphite, graphene, black carbon, fulerene), lamellar sulphides (tungsten and molybdenum), metal salts (boron nitride) and metal oxides (CuO, ZnO, TiO_2 [Cazamir, 2017], which is not mentioned by Rudnik [Rudnik, 2006]), but also linear polymers (polytetrafluoroethylene) [Fessenbecker, 1994]. Among the organic additives that act as friction modifiers are carboxylic acids or derivatives (stearic acid and esters), amides, imides, amines and their derivatives (oleyl amide etc.), phosphoric and phosphonic acid derivatives, organic polymers (methacrylates). Regeneration of the low friction layer depends on the concentration of additives and the conditions in which the tribosystem operates (speed, load, temperature, contamination).

1.6. Specific processes for lubrication with nano additives

Wu et al. [Wu, Y.Y., 2007] propose a model that takes into account the lubricating additive concentration (Fig.1.3). Although the model was created with TiO_2 experiments, it can be used to explain the behavior of lubricants with other nanoscale particles (metal oxides, carbon materials, etc.). The fluid lubrication mechanism with nano additives has been also described in the works [Wo H., 2004], [Wu H., 2013], [Wu J. F., 2009].

The mechanism for reducing friction and anti-wear mechanism of nano particles in lubricants has been investigated and it is based on the following processes [Tang, 2014]:

- the micro-roll process [Chinas-Castillo 2003], [Wu Y. Y., 2007]

- the process of forming a protective film [Alves, 2013], [Gu C., 2009], [Iliuc, 1980], [Yu H., 2008].

- smoothing/leveling process [Liu G., 2004],

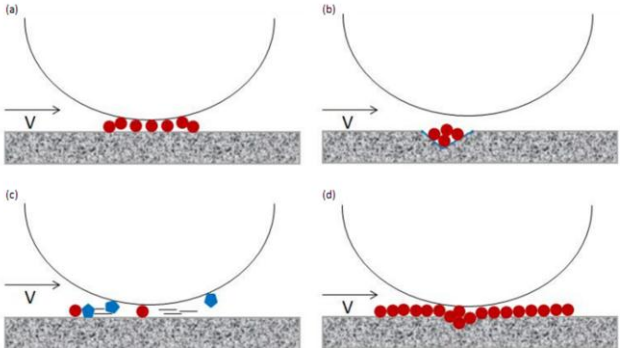

Fig. 1.3. The lubricating mechanism of water based lubricants and TiO_2 as an additive: a) rolling effect, b) mending effect, c) polishing effect, d) effect of protective film [Wu, 2013]

- polishing process [Lee K., 2009], [Chang 2010] (Fig. 1.3).

The first two mechanisms have a direct effect on lubrication [Lee K., 2009]. In the case of rolling, no chemical reactions occur and spherical or oval nanoparticles are willing to roll.

The lubrication mechanism of nanoparticles as friction modifiers includes three types of friction [Tevet, 2011]:

- rolling friction: spherical nanoparticles act as micro or nano ball roller bearings between triboelement surfaces under light load conditions,

- slipping sliding: nanoparticles serve as spacers and eliminate direct metal/metal contact between the asperities of the two triboelements, under higher load conditions,

- rubbing with the third body: exfoliating nanoparticles and their outer layers gradually transfer to the surface texture, providing easier friction under high load conditions, when the third body can be considered a mixture of oil, nanoparticles and wear particles.

The use of nanoparticles as lubricant additives is a top issue of research in the last decades [Tang, 2014], [Akbulut, 2012].

Jayadasa et al. [Jayadasa, 2007] have calculated the advantage of using additives in oils, based on the results of the shear rate and the temperature influence on the viscosity of the additivated lubricant. Wu et al. [Wu Y., 2007] reported increased load capacity fot the additivated lubricants. Many studies were based on a single concentration of the additive. The effect of varying viscosity due to nanoparticle concentration is difficult to model and, therefore, tests become relevant.

A study by Lahouij et al. in 2012 shows how the WS_2 particle protects the direct contact between metal asperities (Fig. 1.4). The ovoid structure functions as a shock absorber and either the structure collapsed, or the particle was fragmented and continued to remain between the two solid bodies. The hollow core of the particle was visible and the deformation was large at the beginning of the stress, but as the load increased, the particle behaved like a variable-elasticity spring, the elastic characteristic actually increasing. Then the particle begins to tear or scissor, and on the second line of photos there are WS_2 exfoliated fragments.

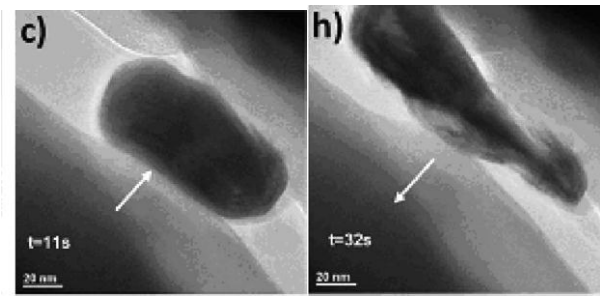

Fig. 1.4. Photos taken from the work of Lahouaiej et al. in 2012, and highlighting the steps through which a particle of WS_2 passes into a loaded contact.

1.7. Carbon nanoparticles as additives in lubricants

The use of nano-carbon materials is more recent - the last decade.

Specialists divide nanocarbon materials into four classes, depending on carbon alotropy: zero dimension, single-dimensional or 1D, two-dimensional or 2D, three-dimensional or 3D.

Carbon materials with size zero. The name is associated with the spherical form of nanoparticles (fulerene). It is not yet clear from the literature if they are also associated with amorphous materials (amorphous carbon).

Unidimensional carbon materials. In this class are, nanowires and carbon nanobar considered nanotubes, which have two of the dimensions much smaller than the other. Their applications are very different, from sensors, to polymeric, ceramic or metallic composites, to liquid lubricant additives.

2D carbon based materials. In this class graphene is included, with a honeycomb arrangement, favorable to anti-wear and friction properties [Joly-Pottuz, 2008], [Eswaraiah, 2011], [Berman, 2015], [Berman, 2013]. For the time being, graphene friction patterns and data obtained at AFM are contradictory. Tribotests that allow for more pertinent comparisons and proximity to actual tribosystems are few and, therefore, the study proposed for this thesis will be useful for the use of graphene in practice.

Lin et al. [Lin, 2011] studied the stability of micro-graphen plates in oil and tested as dispersants: sodium dodecyl benzene sulfonate, stearic acid, dodecyl trimethyl ammonium chloride, oleic acid, sorbitan monooleate and polysorbate. They concluded that from of all these substances, stearic acid and oleic acid are the most suitable dispencers. The optimal concentration of modified graphene was 0.075 wt%, reporting an improvement in wear and

contact loading capacity. The results were superior to the addition of the same oil with natural graphite flakes.

3D nanomaterials of carbon

Although micro-scale diamond particles are used for surface superfinishing, it has been found that at the nano level, these particles act on the principle of bearings, like rollerballs between the two surfaces in sliding. The results on nanodiamonds are contradictory.

Lee [Lee, 2009] studied nanoparticulate graphite in a mineral oil for transmission (220 cSt at 20 °C) (Supergear EP220, SK, Korea), but this oil also had EP additives. The average graphite size was 55 nm. The tested concentrations were 0.1 wt% and 0.5 wt%. The alkyl aryl sulfonate was used as a dispersant. Agglomerations of particles act as a contaminant and increase the risk of generating more abrasive wear by passing agglomerations through the contact and "falling" (continued slipping with local shock in contact).

The conclusions of the study done by Lee and Hwang [Lee, 2009], [Hwang, 2011] are the following.

- The addition of nanoparticle additives to the lubricants enhanced the lubrication characteristics when compared to microparticle additives.

- Nanoparticles in contact take up some of the load and play the role of very small rollers or ball bearings.

- Fibrous particles in oils (CNFs / CNTs, for example) have higher friction coefficients than spherical nanoparticles or close 3D sizes, probably because of the way they get in contact and the fact that spherical particles tend to roll and not to be dragged into contact.

- Fibrous nanoparticles agglomerate more easily than spherical ones and this their thickness becomes larger than the thickness of the lubricant film, resulting in an increase in roughness, an embarrassment of the lubricant circulation, especially when entering into contact.

Black carbon

Carbon is a basic constituent of organic matter [Pierson, 1993]. Carbon is found in nature in the form of compounds. Many of these compounds are essential in the production of synthetic carbon materials and include bituminous and anthracite coal, complex hydrocarbons (petroleum, tar, asphalt) and gaseous hydrocarbons (methane and others), but only two forms of carbon are naturally found: natural graphite and diamond.

Carbon powders and particles are a class of synthetic materials, generically known as carbon black, amorphous carbon, and they are obtained by burning hydrocarbons in insufficient air. Amorphous carbon particles are aggregates of graphite nano crystals, each with only a few cell units, so small that they are not detectable by diffraction techniques. The properties of these materials depend on the size of the particle area.

Graphite is effective in high temperature and high load applications. It is therefore used as a solid lubricant for forging. Other solid lubricants, such as MoS_2, will rapidly oxidize in these processes where the working temperature can reach 760-1200 °C, although MoS_2 has a better lubricating capacity.

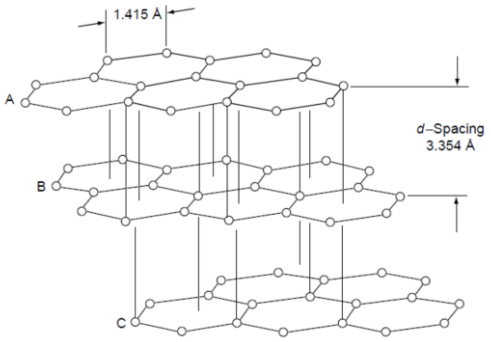

Fig. 1.5. Graphite structure [Berman, 2015], [Pierson, 1993]

Graphite is such a good solid lubricant due to the lamellar plate structure. Its structure is composed of planes of cyclic (hexagonal) carbon atoms. The bonds between the carbon atoms in this plane are strong covalent bonds (Fig. 1.5). The van der Waals forces, the weaker ones, hold together the planes and relay the structure. The distance d of the bond between the carbon planes is larger and therefore weaker as compared to the bond between the atoms located in the same plane. If a force perpendicular to the crystal is applied, the reaction is high. This high yield limit in this direction ensures the load capacity of the solid lubricant. A force perpendicular to the normal load (parallel to the cyclic carbon planes) will move the planes relatively to each other at much lower values: the weak link between the planes allows for shearing the planes in that direction. This results in a cleavage of crystallites. The result is a small resistance opposite to the movement of the planes relative to each other and, thus, the reduction of friction.

Rubbing against metallic or ceramic surfaces, the graphite is transferred to the surfaces, with which it is rubbed, reducing the coefficient of friction to 0.01 [Pierson, 1993] if the transfer is uniform and the film formed does not detach.

The lubricating film is maintained only in the presence of adsorbable vapors such as water vapor, oxygen or contaminant organic gases. In a pure atmosphere of inert gas or nitrogen, in vacuum or at high temperatures, the film is no longer formed or, if formed, it easily breaks. This results in a high coefficient of friction (to 0.1) and wear is severe, with almost five orders of magnitude greater than the vapor environment, the process being known as "dusting". Under these conditions graphite is no longer effective as a lubricant, and additives and compounds are needed to counteract these effects.

Graphene is considered a rising lubricant [Berman, 2015], [Berman, 2015].

In spite of the efforts of developing research for many existing and future applications, their tribological potential as a lubricant remains relatively unexplored. In addition, recent tribological studies based on graphenes, from nano scale to macro scale, and in particular their use as a solid lubricant or additive in lubricating fluids, will be presented.

Graphene, a 2D carbon material, was only stably isolated in 2004 [Novoselov, 2004] but drew the attention of specialists from various fields, the tribology applications being just

on the beginning. Graphene has outstanding properties, which are characterized by reduced friction and wear, from nano to macro scale, being a solid high performance lubricant or an additive in solid lubricants. Being a 2D material, graphene offers unique friction and wear properties that are not typical of other conventional materials. Very high chemical inertia, good strength, and the ability to crack easily between platelets or very smooth surfaces are favorable attributes for a very good tribological behavior. As being very thin, even in many layers, it can be applied to different scales from (nano to macro), including microelectromechanical and nanoelectromecanical systems with sliding, rolling or oscillating contacts in order to reduce friction and wear. The good mechanical resistance of the grafts reduces wear. Lee et al. [C. Lee, 2010] tested the mechanical properties of graphenes and confirmed it to be one of the most resistant materials.

1.8. Conclusions and research directions

From the studied literature, there is a tendency for deep research on additives in industrial fluids, especially those intended for lubrication. Addition with carbon nanomaterials (black carbon, graphite and graphene) can improve the tribological properties of a vegetal oil. Attention should be focused on the dispersion of nano additive and the selection of dispersant.

The purpose of this study is to test, tribologically and rheologically, the influence of carbon nanoaditives on degummed soybean oil. In the literature non-additive or additive vegetal oils were analyzed, but the reported results are still inconclusive and the applications of these oils are based more on market inertia or on the practical experience of users.

From a tribological point of view, the study aims at:

- evaluation of the lubrication regime for test parameters on the four-ball machine, by mapping the lubrication regimes; the theoretical value of the minimum thickness of the lubricant film shall be determined for the considered ranges of loads, speed and viscosities;

- estimating the degree of separation of the two surfaces in contact with the lubricant film, using the Tallian parameter (or the lambda parameter);

- determination of the influence of test parameters and nano additives (as nature and concentration) by experimental determinations on the four-ball tribotester;

- the coefficient of friction;

- the wear process reflected by the wear scar diameter and the ware rate of wear scar diameter,

- evaluation of the influence of the test regime and of the concentration of an nano additive (graphite) on the quality of the used surfaces, an original study made by comparison between 2D and 3D texture parameters).

The autor will study the influence of some parameters, such as load and sliding speed, on the tribological characteristics of the non-additivated soybean oil and additivated with

nano carbon-based friction modifiers (black carbon, graphite, graphene), and based on the results, recommendations will be made on working with nanoadditive lubricants.

From a rheological point of view, based on the experimental data on the influence of shear rate on the shear stress and the temperature on the dynamic viscosity, it is desired:

- the determination of the rheological model (the shear stress variation according to the shear rate) for the formulated lubricants and the determination of the correlation with the theoretical law;

- the determination of the parameters of the viscosity variation model with the temperature and the degree of correlation with this theoretical model.

This study will provide useful data on the use of soybean oil and carbon nano additivated lubricants to produce environmentally-friendly lubricants.

Chapter 2
Theoretical calculation of the lubrication regime, for four ball tribotester

2.1. The lubricant film thickness calculation model

In a lubricated system, the lubricating film formed between the two surfaces may have thicknesses that vary between 10^{-10} m and 10^{-5} m [Cameron, 1973], [Cameron, 1983], [Stachowiak, 2005] [Hamrock, 2004], [Dowson, 1977].

Depending on how the lubricant film is generated between the two surfaces of the tribosystem, the following lubrication regimes can be distinguished [O'Connor, 1968], [Cameron, 1973], [Dowson, 1977], [Hamrock, 2004], [Bloch, 2009], [Booser, 1994], [Bowden, 1956], [Cameron, 1983], [Lansdown, 2004], [Olaru, 2002] (Fig. 2.1):

- the boundary,
- the mixt regime,
- the fluid film regime separating the two triboelements: hydrodynamic (HD), elastohydrodynamic (EHL) regime, hydrostatic (HS) regime.

The configuration of two elastic bodies with convex surfaces in contact was originally considered by Hertz in 1881 [Stachowiak].

Since tests were performed on the four-ball machine, in which all balls are considered spherical and have the same radius (6.35 mm), then it can be assumed that in the calculation model, the balls are perfectly spherical.

The studies conducted by Hamrock and Dowson [Hamrock, 2004], [Dowson, 1977] proposed a method of calculating the thickness of the film, both for the minimum value and the thickness value at the plateau before the minimum thickness (and the center thickness of the lubricant film).

The hypotheses made by Dowson and Higginson [Dowson, 1977] for the EHL lubrication model are:

- deformations are calculated for a solid with equivalent radius R_e on a rigid plane;
- lateral fluid leakage is neglected,
- the pressure limit conditions are: at the entrance, $p_a = 0$ at a great distance from the contact and at the outlet of the contact $\partial p / \partial x = p_a = 0$,
- the lubricant is incompressible,
- thermal effects are negligible in the first phase. These are: viscosity variation with temperature and expansion of the lubricant and contact elements.

The non-newtonian fluid behavior. At high pressures, the density may increase by ~20% and the viscosity may have the following dependence:

$$\eta = \eta_o e^{\alpha \cdot p \cdot - \beta \cdot T} \tag{2.1}$$

where α is the pieso viscosity coefficient and β - the coefficient of thermal viscosity, η_o is the known viscosity at normal pressure and temperature.

Effects of high pressures. Considering an isothermal process (specific to the steady regime), viscosity remains a pressure-dependent function:

$$\eta = \eta_o e^{\alpha \cdot p} \qquad (2.2)$$

For long infinite contact, the Reynolds equation becomes:

$$e^{-\alpha \cdot p} \frac{dp}{dx} = 12 \cdot \eta_o \cdot U \frac{h - \tilde{h}}{h^3} \qquad (2.3)$$

The height of the fluid film h is written:

$$h = h_o + \frac{x^2}{2 \cdot R_e} + w(x) \qquad (2.4)$$

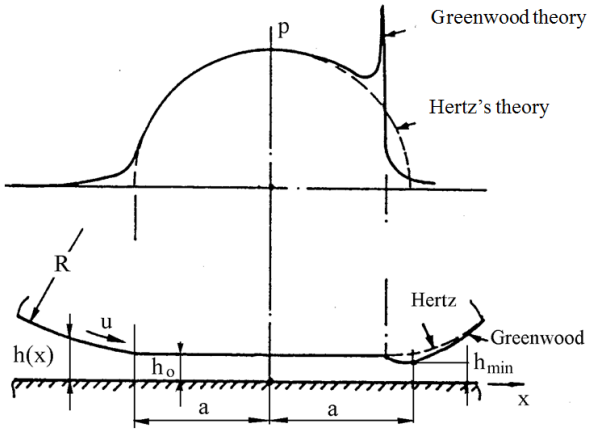

Fig. 2.1 Elastohydrodynamic contact [Dowson, 1977]

where h_o is the minimum thickness of the fluid film if the bodies are perfectly rigid, $h' = x^2/(2R_e)$ is determined by the theoretical (parabolic) shape of the interstitial, and the last term is the elastic deformation of the contact area, similar to that obtained for a Hertzian contact. R_e is the equivalent radius of curvature, $w(x)$ is the component of the thickness of the film resulting from the elastic deformation of the solid bodies and it is estimated from the classic model in the elastic semi-space, [Dowson, 1977]:

$$w(x) = -\frac{2}{\pi \cdot E'} \int_{s_1}^{s_2} p(s) \ln(x - s)^2 \, ds + C$$

The calculation formulas developed by specialists [Dowson, 1977], [Hamrock, 2004], [Olaru, 2002] and could be applied to any type of contact (punctual, linear or elliptical). They apply to a large number of combinations of contact materials, including steel on steel, and for maximum pressures up to 4 GPa.

$$h_{min} = 3{,}63 \cdot R_e \cdot \left(\frac{U \cdot \eta_0}{E' \cdot R_e}\right)^{0{,}68} \cdot (\alpha \cdot E')^{0{,}49} \cdot \left(\frac{W}{E' \cdot R_e^{\,2}}\right)^{-0{,}073} \cdot \left(1 - e^{-0{,}68 \cdot k}\right) \qquad (2.6)$$

where h_{min} – the minimum thickness of the lubricant film, [m]; U – the speed of the surfaces when in contact, [m/s]; $U = (U_A + U_B)/2$, U_A and U_B refers to body speeds A and B, respectively; η_0 – the dynamic viscosity of the lubricant at atmospheric pressure [Pa·s]; E' – Young equivalent module, [Pa];

$$\frac{1}{E'} = \frac{1}{2} \cdot \left[\frac{1 - \nu_A^2}{E_A} + \frac{1 - \nu_B^2}{E_B}\right] \qquad (2.7)$$

ν_A, ν_B – Poisson coefficients for the contact bodies A and B, respectively; E_A, E_B – the Young elastic modulus for the contact bodies A and B respectively,[Pa]; R_e – equivalent radius of the contact, [m];

$$\frac{1}{R_e} = \frac{1}{R_A} + \frac{1}{R_B} \tag{2.8}$$

R_A, R_B – the radius of balls (spheres) in contact A, respectively B, [m]; α – the pieso viscosity coefficient, [m^2/N];

$$\alpha = \frac{0,0129 \cdot \ln\left(10^4 \cdot \eta_0\right)}{p_H^{0,25}}, \text{ [MPa}^{-1}\text{] [Paleu, 2002] ,[Gold, 2002]}$$

(2.9)

p_H – Hertzian pressure, [MPa], W – contact load, [N], k – the ellipticity parameter,

$$k = \frac{a}{b} \tag{2.10}$$

with a – the contact ellipse half axe in the transverse direction, [m]; b – the contact ellipse half axe in the direction of sliding, [m]. In the case of punctual contact, k = 1.

For the four-ball test, the contact between two balls is characterized by:

- contact load $$W = \frac{F}{3 \cdot \cos(\alpha)} = \frac{F}{3 \cdot \cos(35,264°)} \text{ [N]} \tag{2.11}$$

- sliding speed $$U = \frac{U_A}{2} = \frac{1}{2} \cdot \frac{2 \cdot \pi \cdot n}{60} \cdot \frac{R_A}{\sqrt{3}} \text{ [m/s]}, \; U_B = 0 \tag{2.12}$$

where F – axial loading applied to the spindle of the four-ball machine, [N]; n – the spindle angular speed of the four-ball machine, [rpm].

The thickness of the lubricant film may also be expressed by the following adimensional factors [Cameron, 1983], [Dowdon, 1977], [Olaru, 2002]:

- the thickness of the film: $$H = \frac{h_{min}}{R_e} \tag{2.13}$$
- the speed factor: $$U = \left(\frac{U \cdot \eta_0}{E' \cdot R'}\right) \tag{2.14}$$
- the material factor: $$G = \left(\alpha \cdot E'\right) \tag{2.15}$$
- the load factor: $$W = \left(\frac{W}{E' \cdot R_e^{\,2}}\right) \tag{2.16}$$
- the contact shape factor, k, (elliptic factor) (2.17)

In the case of contact between two identical spheres, the equation becomes:

$$H = 3,63 \cdot U^{0,68} \cdot G^{0,49} \cdot W^{-0,073} \cdot \left(1 - e^{-0,68 \cdot k}\right) \tag{2.18}$$

In general, there are four lubrication regimes (film full) [Cameron, 1983], [Dowdon, 1977], [Olaru, 2002], [Stachowiak, 2005] each characterized by operating conditions and material properties: isoviscous-rigid (IVR) piesoviscous-rigid (PVR), isoviscous-elastic (IVE), piesoviscous-elastic (PVE).

The lubricant film thickness equations have been developed for each of these regimes. The calculation model is based on the introduction of a set of adimensional parameters used for calculating the thickness of the lubricant film [Stachowiak, 2005], [Stachowiak, 1993]:

- the adimensional parameter of the film thickness $$\overline{H} = H \cdot \left(\frac{W}{U} \right)^2 \qquad (2.19)$$
- the adimensional parameter of viscosity $$G_V = \frac{G \cdot W^3}{U^2} \qquad (2.20)$$
- the adimensional parameter of elasticity $$G_E = \frac{W^{8/3}}{U^2} \qquad (2.21)$$
- the adimensional parameter of ellipticity,k (2.22)

The formula for calculating the adimensional thickness of the lubricant film for the four lubrication regimes is [Hamrock, 2004], [Stachowiak, 2005]:

isoviscous-rigid regime

$$\left(\overline{H}_{min}\right)_{IVR} = 128 \cdot k^{\pi/2} \cdot \left[0{,}131 \cdot \operatorname{arctg}\left(\frac{k^{\pi/2}}{2} \right) + 1{,}683 \right]^2 \cdot \left(1 + \frac{2}{3} \cdot k^{-\pi/2} \right)^{-2} \qquad (2.23)$$

piesoviscous-rigid regime

$$\left(\overline{H}_{min}\right)_{PVR} = 1{,}66 \cdot G_V^{2/3} \cdot \left(1 - e^{-0{,}68 \cdot k} \right) \qquad (2.24)$$

isoviscous-elastic regime

$$\left(\overline{H}_{min}\right)_{IVE} = 8{,}70 \cdot G_E^{0{,}67} \cdot \left(1 - 0{,}85 \cdot e^{-0{,}31 \cdot k} \right) \qquad (2.25)$$

piesoviscous-elastic regim

$$\left(\overline{H}_{min}\right)_{PVE} = 3{,}42 \cdot G_V^{0{,}49} \cdot G_E^{0{,}17} \cdot \left(1 - e^{-0{,}68 \cdot k} \right) \qquad (2.26)$$

Depending on the contact time and regime, the minimum thickness of the lubricant film is calculated:

$$h_{min} = \left(\overline{H}_{min}\right) \cdot R_e \cdot \left(\frac{U}{W} \right)^2 \qquad (2.27)$$

Hamrock [Hamrock, 2004] develops a method of identifying the lubrication regime in the case of punctual contact, by producing, for each ellipticity parameter k, a map of the lubrication regimes according to two non-dimensional parameters, the viscosity parameter, G_V, and of elasticity, G_E. The methodology is also presented by Stachowiack [Stachowiack, 2005] and Olaru [Olaru, 2002].

The construction of the lubrication map for punctual contact (characterized by certain solid body materials and a particular lubricant) is performed in a double logarithmic

coordinate system, with the dimensional elasticity parameter G_E on the abscissa and the adimensional viscosity parameter G_V on the ordinate axis. In the following maps, broken lines delimit the four lubrication regimes.

The mapping methodology of the lubrication regimes for a certain contact, characterized by the dimensional elliptic parameter k, contains steps [Georgescu, 2015], [Olaru, 2002], [Hamrock, 2004].

1. For the value of the adimensional elliptic parameter k, the adimensional parameter of the thickness $\left(\overline{H}_{min}\right)_{IVR}$ of the lubricant film is calculated, with (2.23).

2. The parameter $\left(\overline{H}_{min}\right)_{IVR}$, determined at step 1, equals the adimensional thickness of the lubricating film thickness $\left(\overline{H}_{min}\right)_{PVR}$, given by (2.24) and determine the adimensional viscosity parameter $G_{V,1}$:

$$G_{V,1} = \left[\frac{\left(\overline{H}_{min}\right)_{IVR}}{141\cdot\left(1-e^{-0,0387\cdot k^{\pi/2}}\right)}\right]^{1/0,375} \tag{2.28}$$

3. For the value of k imposed, along with its value $\left(\overline{H}_{min}\right)_{IVR}$, determined at step 1, and the value of $G_{V,1}$, determined at step 2, determine the elasticity parameter $G_{E,1}$ is determined with the relation:

$$G_{E,1} = \left[\frac{\left(\overline{H}_{min}\right)_{IVR}}{3,42\cdot G_{V,1}^{0,49}\cdot\left(1-e^{-0,68\cdot k}\right)}\right]^{1/0,17} \tag{2.29}$$

A point $A_{1,1}$, is obtained which has the coordinates $G_{E,1}$ and $G_{V,1}$, representing the first point of the delimitation line between the lubrication regimes PVE and PVR. The boundary between the IVR regime and the PVR regime is drawn, drawing a horizontal line from point $A_{1,1}$ to the ordinate axis.

4. With the same values for the dimensional parameters k and $\left(\overline{H}_{min}\right)_{IVR}$, the adimensional elasticity parameter $G_{E,2}$, is determined with the relation:

$$G_{E,2} = \left[\frac{\left(\overline{H}_{min}\right)_{IVR}}{8,70\cdot\left(1-0,85\cdot e^{-0,31\cdot k}\right)}\right]^{1/0,67} \tag{2.30}$$

5. For the same values for the parameters k and $\left(\overline{H}_{min}\right)_{IVR}$, together with the value of $G_{E,2}$, determine the new non-dimensional viscosity parameter $G_{V,2}$, is determined with the relation:

$$G_{V,2} = \left[\frac{\left(\overline{H}_{min}\right)_{IVR}}{3,42 \cdot G_{E,2}^{0,17} \cdot \left(1 - e^{-0,68 \cdot k}\right)} \right]^{1/0,49} \tag{2.31}$$

A point $A_{1,2}$, is obtained, having the coordinates, $G_{E,2}$ and $G_{V,2}$, which represents the first point of the boundary line between the PVE and IVE lubrication regimes. The points $A_{1,1}$ and $A_{1,2}$ are joined together with a straight line and the border between the IVR regime and the PVE regime is obtained. The boundary between the IVR regime and the IVE regime is drawn, leading a vertical line from point $A_{1,}$ to the abscissa axis.

6. Choose a new value for $\left(\overline{H}_{min}\right)_{IVR}$, higher than the previous one, and repeat steps 2 through 5 to obtain new $A_{i,1}$ and $A_{i,2}$ points. The points $A_{1,1}$, $A_{2,1}$, ..., $A_{i,1}$ unite and determine the boundary between the PVR and PVE regimes and the points $A_{1,2}$, $A_{2,2}$, ..., $A_{i,2}$ determine, by union, the frontier between the PVE and IVE regimes.

2.2. Calculated lubrication regimes for ball on ball sliding contact, with soybean oil and nano additivated lubricants

In the calculation models of the thickness of lubricant film, values of dynamic viscosity were used, η_0, obtained by processing the experimental results (see chapter 5). For each lubricant, the lubrication regime has been calculated for different working conditions. The working regime is characterized by sliding speed and normal force. Calculations were performed for combinations (F, v), with the following values: for speed v = 0,38 m/s, v = 0,53 m/s and v = 0,69 m/s and force (F = 100 N, F = 200 N şi F = 300 N).

The author has used a program in Excel [Georgescu, 2015] that allows rapid calculations for various combinations, including ball material, lubricant (temperature and pressure-dependent viscosity, by α and β parameters), sliding speed, load.

Hypothesis: Stabilized lubrication regime (constant temperature, constant viscosity at working pressure and temperature).

Taking into account the results of the effect of temperature on the dynamic viscosity, lubrication regime maps were drawn, for 20 °C and 45 °C.

In the following figures, the details of lubrication regimes are given only for concentrations of 1%. In Fig 2.3, the test regimes are positioned for the temperature of 20°C.

For all lubricants used in the four-ball tribotester (Figures 2.7 and 2.8), the lubrication regime is piesoviscous-elastic (PVE), very close to the IVE regime, for all ranges of speed and axial loads and viscosities considered in this test plan. The increase in axial load, speed and viscosity only brings near the isoviscous-rigid regime (IVR).

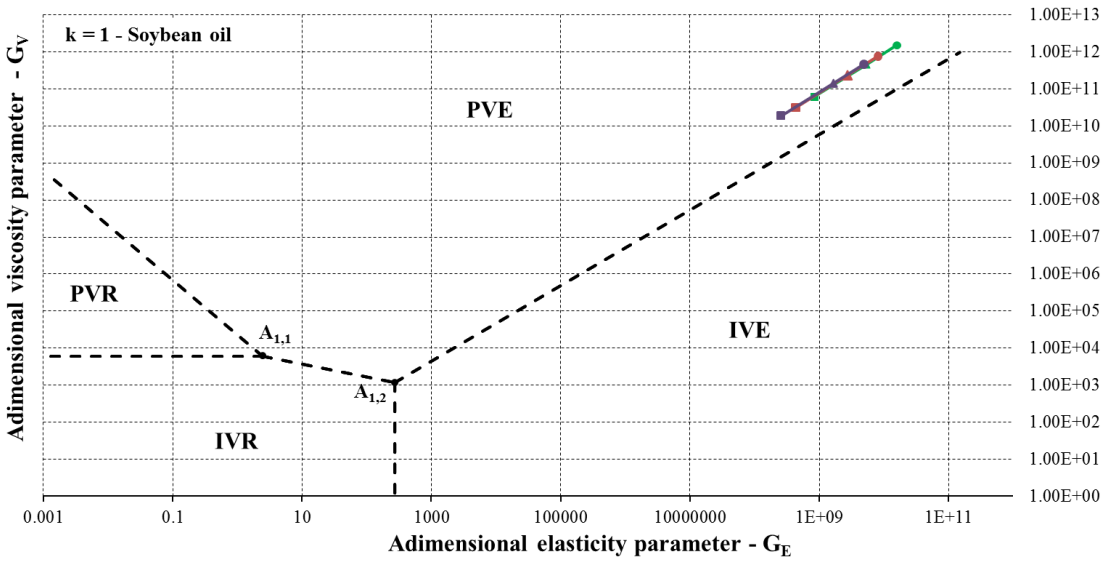

Fig. 2.2. Map of lubrication regimes for k = 1, soybean oil, isothermal regime (20 °C)
Legend: color represents speed (green v = 0,38 m/s, red v = 0,53 m/s, blue v = 0, 69 m/s), the symbols are for the load on the machine axle:● – F = 100 N; ▲ – F = 200 N; ■ – F = 300 N

2.3 Calculation of minimum thickness of the lubricant film

After identifying the lubrication regime, the minimum thickness of the lubricant film was calculated using the relations (2.26) and (2.27), for all analyzed lubricants and for all axial load speeds. In terms of dynamic viscosity, calculations were made for experimentally determined values in Chapter 5, for temperatures of 20 °C and 45 °C.

It is found (Fig. 2.3) that the minimum thickness of the lubricant film depends to a great extent on the sliding speed and the viscosity of the lubricant, respectively on the adimensional speed parameter U, for all analyzed lubricants. The highest minimum film thickness is obtained for soybean oil (which has the highest dynamic viscosity) and the smallest for soybean oil additivated with nano graphite and nano graphene (with the lowest dynamic viscosity [Șolea, 2013]).

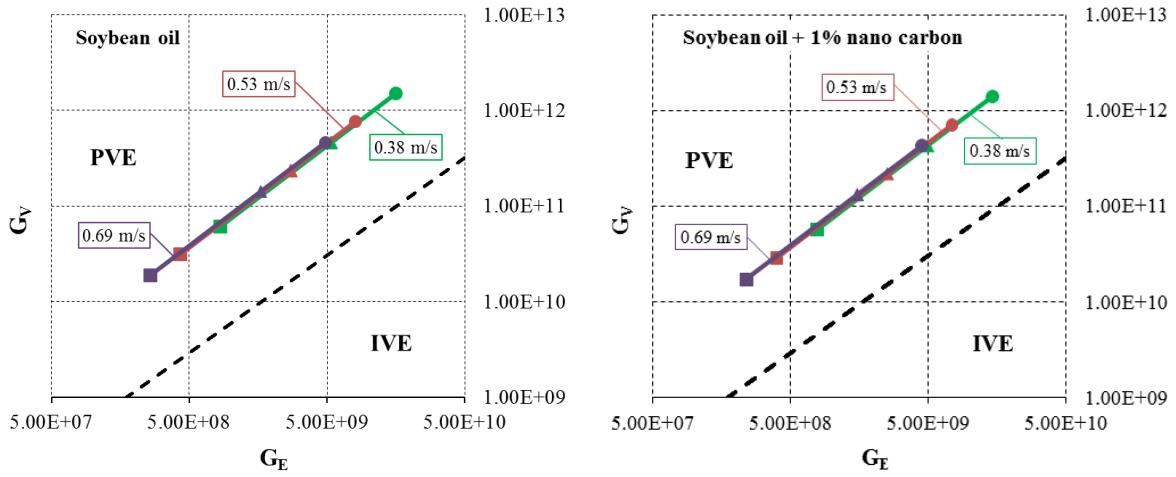

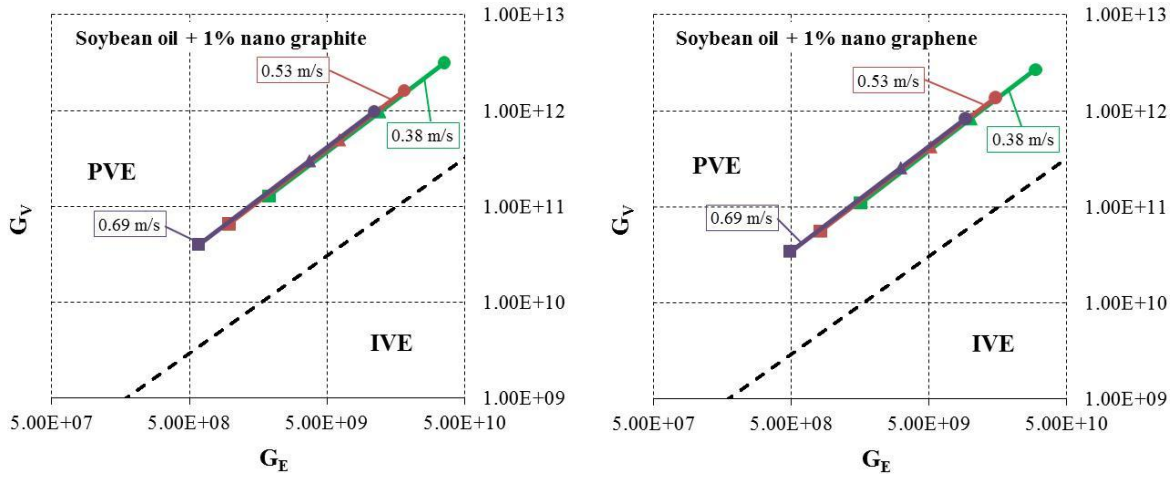

Fig. 2.3. Details of maps lubrication regime for lubricant additivated with nano carbon (20°C)

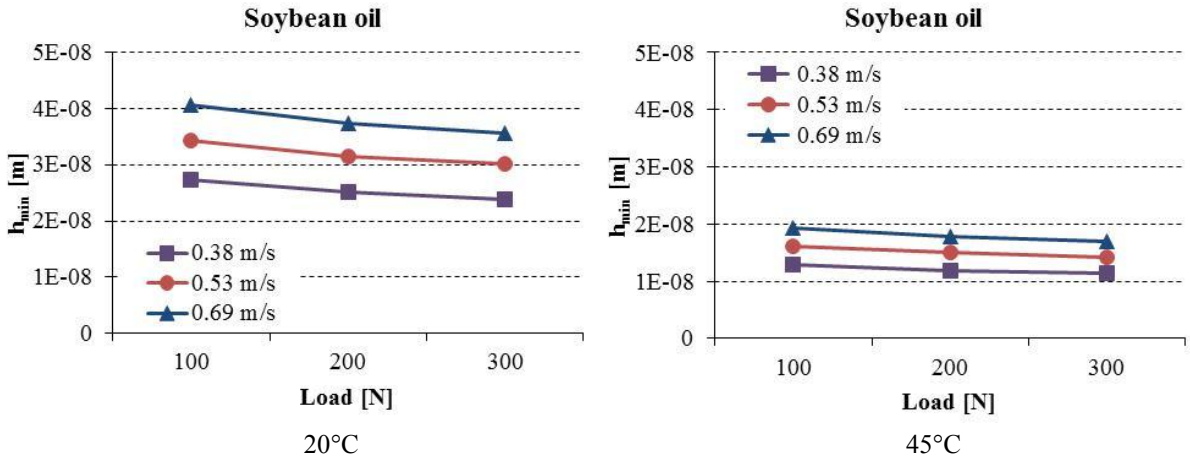

20°C 45°C

Fig. 2.4. Influence of axial load and sliding speed on calculated value of the minimum thickness of lubricant film for non-additivated soybean oil

If one compare the two graphs in Fig. 2.4, one may notice:

- all curves are similary maintained,
- theoretical thickness is 10^{-8} m
- the influence of the load is relatively weak compared to the influence of speed,
- at both temperatures, the highest thickness is obtained for the highest velocity (v = 0.69 m/s) and slightly decreases with the load,
- the temperature has a very strong influence, h_{min} (20 °C) is about twice as high as h_{min} (45 °C),
- in addition, h_{min} values at 45 °C are more grouped within a narrower range,
- speed has a lower influence on higher temperature, in other words, it has a lower influence on fluids with low dynamic viscosity.

The evolution of h_{min} with the load is small, reflecting the conclusions of Dowson and Hamrock that the load factor influences less the thickness of the as film compared to the velocity factor [Dowson, 1977], [Hamrock, 2004]. At 45 °C, the influence of the load is even lower, thus the curve slope is small.

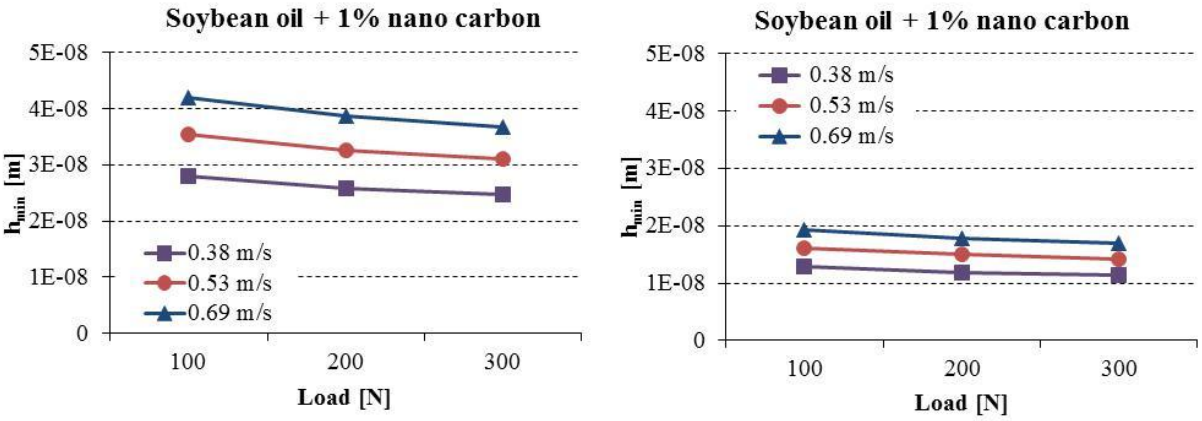

20°C 45°C

Fig. 2.5. The influence of axial load and sliding speed on the calculated minimum thickness of the lubricant film, for the class of lubricants additivated with amorphous nanocarbon

It can be noted:

- the influence of the additive concentration carbon black at 20 °C is almost unobservable. Table 2.1 gives some values of h_{min} for the regimes with F = 300 N; h_{min} (non-additivated soybean oil) is just a little smaller than h_{min} (c = 0,5%) and h_{min} (c = 1%),

- h_{min} has a slight growth trend with the additive concentration even with non-additivated soybean oil.

For example, at F = 100 N and v = 0.38 m/s, the values obtained are h_{min} (c = 0.25%) = $2.24 \cdot 10^{-8}$ m and h_{min} (c = 0.5%) = $2,4 \cdot 10^{-8}$ m.

At the temperature of 45 °C, the trend remains, but the differences are smaller.

Table 2.1. Minimum film thickness, nano carbon, F = 300 N

	20°C				**45°C**			
Speed	**Concentration of the additive (%wt)**							
	0	**0.25**	**0.5**	**1**	**0**	**0.25**	**0.5**	**1**
	h_{min} (x 10^{-8} m)							
0.38 m/s	2.39	2.24	2.4	2.5	1.1	0.93	1.1	1.1
0.53 m/s	3.01	2.82	3.0	3.1	1.4	1.2	1.4	1.4
0.69 m/s	3.57	3.34	3.6	3.7	1.7	1.4	1.7	1.7

At 20 °C, the influence of additive concentration resembles that obtained for nanocarbon, with lower values. At 45 °C, the influence of concentration of the additive produced very close curves and very little influence of the concentration, h_{min} is almost the same for all the considered concentrations considered, being justified by the very close values for the viscosity of the nanoparticulate lubricants at 45 °C. The values for h_{min} for lubricants additivated with graphene are below $1 \cdot 10^{-8}$ m.

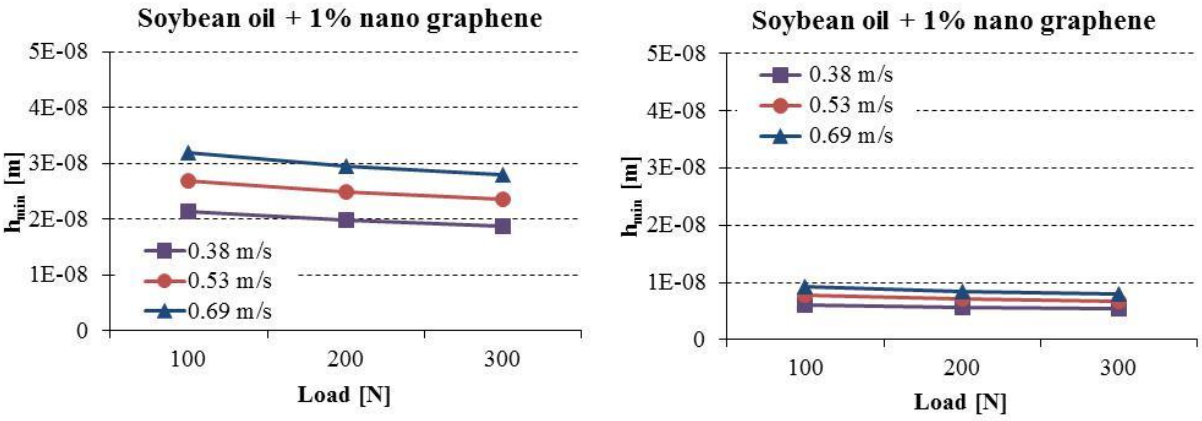

20°C 45°C

Fig. 2.6. Influence of axial load and sliding speed on the calculated minimum film thickness of the lubricant for the class of lubricants additivated with nanographene

Table 2.2. Minimum film thickness, nano graphene, F = 300 N

	20°C				**45°C**			
Speed	**Concentration of the additive (%wt)**							
	0	**0.25**	**0.5**	**1**	**0**	**0.25**	**0.5**	**1**
	h_{min} (x 10^{-8} m)							
0.38 m/s	2.39	2	2	1.9	1.1	0.41	0.54	0.54
0.53 m/s	3.01	2.5	2.5	2.4	1.4	0.52	0.68	0.68
0.69 m/s	3.57	2.9	2.9	2.8	1.7	0.62	0.81	0.81

2.4. Conclusions based on the assessment of theoretical lubrication regimes

Maps of the lubrication regimes have been drawn and the lubrication regimes have been identified in the case of four-ball testing machine (contact point, k = 1), for the three categories of additivated lubricants and for the non-additivated soybean oil. It has been found (see Figures 2.2 and 2.3) that, for all analized lubricants, the lubrication regime is piesoviscous-elastic (PVE).

The minimum theoretical thickness of the lubricating film (for the determined lubricating regime) was calculated for all analyzed lubricants and for all the dynamic ranges of axial loads, sliding speed and dynamic viscosity the author considered. The obtained thicknesses of the lubricant film are very close and comparable to the roughness value Ra of the initial surfaces in contact.

Figure 2.7 graphically shows the influence of the nature and concentration of the additive on the theoretical minimum thickness at 20 °C and 45 °C. The most severe test regime was chosen (F = 300 N, v = 0,69 m/s), but the trends are the same, taking into account the graphs in Figures 2.2 and 2.3.

The following conclusions could be formulated:

- for non-additivated soybean oil, with the increase in temperature, h_{min} is decreasing,

- for all regimes, h_{min} (soybean oil) is higher except h_{min} (nano carbon, c = 1%) and h_{min} (carbon, c = 1%) at 20 °C, but at 45 °C the values are equal,

- the addition of nano carbon has low influence on h_{min},

- when temperature rises, all analyzed lubricants had a lower h_{min}. the ratio between h_{min} (20 °C) and h_{min} (45 °C) ranging between 2 for soybean oil and nano carbon lubricants and 5 to 6 times for nano graphite and nano graphene.

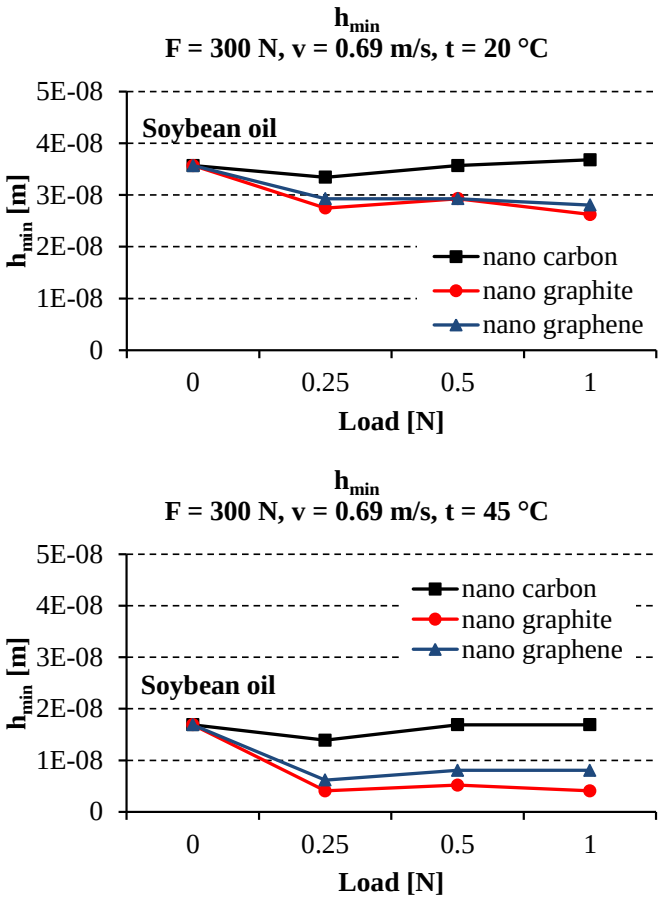

Fig. 2.7. Influence of the nature and concentration of the additive on the theoretical minimum thickness of lubricant film

If the influence of the nature of the lubricant is analyzed, it is found that the amorphous nano carbon does not significantly influence h_{min} at either 20 °C or 45 °C, the evolution of h_{min} being close to h_{min} (soybean oil).

The other two nanoadditives have a more reduced h_{min}, but the influence of their nature (one being considered with a 3D structure - graphite, the other with a 2D graphene structure) is very low at 45 °C and almost non-measurable at 20 °C.

Chapter 3
Laboratory formulation of lubricants and testing methodology on four-ball machine

3.1. Testing lubricants on the four-ball machine

Laboratory tests are required for product control [Gold, 2002], [Holmberg, 2005], [Stachowiak, 2004], being applied in industry and research. Test methods determine whether the product has the physical, chemical and performance properties as specified in the product catalogs. The equipment with which these tests can be performed can be included in two main groups:

- laboratory equipment that model tribological processes that characterize industrial tribosystems or generate friction processes under well defined conditions [Erhan, 2002], [Erhan, 2005], [Honary, 2011], [Stachowiak, 2004]; many are used to obtain comparative data;
- laboratory equipment using systems or sub-system from actual technical systems, monitored by appropriate measuring devices [Gold, 2002].

At the final stage of formulating a new lubricant, it is necessary to test it under actual operating conditions or under very close conditions to those that will be created under normal or even abnormal operating conditions. The actual operating conditions are characterized by a wide variety of operating parameters and, as a result, determinations have to be done on a large number of samples, with repeated tests under the same conditions. The cost of research increases significantly for real-time tests. In order to reduce costs, specialists [Czichos, 2006], [Erhan, 2002], [Gold, 2002], [Stachowiak, 2004] recommends the laboratory research phase, even if test systems are simple but rigorously controlled as compared to those in practice. For laboratories, tribotesters are very useful because they allow rigorous parameter control and accurate and continuous monitoring. One of them, recommended for its simplicity, is the four-ball test [Czichos, 2006], [Gold, 2002], [Stachowiak, 2004].

The four-ball machine is designed to measure the durability of the oil film in the sliding friction and the friction moment measurement [Chang, 2010].

The principle of testing the lubricant with this tribosteter (Fig. 3.3a) is based on 4 technically identical balls, with a diameter of 12.7 mm, placed in the form of a regular tetrahedron. The three lower balls are positioned in a steel support and fixed with a ring and a clamping nut, over which the lubricant to be tested is cast. The test can be done with or without temperature control. The fourth ball is fixed in a special sleeve and positioned at the bottom of a rotary shaft, driven by a constant or variable speed electric motor (200 rpm - 3000 rpm). It rotates relative to the three fixed balls with the loads and speeds desired by the operator. A section of the 4-ball fastening assembly is illustrated in Figure 3.3b. Loads are

applied to the balls using discs positioned on a load lever (they can apply forces between 60 N and 6 kN). The cup assembly is supported, above the loading lever, by a disc that rests on an axial bearing, thus allowing horizontal movement and automatic alignment of the three lower balls in contact with the fourth ball. The measured performance indicators are the coeficient of friction and wear scar diameter, which overall determines the ability of the lubricant to prevent scratching and wear of the surface. The friction moment exerted between the test balls is measured by means of a tensiometric mark trapped between the fixed arm of the machine and the cup assembly arm, which is connected to a recording device and then to a computer for data acquisition.

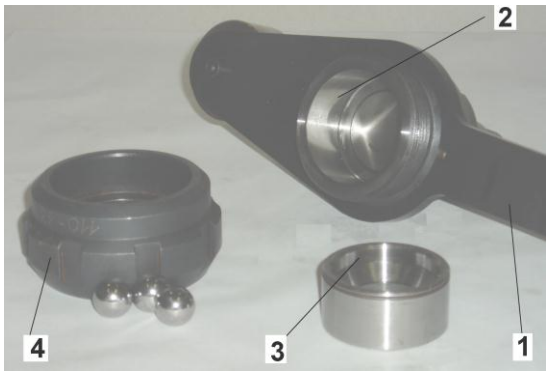

Fig. 3.1. Fixed balls cup. 1 - lever on which the tensiometric mark is mounted , 2 - Fixed balls cup, 3 - ball fastening ring, 4 - ball fastening nut

Abdullah [Abdullah, 2016] tested according to ASTM, a nano additive oil with 0.5 wt% of 70 nm hBN in a diesel engine oil SAE15W-40, obtained by sonication. The seizure point was low and the adhesion wear traces were larger and more frequent on nano additivated oil. Such studies have led to the setting of test parameter intervals.

Figure 3.3 shows the four-ball in the laboratory "Lubritest" of "Dunărea de Jos", University with the load of 6000 N (manufactured by Hansa Press- und Maschinenbau GmbH, Germany). It mainly consists of: electric motor (1), machine body (2), loading system (3), electric control and monitoring panel (4), support frame (5). The system for measuring and monitoring the friction torque was carried out at the "Dunarea de Jos" University of Galati. The equipment also includes an electronic timer, which can read with a precision of 0.2 s.

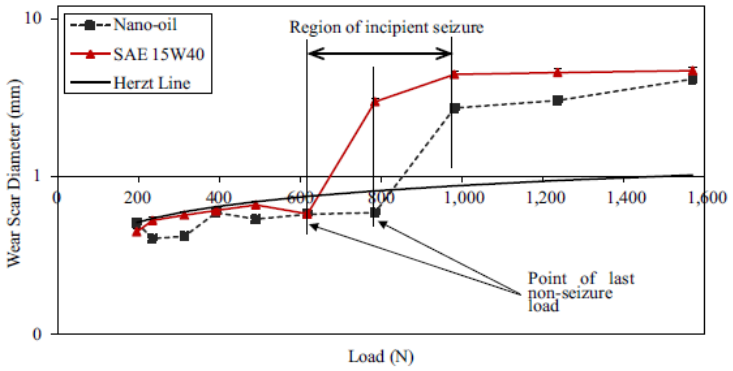

Fig. 3.2. Wear results [Abdullah, 2016]

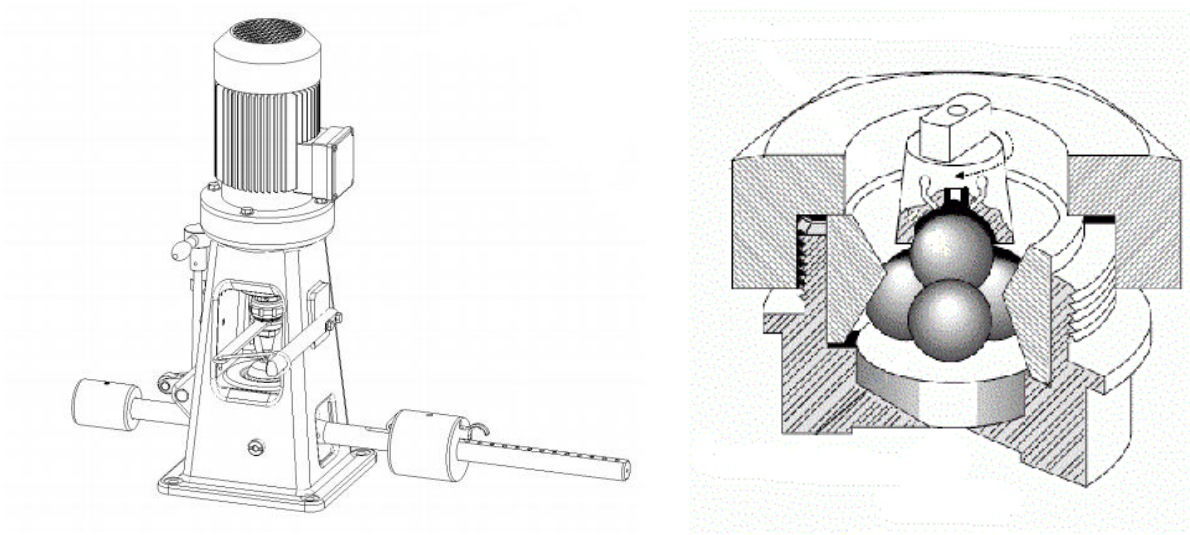

a) b)

Fig. 3.3. (a) Illustration of the four-ball machine;
(b) the 4-ball fastening system (3 fixed balls and a mobile ball) during testing

The four-ball machine performs a sliding motion between the ball attached to the machine shaft and the three other balls in the cup. The four-ball machine (Fig. 3.4) consists of a vertical shaft ending with an element (1), which allows for mounting and fixing of a movable ball (2). It acts on another three balls, fixed in a cup-shaped piece by means of a threaded piece (4) and a conical piece (5). The loading is obtained by means of a lever (3), visible in Fig. 3.3. One point of the lever acts on the cup, with the fixed balls and the other is loaded with various weights, at different distances.

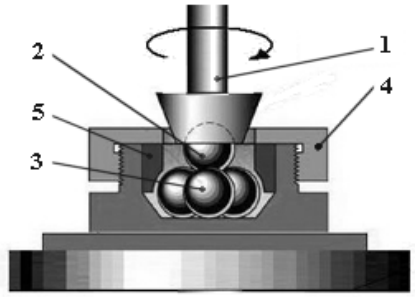

Fig. 3.4. Main parts of the four-ball tribotester

The diameters of the four balls are 12.7 mm. The balls are made by SKF, specially treated, with high precision (± 0.0005 mm), high hardness (62 ... 65 HRC) and outstanding surface quality (Ra = 0.02 ... 0.03 μm).

The test procedure is carried out in stages, following the order:

- the 4 test balls, the fixed balls cup, and the ball sleeve that rotates, are cleaned from possible impurities;
- the balls are left to degrease in isopropyl alcohol for 2 minutes;
- the fixed balls cup is placed in the tightening bracket;
- after drying, place the three balls in the cup and center in position with a fastening ring;
- the assembly is tightened with the locking nut, at a torque of 68 N·m ± 7 N·m;
- add sufficient test lubricant inside the cup (8-10 ml), so that the three balls are covered by the fluid at least 3 mm;

- the fourth ball is knocked into the holder and then placed in the mandrel of the tribosystem;
- it is checked that it can not be rotated relative to the ball holder;
- the ball cup assembly is centered under the spindle and in contact with the fourth ball;
- it must be able to rotate freely around the axis of the fourth ball;
- place the necessary weights on the load lever to have the desired load;
- they are placed slightly, avoiding the shock that can permanently deform the balls;
- check, by rotating the cup, that the three balls are centered on the upper ball;
- fix the tensometric mark between the fixed tribosystem arm and the lubricant bowl arm;
- start the friction moment reader and fix it to a scale equivalent to that of the friction force; it must be brought to 0 before the tribotester starts up;
- start the computer software to acquire data during the test;
- start the engine and the timer;
- at the end of the test period, determined by the operator, the engine stops automatically;
- remove the load from the balls and save the data in .xls format.

3.2. Tribological parameters measurable by tests on the four-ball machine

In this study, there were analyzed the coefficient of friction and two parameters dependent on the wear scar diameter of the fixed balls.

The coefficient of friction**.** For the measurement of the frictional force, the author used a tensometric bridge (connected between the machine arm and the three-ball fixation arm), the signal of which was taken over by a Scout 55 acquisition system and transmitted to a computer (Figure 3.5). Data acquisition and processing was performed using the CATMAN® EXPRESS 4.5 software. Details of the resistance (friction) torque measurement system are given in [Solea, 2013]. Starting from the friction force values, the friction moment and coefficient of friction were determined.

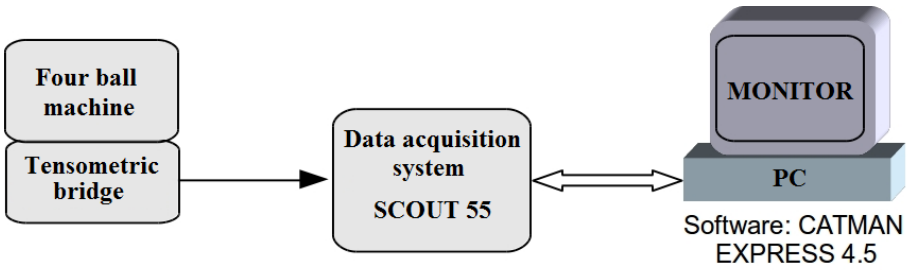

Fig 3.5. The block diagram of the data acquisition system, as it was done by Șolea [Șolea, 2015]

Wear evaluation can be done with one of the following parameters:

- WSD (average diameter of wear mark for fixed balls: average of six measured diameters, two on each ball, one measured in the sliding direction, the other perpendicular to it),

- wear rate of wear scar diameter.

3.3. Methodology for obtaining the soybean oil based lubricants and carbon based nano additives

The materials tested for this study are lubricants based on soybean oil supplied by Prutul Galati and additives of nano carbon materials in various concentrations (0.25 wt%, 0.5 wt% and 1.0 wt%). The composition in fat acids of the soybean oil is shown in Table 3.1.

Table 3.1. The characteristic fatty acid composition for the tested soybean oil

Acid	Symbol	Concentration, %wt
Miritic acid	C14:0	0.11
Palmitic acid	C16:0	12.7
Palmitoleic acid	C16:1	0.13
Heptadecanoic acid	C17:0	0.05
Stearic acid	C18:0	5.40
Oleic acid	C18:1	21.60
Linoleic acid	C18:2	52.40
Linolenic acid	C18:3	5.70
Arachidic acid	C20:0	0.25
Gondoic acid	C20:1	0.20
Eicosadenic acid	C20:2	0.50

Additives were supplied by PlasmaChem [PlasmaChem, 2016]:

- **nano amorphous carbon:** average particle size ~ 13 nm, specific surface area ~ 550 m²/g,
- **nano graphite:** average particle radius: 400 - 450 nm,
- **nano grafene**: nano plates with a thickness of 1.4 nm and a particle size of up to 2 microns.

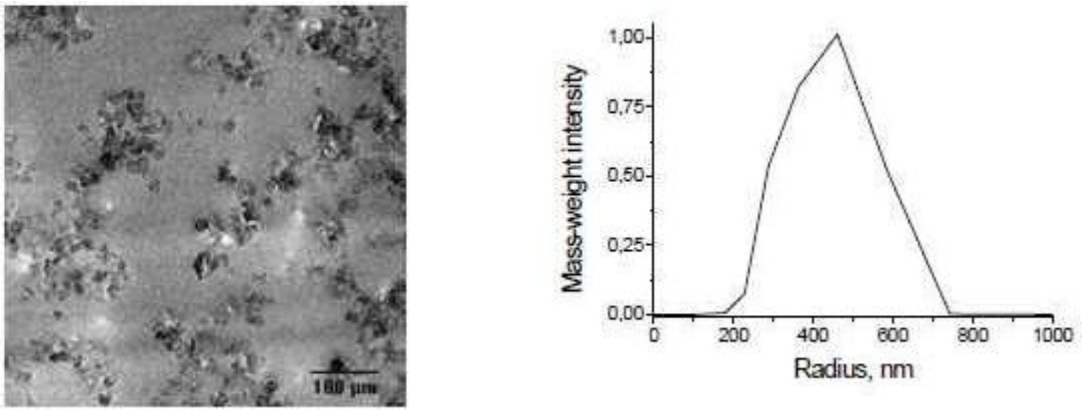

a) Amorphous carbon, nano powder b) Graphite particles rays dispersion

Fig. 3.6 Characteristics of nano additives [PlasmaChem, 2016]

The problem to be solved with such an anti-wear additive is its dispersion in oil. Thus, since the tested base oil is a mixture of fatty acid triglycerides (Table 3.1), the author proposed a method of obtaining a good dispersion. The formulated lubricants were obtained in a small amount of 200 ml each. The steps followed in this laboratory technology were similar to those presented by Cristea [Cristea, 2017]:

The mass ratio of the additive in the dispersing agent is 1:1, with an accuracy of 0.1 mg,

- mechanical mixing of the additive and an equal amount of guaiacol (supplied by Fluka Chemica) with the chemical formula C_6H_4 (OH) OCH_3 (2-methoxyphenol) for 20 minutes; this dispersing agent is compatible with both the additive and the soybean oil;

- gradually adding the soybean oil, measured to obtain 200 g of lubricant with the desired additive concentrations, by mixing with a magnetic homogenizer during 1h.

- ultrasonication + cooling 200 g of lubricant for 5 minutes using the Bandelin HD 3200 (Electronic GmbH & KG Berlin) sonicator; the lubricants are heated to about 70 ° C; the cooling time was 1 hour; this ultrasonic + cooling step is repeated 5 times to obtain a total of 60 minutes of ultrasonication. The parameters of the ultrasonic regime are: 100 W power, frequency 20 kHz ± 500 Hz, continuous mode.

3.4. Testing methodology on four-ball machine

Testing methodology includes the establishment of materials, the production of lubricants at laboratory scale, their testing, data interpretation, non-destructive analysis of wear traces by optical microscopy and SEM, 3D profilometry).

The test parameters for each tested lubricant were**:**

- loading force - 100 N, 200 N and 300 N (± 5%).

- sliding speeds of 0.383 m/s, 0.537 m/s and 0.691 m/s, corresponding to the spindle speeds of the four-ball machine 1000 rpm, 1400 rpm and 1800 rpm (± 6 rpm),

- test time - 60 minutes (± 1%),

- the concentration of each additive in the formulated lubricants is 0.25%, 0.50% and 1% (wt), respectively.

Lubricants that have been tested have been inserted into the fixed balls cup to cover these balls. The amount of oil used for each test was 10 ml. After each test, the ball fastening system and the balls were cleaned and degreased with isopropyl alcohol and ethyl ether, then dried in air stream.

Measurement of wear trace diameters was performed with the Neophot 2 optical microscope. In accordance with the procedure of SR EN ISO 20623: 2004 [SR EN ISO 20623: 2004], three wear marks were obtained for each test, these being located on the three fixed balls. Two diameters, the first diameter measured along the sliding direction, the second diameter measured perpendicular to the first, were measured for each wear trace. With three traces of wear, six diameters were obtained and their mean value was calculated. This value represents the diameter of the wear scar reported for each of the tests performed. The same method of obtaining the wear diameter is also given in specialized reports [Cristea, 2017], [Tiong, 2012], [Czichos, 2002].

Chapter 4
Experimental results on the tribological behavior of formulated lubricants tested on the four-ball machine

4.1. Tribological parameters

To assess the quality of lubricants, it is important to establish the test methodology (equipment, parameters and investigations during and after testing). Their selection depends primarily on the practical use for which the lubricant is tested and a tribotester approaching as much as possible to the technical system in which the lubricant will be introduced is desirable.

Tribological tests can be grouped in severe tests and tests under normal working conditions.

In this paper the tests are performed for normal working regimes with liquid lubricants.

The following coefficients of friction were analyzed:

- instantaneous value (i.e. at t time)

- mean value over the duration of the test (1 hour in this study, with 7200 recorded values with a sampling of two records per second)

- average value over the last 10 minutes of the test (argumentation: there are research reprezent for in 10 minutes, 5 minutes, it is considered to be a stabilized domain)

- the variation interval of the friction coefficient for 1h and for the last 10 minutes,

Wear parameters

Wear scar diameter (WSD) is characteristic of the four-ball machine and many authors also give the results of wear using this parameter.

WSD is the arithmetic mean is the mean of the six measurements, two on each of the three fixed balls of a test. For each ball, the wear diameter was measured in the direction of sliding and perpendicular to it.

WSD wear rate

Since the duration of the test is 1 h, the sliding distances are different for different speeds:

L_{1000} (v = 0.38 m/s) = 1378.8 m; L_{1400} (v = 0.53 m/s) = 1933.2 m; L_{1800} (v = 0.69 m/s) = 2487 m.

It is possible that the simple graph of the WSD dependence on additive concentration, load and speed is not relevant due to the difference in the sliding distances, and then, on the basis of the literature [Holmberg, 2012], the wear can be also evaluated by another parameter, called the wear rate, where:

$$w = \Delta V / (F \cdot L) \quad (4.1)$$

where ΔV – variation in sample volume (volume of removed material), F – loading force; L – sliding distance.

The product $F \times L$ is the mechanical work done by the tribosystem, in other words, the wear rate shows the loss of volume material for the mechanical work unit performed by the system, the wear rate of WSD (wear scar diameter) is:

$$w(WSD) = \frac{WSD}{F \times L} \quad [mm/N \cdot m] \quad (4.2)$$

where WSD is the wear scar diameter average for a test, F - the load applied on the four balls, L - the sliding distance.

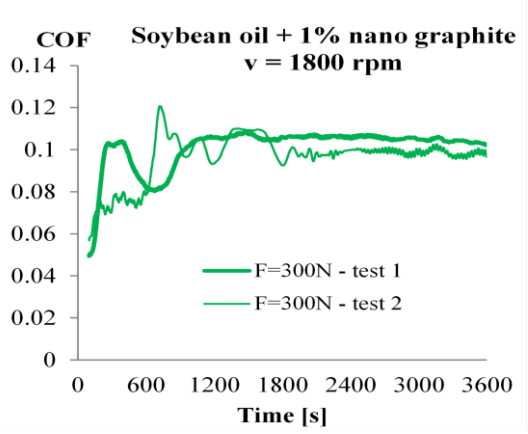

Fig. 4.1. Evolution of COF in time for two tests done with the same parameters

Repeatability (intradetermination accuracy) and bias (difference between measurements). Each set of parameters (F, v, c) was repeated twice, and Figure 4.1 shows the evolution of the friction coefficient (COF) over time for two tests performed with the same parameters to evaluate the repeatability. F is the force on the machine axis, v - the sliding speed between the fixed ball and the spinning ball, and c - the mass concentration of the additive in the soybean oil.

4.2. Using maps in tribological analysis

All maps were represented using a spline interpolation, and the surfaces are "compelled" to include experimental data. A point on a wear map is a test for the same set of parameters (F [N], v [m s], C [%]) where F is the normal load on the 4 ball tribotester (F = 100 N, 200 N and 300 N), v is the sliding speed (0.38 m/s, 0.53 m/s and 0.69 m/s) and c is the mass concentration of nano additive (0%, 0.25%, 0.5%, 1.0%).

In this study, the friction coefficient maps (average value for each test of the two with the same parameters) and the wear-rate maps were done under the same conditions. These are useful in assessing trends and determining test regimens for which the tribological parameters and, thus, the tribological behavior of the system, is better.

From the documentation available, an analysis of tribological behavior based on maps for several parameters (here COF and w(WSD)) is made for the first time.

4.3 Analysis of tribological parameters for the non-additivated soybean oil

The graphs in Fig. 4.2 are done using a moving average for 200 values. The author chose this representation to highlight the friction coefficient trend evolution over the 1 hour test for which 7,200 values were recorded (of 2 values per second).

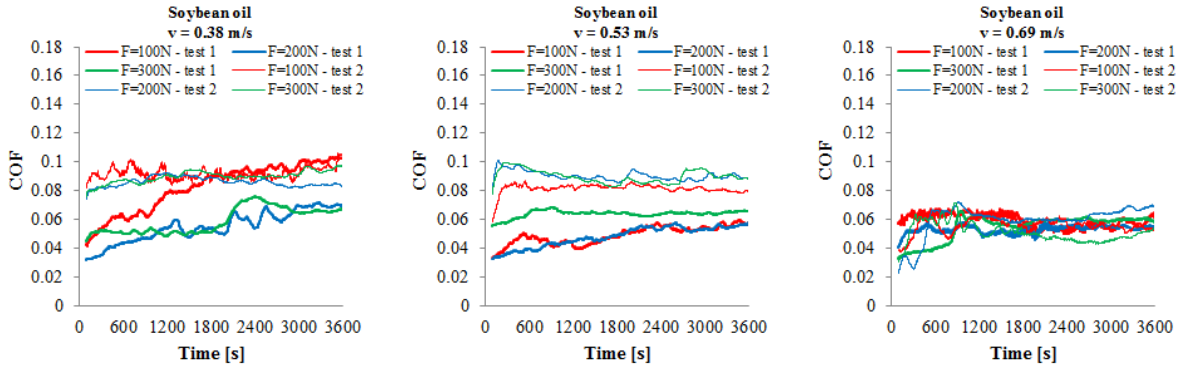

Fig. 4.2 The evolution of COF over time, depending on to load and speed, for two tests with the same parameters (F, v)

Lower values for v = 0.69 m/s indicate a full-film regime based on these tests, the author recommending a higher speed regime for the non-additive soybean oil. Friction is more unstable at the low speed v = 0.38 m/s. The COF value is close to 0.1, which means that the working mode tends to a mixed one or a boundary lubrication. And at low forces, COF oscillations reflect the instability of the regime. Except for the regime (F = 100 N and v = 0,38 m/s), COF does not depend on the combination of parameters (F, v). The results obtained for the soybean oil are in line with the discussions in Şolea [Şolea, 2013] and [Georgescu, 2015], but the author has increased the studied intervals for forces and speeds.

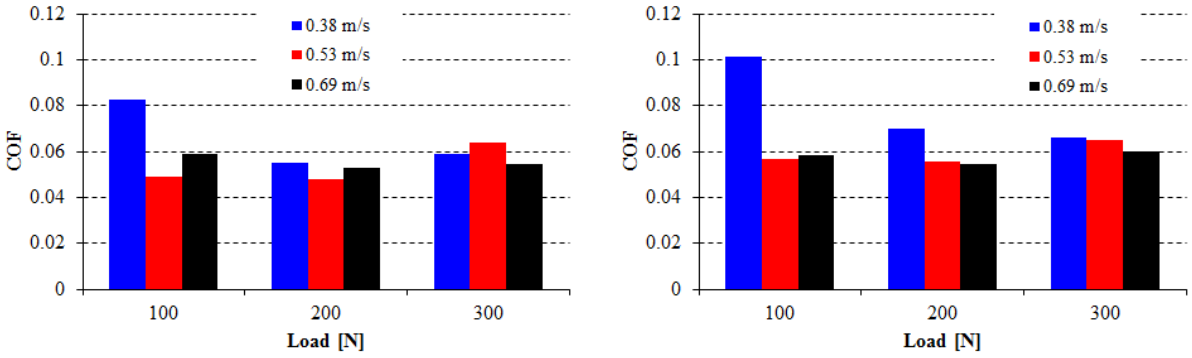

a) average for 1 hour b) average for the last 10 min

Fig. 4.3. The average of COF values over the entire test (a) and the last 10 min (b)

Wear parameters

A representation of the wear rate as in Fig. 4.4 helps the researcher to observe the evolution trends of the parameter of interest according to two variables, here the tribotester load and the sliding speed of the rotating ball on the three fixed balls. For the range of analyzed loads and speeds, non-additivated soybean oil had a downward trend with increasing load and speed. This trend is consistent with Dowson and Higginson's argument on generating the EHD film [Dowson, 1977], although the demonstration is made for a linear contact, but this also applies to punctual contact, as seen in Crețu's works [Crețu, 2009]. They

have shown that the speed factor

$$U = \eta_o \left(U_1 + U_2 \right) / \left(2E' \cdot R_e \right)$$

has the greatest influence on the minimum thickness of the fluid.

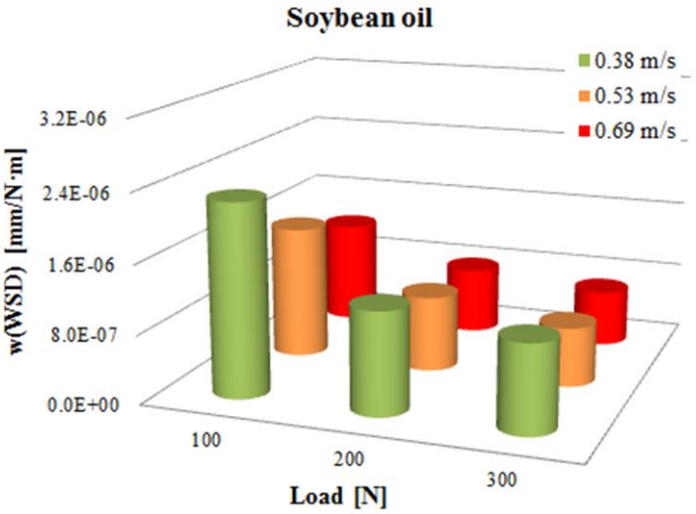

Fig. 4.4. WSD wear rate for the non-additivated soybean oil

For low-viscosity oils, the G-factor can not participate in film formation to the same extent as the viscous oils at the working temperature of the contact. [Cameron, 1983] [Gold, 2002]. In addition, vegetal oils are characterized by a high viscosity index, i.e. the variation of this characteristic with the temperature is low, especially at temperatures above 50 - 60 °C.

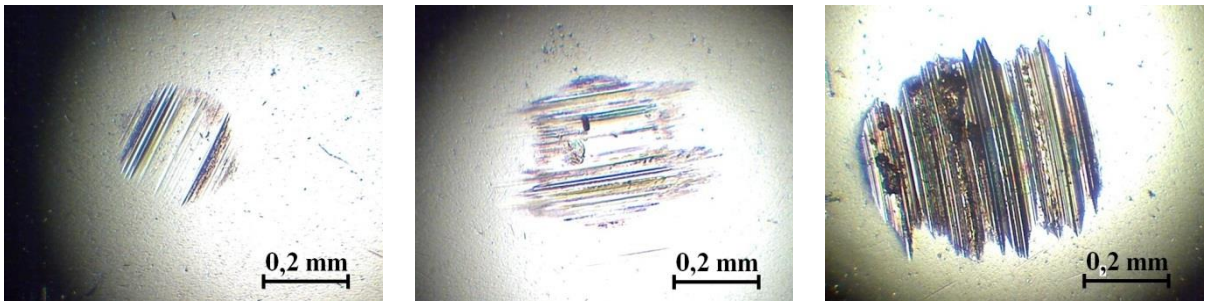

F = 100 N F = 200 N F = 300 N

Fig. 4.5. The wear scars obtained with the soybean oil without additives v = 0,69 m/s

In Figure 4.5 the wear scars for the non-additivated soybean oil test are presented for v = 0.69 m/s. One may notice the wear scar increases proportionally to the load, but this optical microscope study also reveals how the wear process develops. at F = 100 N, it is noticed abrasive wear, but not on the entire contact area. It is possible to partially regenerate a lubricant film (the fluid pressure is higher in this area) in the central area (not seen or slightly worn). At F = 200 N, the abrasive wear is evident throughout the wear scar and there is also a spot where the ball material has been smeared due to a local adhesion process. At F = 300 N, wear results in a heavy abrasive wear, with multiple pitting areas.

The analysis of wear data has to be done carefully because, depending on the wear parameter discussed, the results can show some different aspects. For example, if you analyze Fig. 4.6, it is noted that WSD increases with the load and the speed dependence is relatively poor, but the wear rate is substantially reduced with the increase of the load. This difference between wear parameters was obtained because the four-ball test was done for 1 hour for all its variables (load sliding speed and additive concentration). This time interval has been retained in order to compare the results obtained by the author with the results of the literature, in which the vast majority of the four-ball test reports are done for 1 hour irrespective of the test speed. It is true that many papers do not vary speed as a test parameter [Ossia, 2010], [Cretu, 2014].

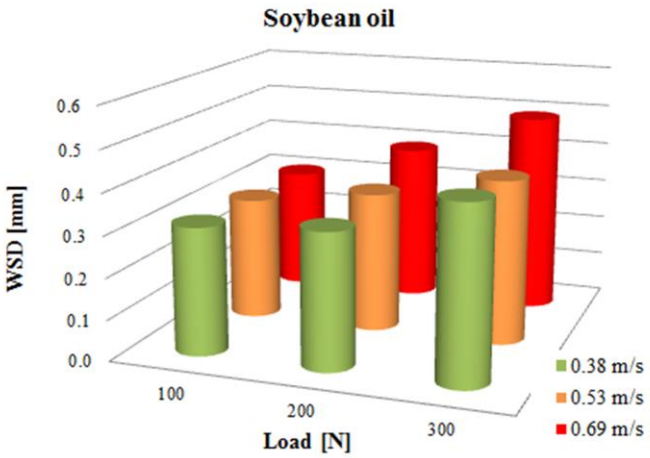

Fig. 4.6. WSD for non-additivated soybean oil at different test speeds

The conclusion is that for the variation of several test parameters (here the variation of the sliding speed, also determines the sliding distance variation), the interpretation of the data has to be done carefully and taking into account that keeping constant a test parameter (here, time) can vary other important parameters the sliding distance).

4.4. Lubricants additivated with nano black carbon

SEM investigations show that nano carbon is on the friction surfaces as nano agglomerations (Fig. 4.8), unevenly distributed over the texture of the surface. These particles or agglomerations appear to be rolled up and are likely to act as nano rolling elements, which explains low friction coefficients during the test (Fig. 4.9). The problem is that, these particles are not uniformly distributed over the contact surfaces, producing a preferential wear on the particle-free areas. As the particles migrate in motion, these areas prone to direct contact. This may be the explanation for the variation of the friction coefficient over time and with large amplitudes (Fig. 4.9). The friction coefficient plots of Fig. 4.9 are done using a moving average of 200 values, the recorded samples being of 2 values per second. The discussion of the evolution of the friction coefficient over time is based on the comments done by Czikos [Czichos, 2006].

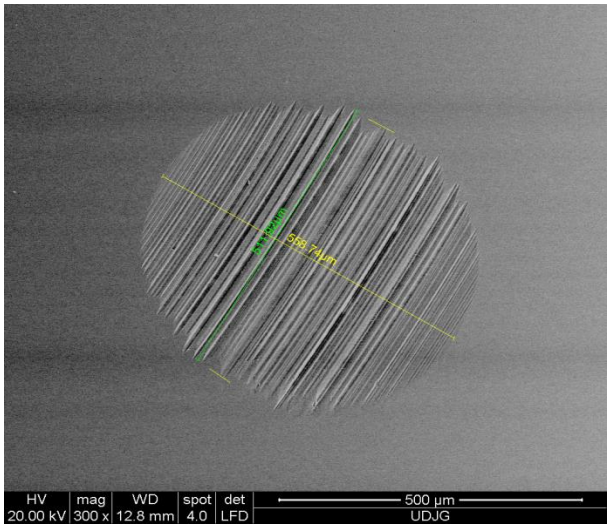

Fig. 4.7. Exemple of WSD measurement. Test conditions: v = 0.38 m/s, F = 200 N, time 1 h, lubricant: soybean oil +1% nano black carbon, ball 1

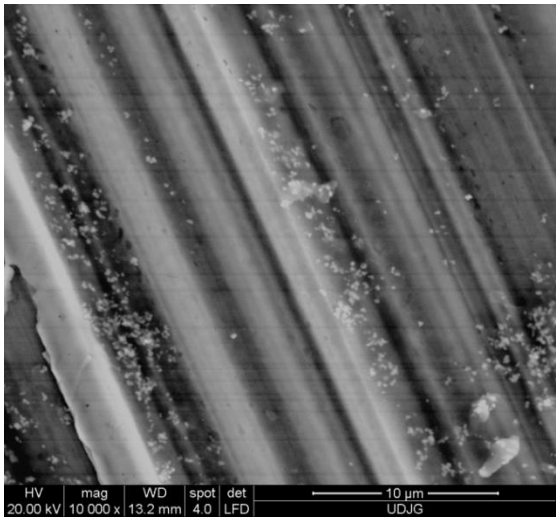

Fig. 4.8. Particles of nano black carbon on wear scar. Test conditions: v = 0,38 m/s, F = 200 N, time 1 h, lubricant: soybean oil +1% nano black carbon

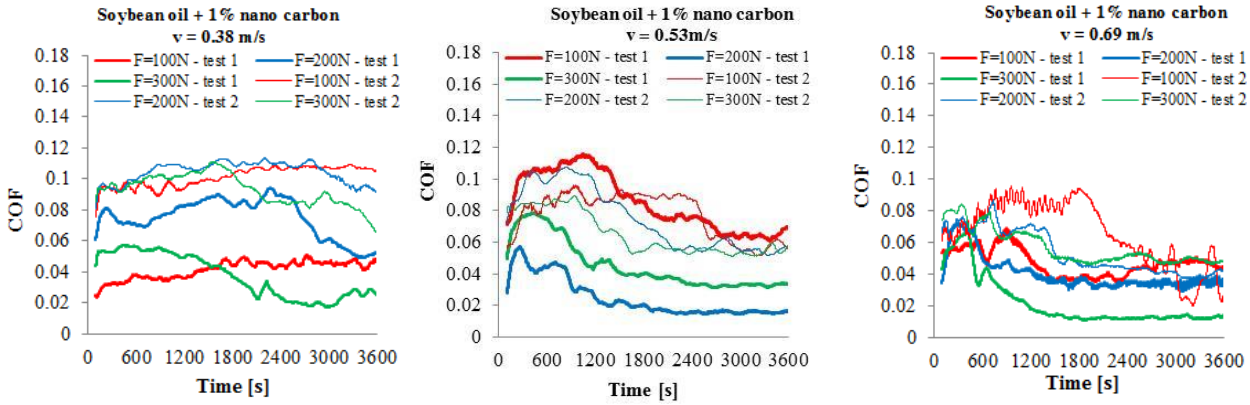

Fig. 4.9The evolution of COF over time, depending on load and sliding speed for two tests with the same parameters (F, v)

Thus, the coefficient for the soybean oil with nano carbon is spread on a large interval for the lowest speed, but at v = 0.69 m/s, after a period with high values, COF evaluates in a narrow interval, under 0.06 meaning a full lubrication. (Fig. 4.9). For added lubricants, the tendency is to reduce the friction coefficient after a period of operation of 10 ... 15 minutes. Analyzing Figure 4.10, it is noted that at a concentration of 1.0% of nano-carbon, the friction coefficient becomes lower for higher load (F = 300 N) and high speed (v = 0.69 m/s). Also, this regime gives less influence on WSD (Fig. 4.10). Under the minimum test load (F = 100 N), the COF oscillation range is the highest.

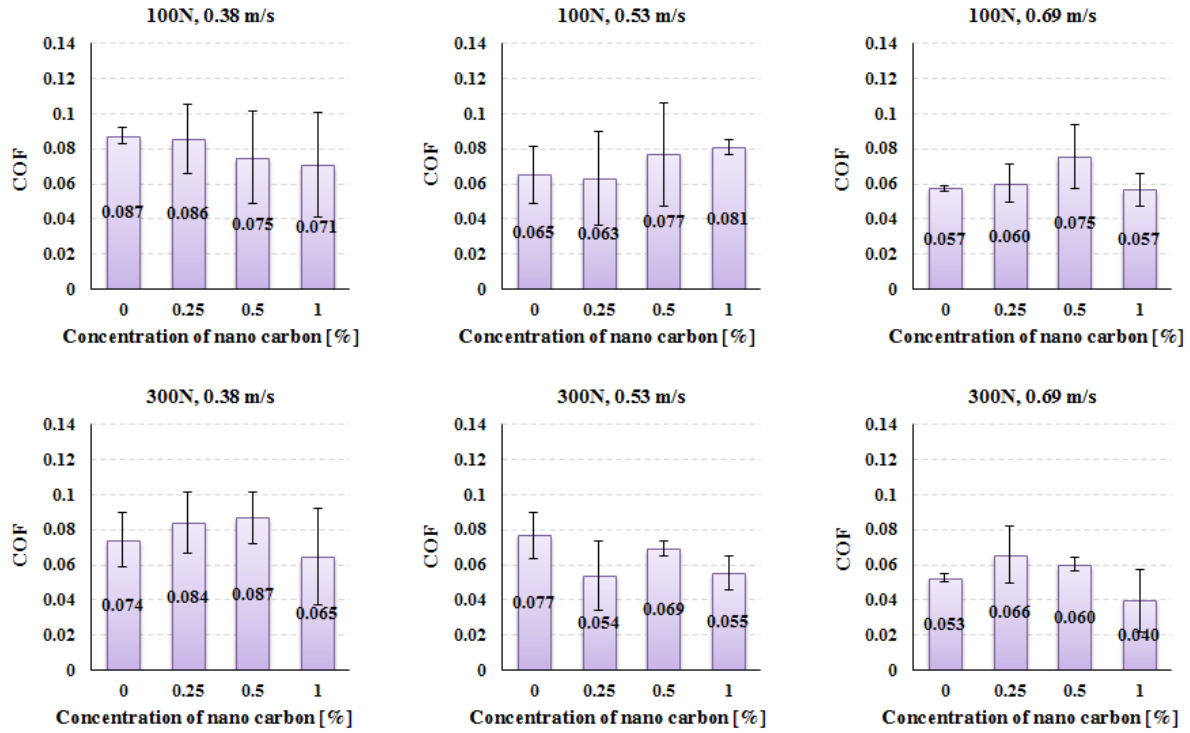

Fig. 4.10. COF (average values during a test of 1h, two tests with the same parameters)

For nano carbon additivated lubricants, mean COF values below 0.1 were obtained for all tests. The maximum values did not exceed 0.1, except for the regime F = 100 N, v = 0.38 m/s and v = 0.53 m/s and for F = 300 N, v = 0.38 m/s but just a little over 0.1.

Addition of nano carbon in soybean oil resulted in a COF decrease trend for extreme test regimens (F = 100 N, v = 0.38 m/s) and (F = 300 N, v = 0.69 m/s). In the remaining combinations of test parameters, the influence of additivation on COF is not obvious.

If the first column (v = 0.38 m / s) in Fig. 4.11 is analyzed, it can be seen that WSD increases for amorphous carbon in soybean oil, the increase being lower at low loads (F = 100 N).Also on the same graphs, WSD is not clearly influenced by the additive concentration. At v = 0.69 m/s, the WSD is always higher than the value obtained with without additive soybean oil.

This partial analysis would show that nano carbon addition to reduce wear is not warranted, at least for the range of tested (F, v) regimens tested.

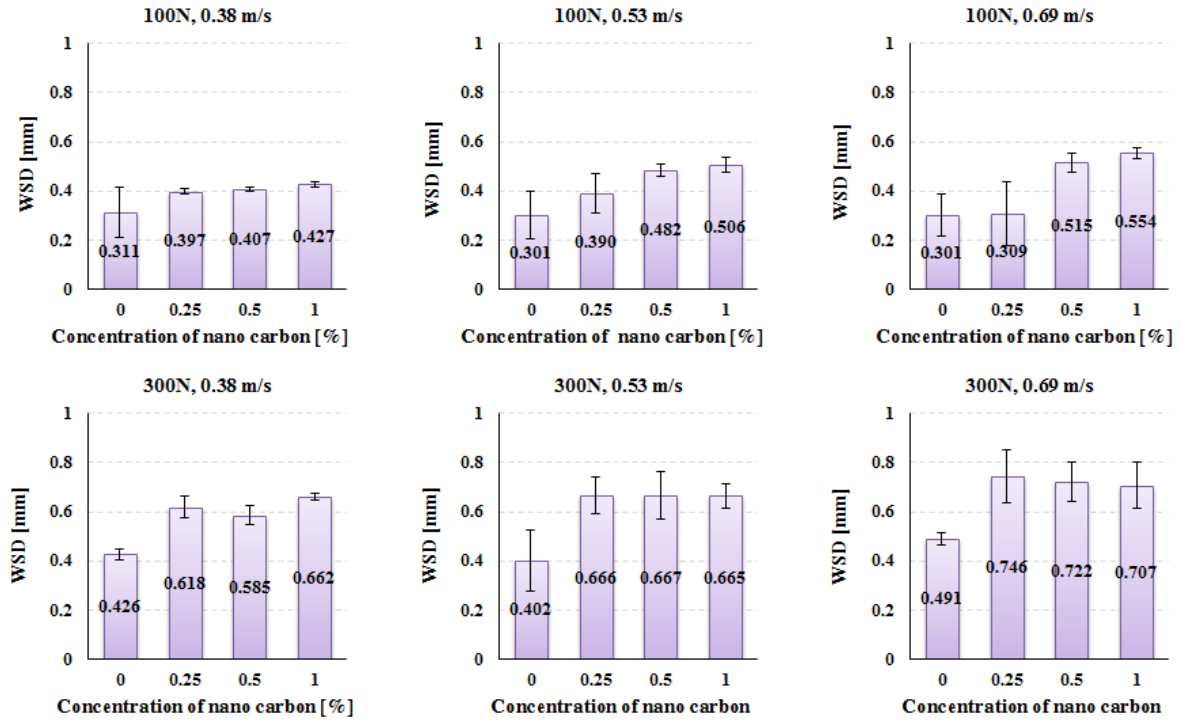

Fig. 4.11 WSD for lubricants with nano carbon

For nano carbon additivated lubricants, WSD is less sensitive to concentration, especially for F = 300 N. The non-additivated soybean oil can be recommended for light regimes (equivalent to F = 100 ... 200 N and speed v = 0.38 ... 0.69 m/s) The almost linear dependence of WSD on the concentration of this additive is only observed for combinations with F = 100 N. For the tested regimes (F = 100 N ... 300 N and v = 0.38 ... 0.69 m/s), the results are not in the favor of nano carbon additivation of the soybean oil.

The addition of nano carbon increases WSD. By comparing only the additivated oils at low speed, when the load increases, WSD also increases. Under the load of 200 N and 300 N, WSD is lower in relation to sliding speed and load, for concentrations of 0.5% and 1.0% nano carbon.

This anti-wear additive does not have a very clear influence on improving the tribological behavior of the soybean oil. Although the friction reduction mechanism exists in the presence of the additive, which is the interposition of carbon nano particles between the friction surfaces, and having a third body friction, the migration of these particles (because they are not bonded to the surfaces) and the uneven distribution in the contact the tribosystem behave more unstable than the neat soybean oil. In a statistical approach, at some point, it could come in contact with particles sufficiently to reduce friction and wear, but during operation there could be times when this number is low enough to have a mixt contact, and the oscillations between these two situations could explain the variations in friction coefficient and higher values for WSD.

Since particle distribution is not even in contact during operation, this type of anti-wear additive can not help to improve tribological behavior because it does not reduce the friction coefficient and does not reduce the wear scar diameter as compared to those produce with neat soybean oil. The author believe that the additive should be bonded (physically or chemically) for better results.

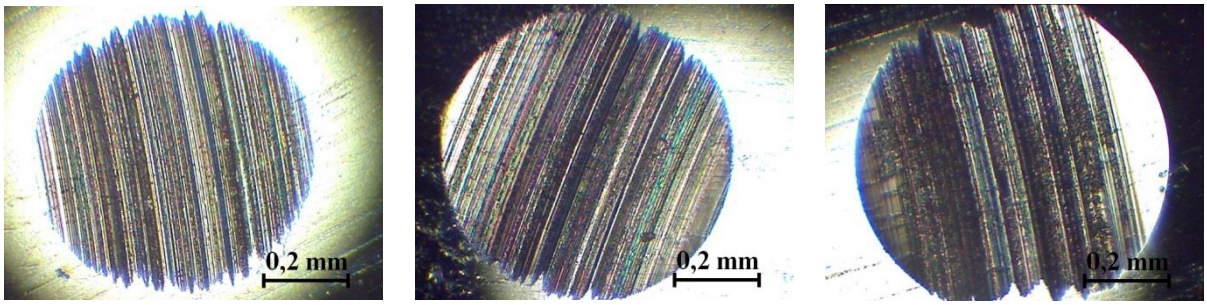

v = 0,38 m/s v = 0,53 m/s v = 0,69 m/s

Fig. 4.12 Wear scar obtained with soybean oil + 0.25% nano carbon, F = 300 N

From Figure 4.12, it is noticed that the wear pattern did not increase too much with the speed, but the quality of the surface has considerably worsened, which justifies the profilometry study in Chapter 6. The wear rate helps more to determine the influence of the concentration of this nano additive. In these graphs, the neat oil is not given. Comparison with unadulterated oil is highlighted on the maps of the conclusions.

It can be noted:

- a decrease of w(WSD) with load for all concentrations and speeds, for the additivated lubricants,
- the slope of the speed dependence for the same load is lower,
- at v = 0.38 m/s, the influence of the additive concentration is insignificant,
- the additivation would be justified in the field of high force for all speeds.

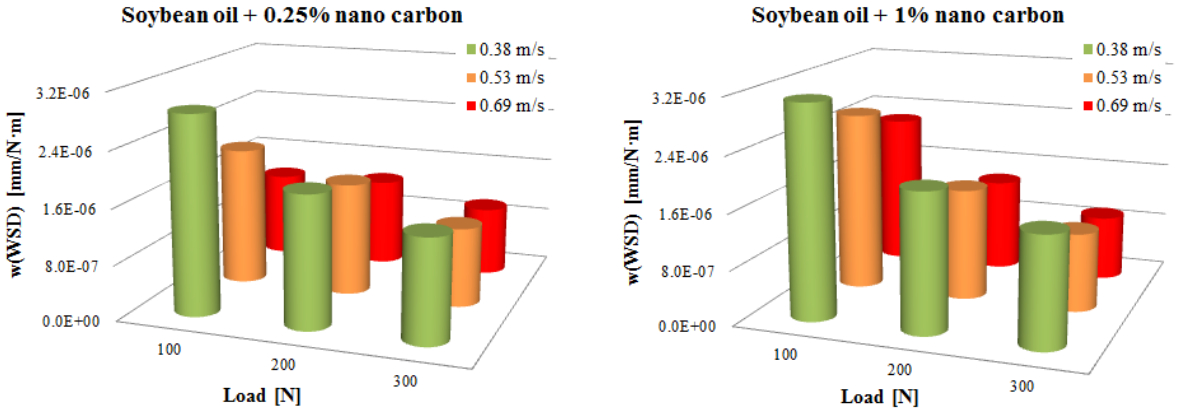

Fig. 4.13. WSD wear rate for amorphous nano carbon-additivated lubricants

4.5. Lubricants additivated with nano graphite

Figure 4.14 shows the evolution over time of COF for all tests performed with soybean oil additivated with nano graphite. There is a narrowing of its evolution range for v = 0.69 m/s for all loads and a scattering of higher COF values for low speeds and loads.

Analyzing Fig. 4.15, it can be noticed that, at F = 100 N (first horizontal line) the nano additive does not dramatically alter COF average. At high load (F = 300 N), COF increased for all additivated soybean oils as compared to the neat oil.

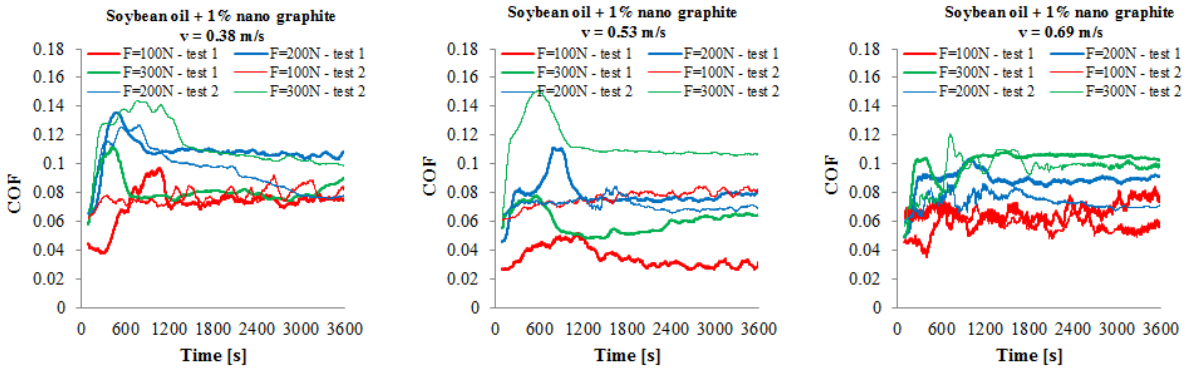

Fig. 4.14. The evolution of COF over time according to load and speed for two tests with the same parameters (F, v)

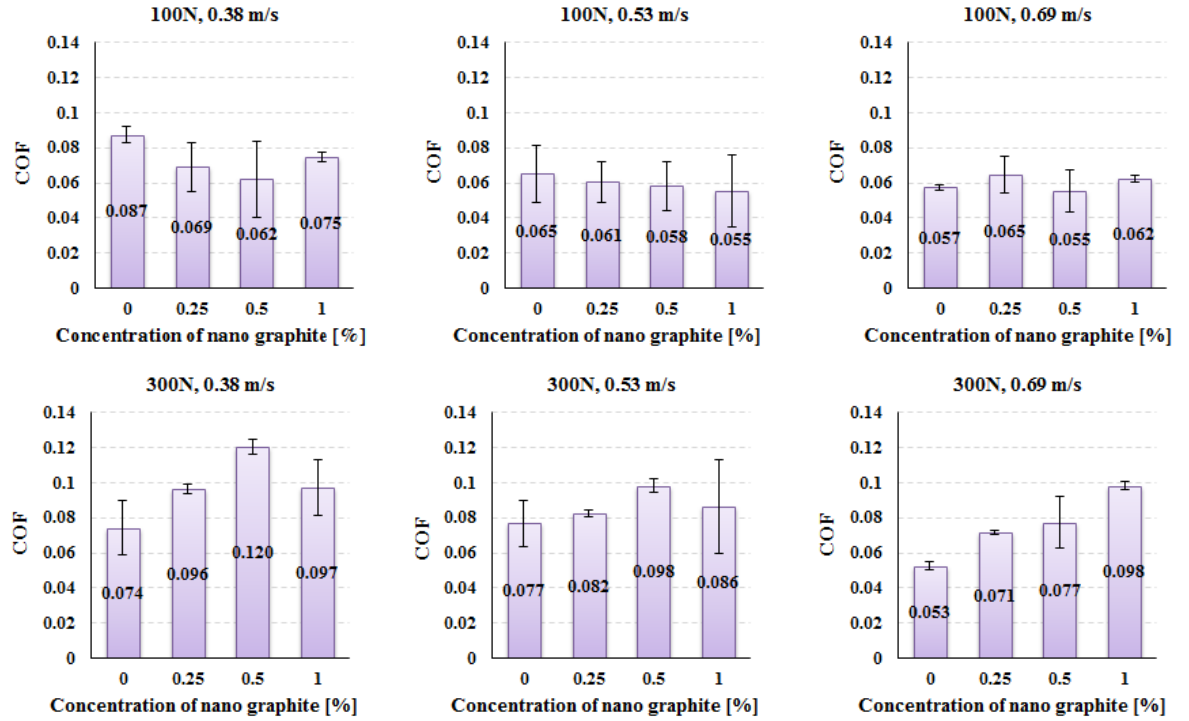

Fig. 4.15.Average values and mean seatteing intervals for two tests performed with the same parameters (F, v, c)

The explanation would be that the graphite does not cover the entire surface of the contact, but is only in contact in the form of nano rolls, the friction being zonal. Direct friction areas and friction areas with the third body. It appears that the presence of graphite prevents the generation of EHD film as COF values higher, towards 0.1, especially for F = 300 N.

Wear parameters

For all tested regimes, average wear scares are obtained in a narrow range and the spreading ranges are high. No lower average COF values than those for the soybean oil have been obtained, except for tests: (F = 100 N, v = 0.38 m/s), (F = 100 N, v = 0.53 m/s), with a concentration of 0.25%. But the differences are too small to highlight a trend and the influence of the additive or the test regime.

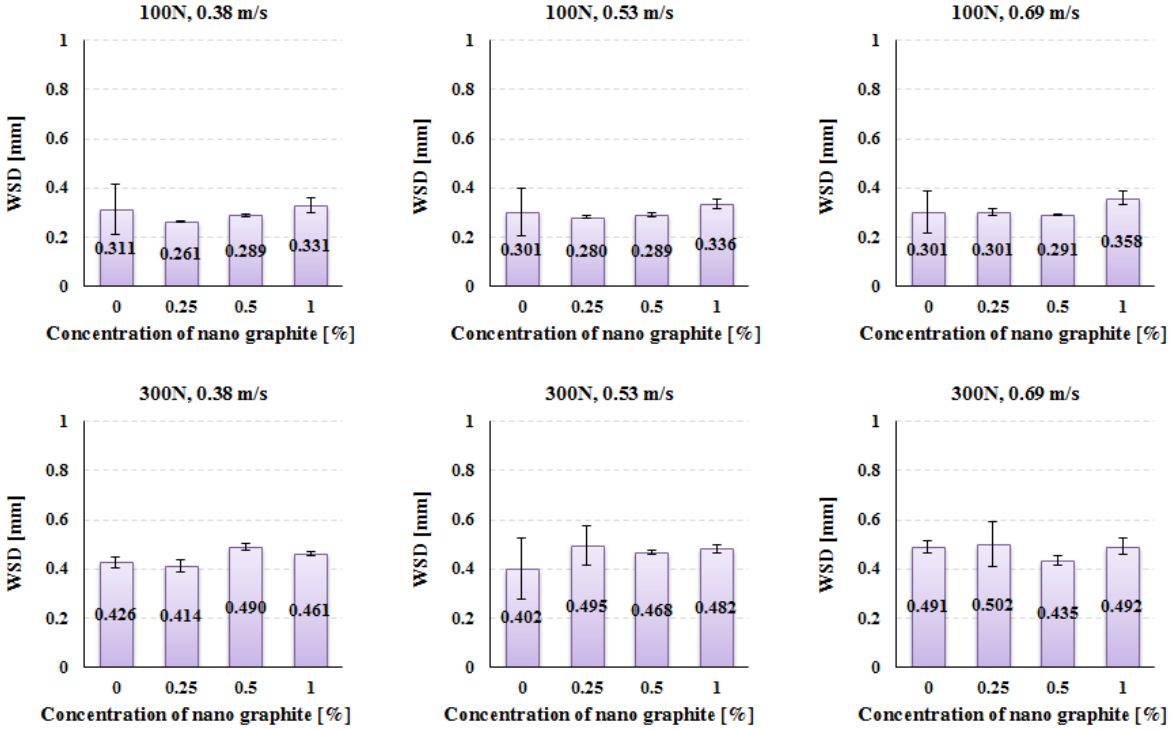

Fig. 4.16. WSD for lubricants additivated with nano graphite

High wear rate at low load and speed implies more intense abrasion, which occurs if the lubricant film does not form and if the additive does not protect the contact (may be in the form of local agglomerations that oscillate COF but when migrating into contact allows one triboelement to fall over the other, in direct contact and higher load than if it had not encountered the graphite agglomerations.

Analyzing the photos in Fig. 4.17, it can be noticed that the nature of the wear pattern does not change significantly, resulting from the abrasive wear process and with rare adhesive wear spots at higher loads.

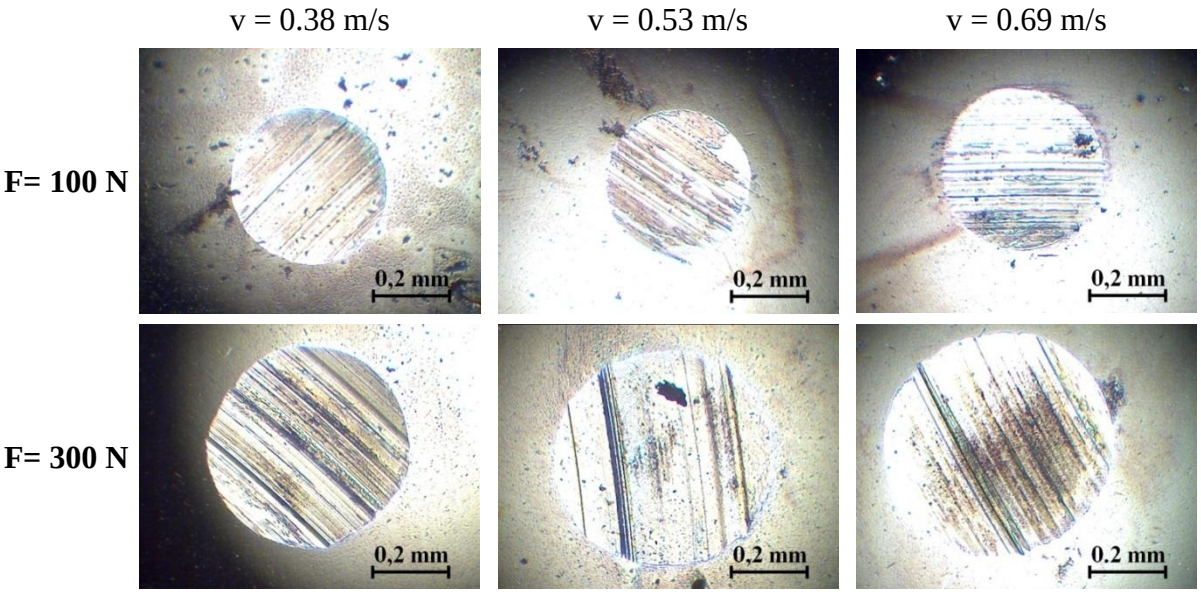

Fig. 4.17. Photos of the wear scars of the soybean oil + 1% nano graphite

It can be noted:

- comparing the graphs in Fig. 4.18, they are similar in appearance, regardless of the concentration of the nano additive,

- the wear rate decreases with increasing load,

- for load F = 300 N, the wear rate of WSD less influenced by speed.

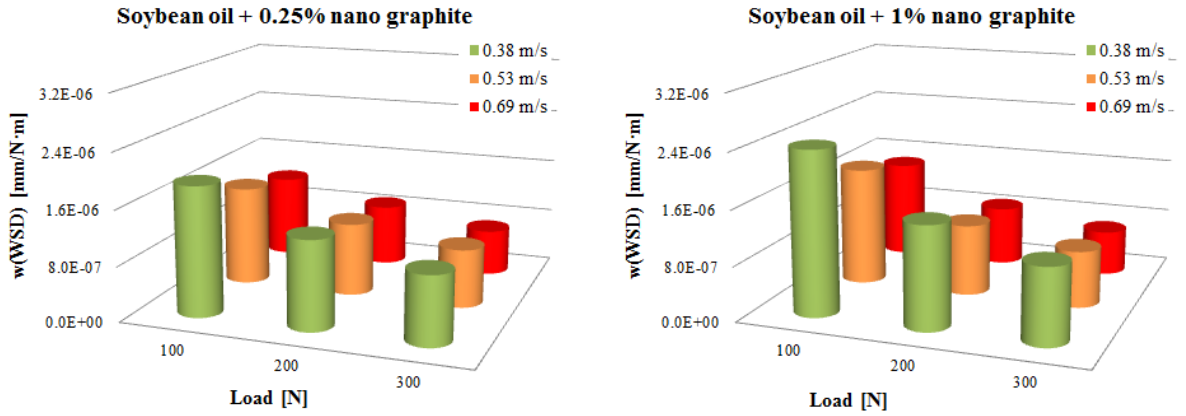

Fig. 4.18 WSD wear rate for nano graphite additivated lubricants

4.6 Lubricants additivated with graphene

The evolution of COF over time is given in Fig. 4.19, better evolution for the highest concentration. COF variations have short cuts or growth levels, which can be explained by the dynamics of COF components (dry friction, third body rubbing in areas with graphene nanoparticle, partial fluid friction).

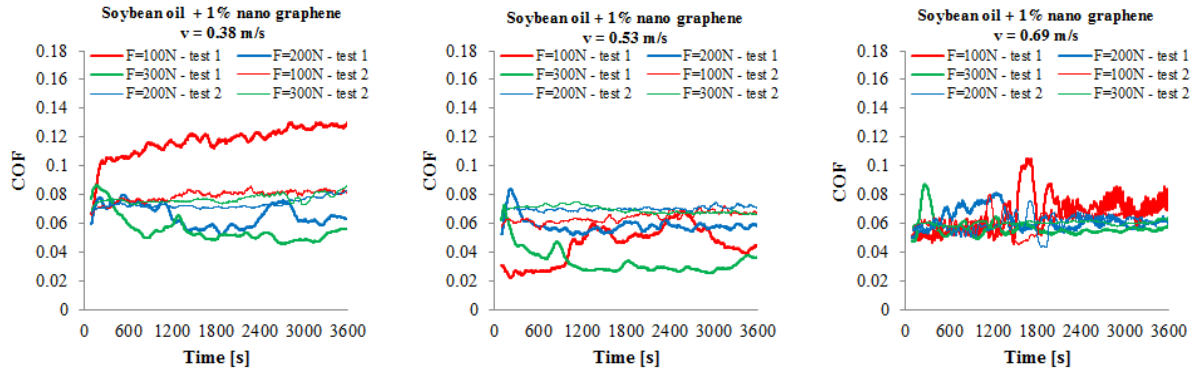

Fig. 4.19 The evolution of COF in time, depending on load and speed, for two tests with the same parameters (F, v)

The addition of graphene does not improve COF but keeps it very close to the values of neat soybean oil.

At v = 0.38 m/s, the highest values were obtained irrespective of the concentration of the additive, suggesting that the improvement in friction (in the sense of reducing it) is due to the increase in speed, [Dowson, 1977] and not on the additive, but the graphene does not prevent the formation of the film.

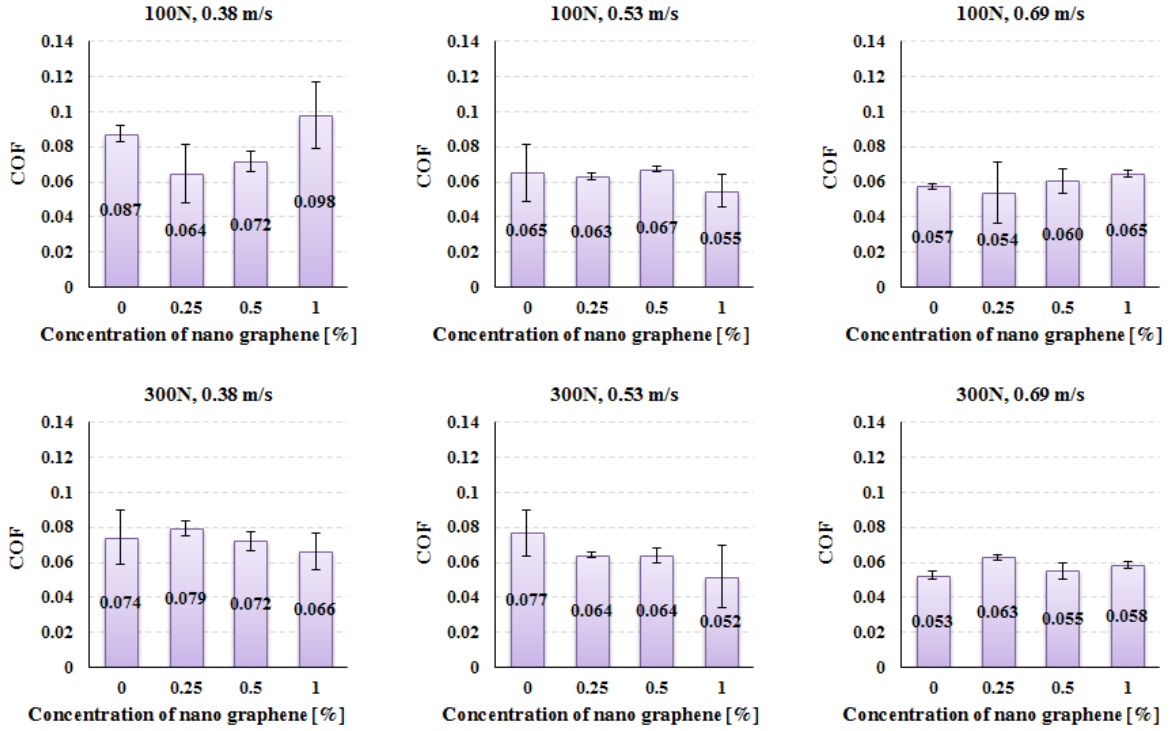

Fig. 4.20. Average values and spread range for two tests performed with the same parameters (F, v, C)

Wear parameters

WSD analysis is inconceivable to determine the influence of this additive and test regime.

From Fig. 4.22, it is noted that, for F = 100 N the WSD size increases with speed, but for F = 300 N, WSD does not significantly increase, but the texture of the surface visibly changes. Analyzing the graphs in Fig. 4.21 for WSD and WSD photos, the importance of correlation in the interpretation of several tribological parameters is point out.

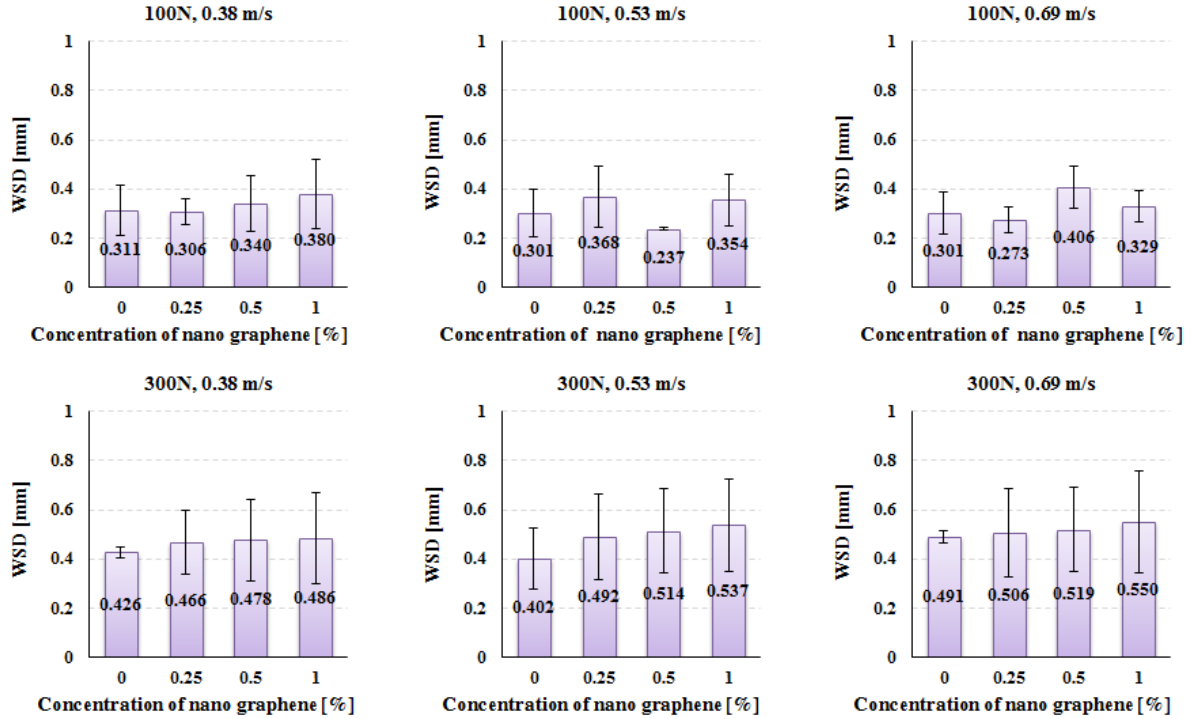

Fig. 4.21. Wear trace diameter for nano graphene lubricants

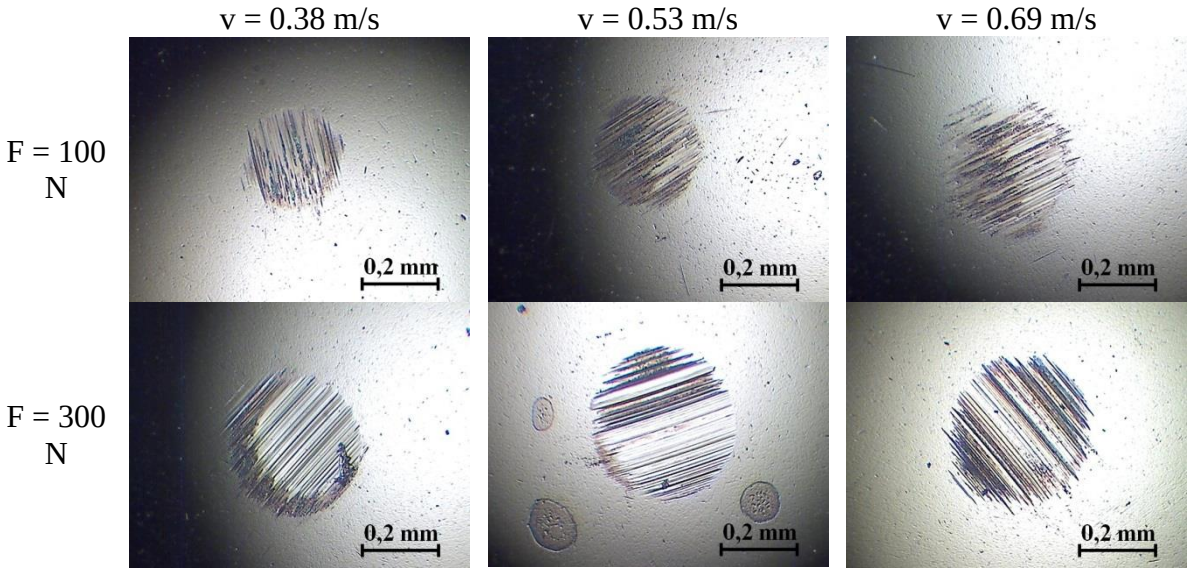

Fig. 4.22 Optical microscope photos of wear scar diameter, after testing with soybean oil + 0.5% nano graphene

It can be noted:

- high values for the mildest test regime (F = 100 N and v = 0.38 m/s). One could argue that contact oscillations do not keep the additive in contact,

- the lowest value for the most severe regime (F = 300 N, v = 0.69 m/s), explained by forming the EHD film and maintaining the nano additive in contact,

- the graphs in Fig. 4.21 show a trend of very small increase of WSD whit additive concentration, more visible at F = 300 N.

- the wear rate of WSD (Fig. 4.23) are similar for 0.25% and 1% meaning the additive concentration (0.25%...1%) does not influence to much the wear.

It seems that the wear is made in stages and is smaller for longer sliding distances.

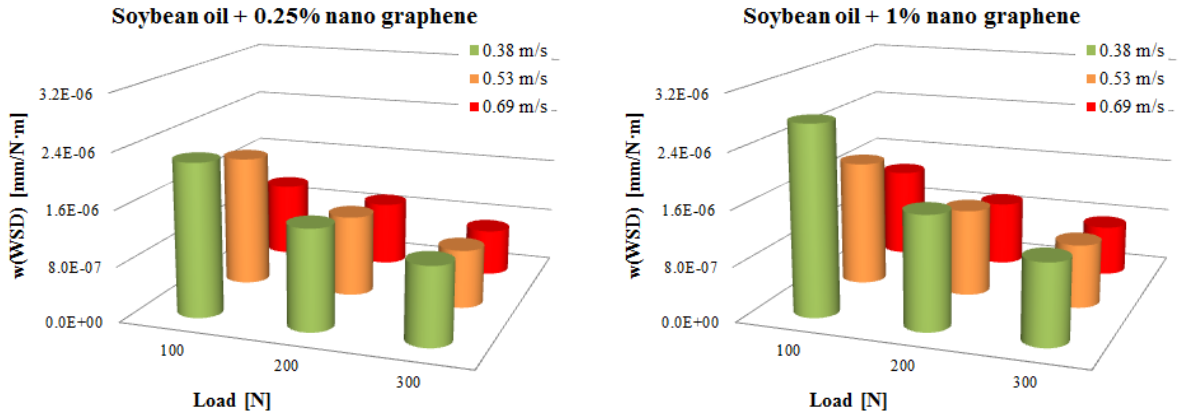

Fig. 4.23. WSD of lubricant additivated with nano graphene

4.7 Comparative analysis of experimental results

COF for nano carbon additivation of soybean oil

At speeds v = 0.38 m/s and v = 0.53 m/s, COF has no obvious trend.

At v = 0.69 m/s, it has a clear tendency to decrease in the range of additive concentration, for the maximum value of the nano carbon concentration and for high loads (200 ... 300 N).

COF for nano graphite additivation of soybean oil

For the most severe regime, the highest average was obtained. It would mean that graphite prevents the formation of a film or that it is in the form of large agglomerations and rubbing over them, increasing friction. The lowest COF values were obtained for unadulterated oil and the additivated lubricant with higher concentrations, but up to F = 200 N.

COF for the additivation with nano graphene of soybean oil

At v = 0.68 m/s, COF oscillates in a very small interval.

At load F = 100 N, regardless of speed, COF increases. It results that nanoparticles are not kept in contact because of too less pressure on them.

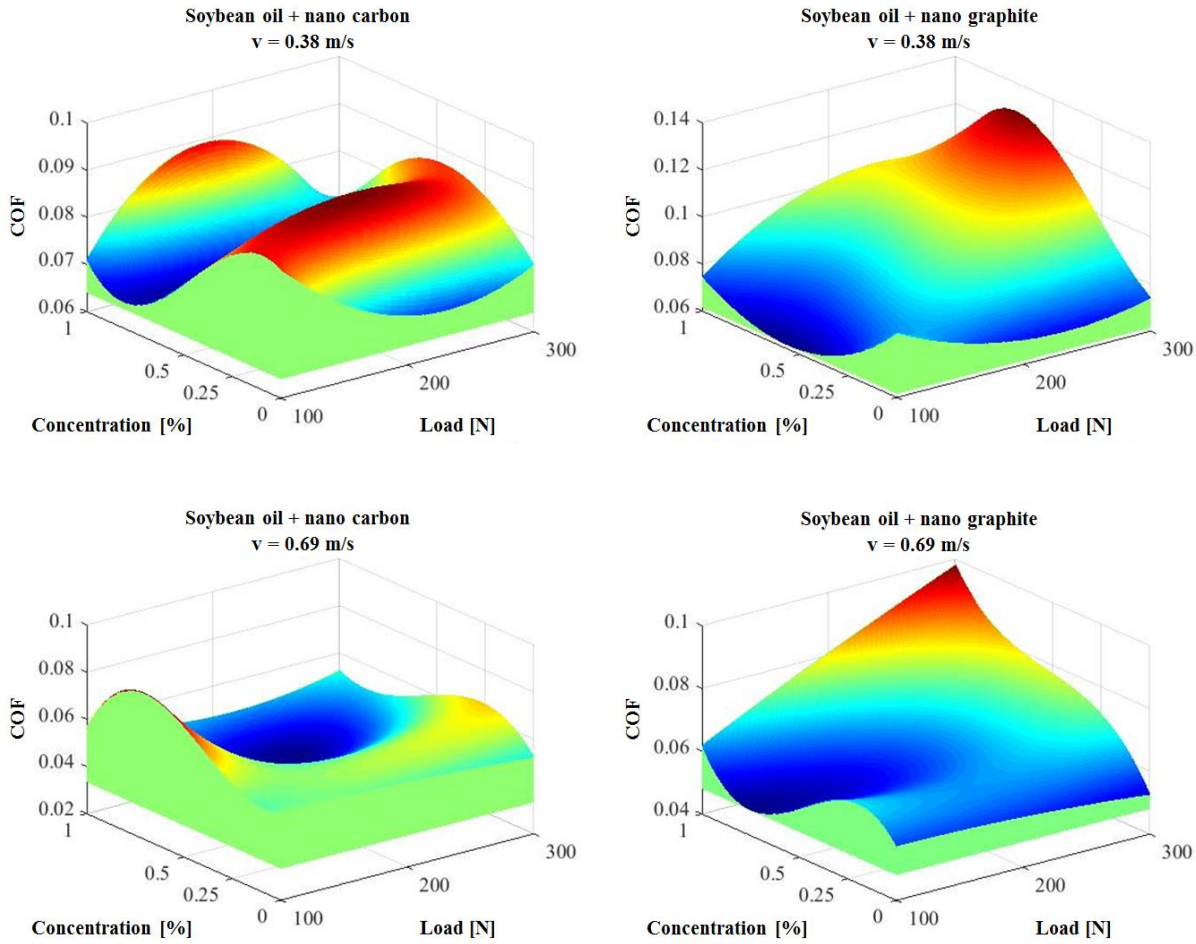

Fig. 4.24 COF maps for lubricants tested at extreme speed conditions

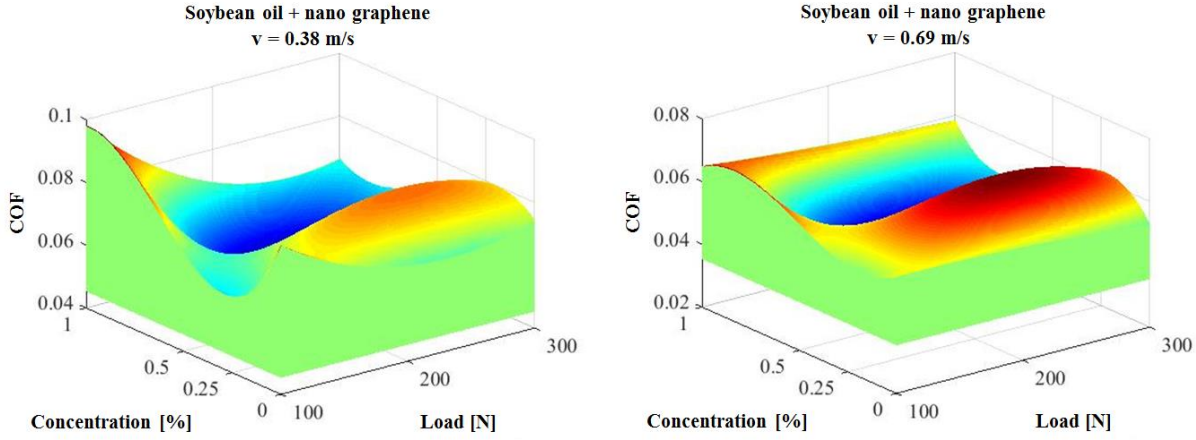

Fig. 4.25. COF maps for lubricants tested at extreme speed conditions

Wear parameters

The influence of the quality of the additive is manifested not only by the minimum value, but also by the domain of the map area for which the minimum values of w(WSD) are obtained. The greatest wear "depression" at this concentration was obtained for graphite and then for graphite.

For carbon, the low wear rate area is narrower. At v = 0.38 m/s and the lowest load, tested the lowest value of w(WSD) is obtained for graphite.

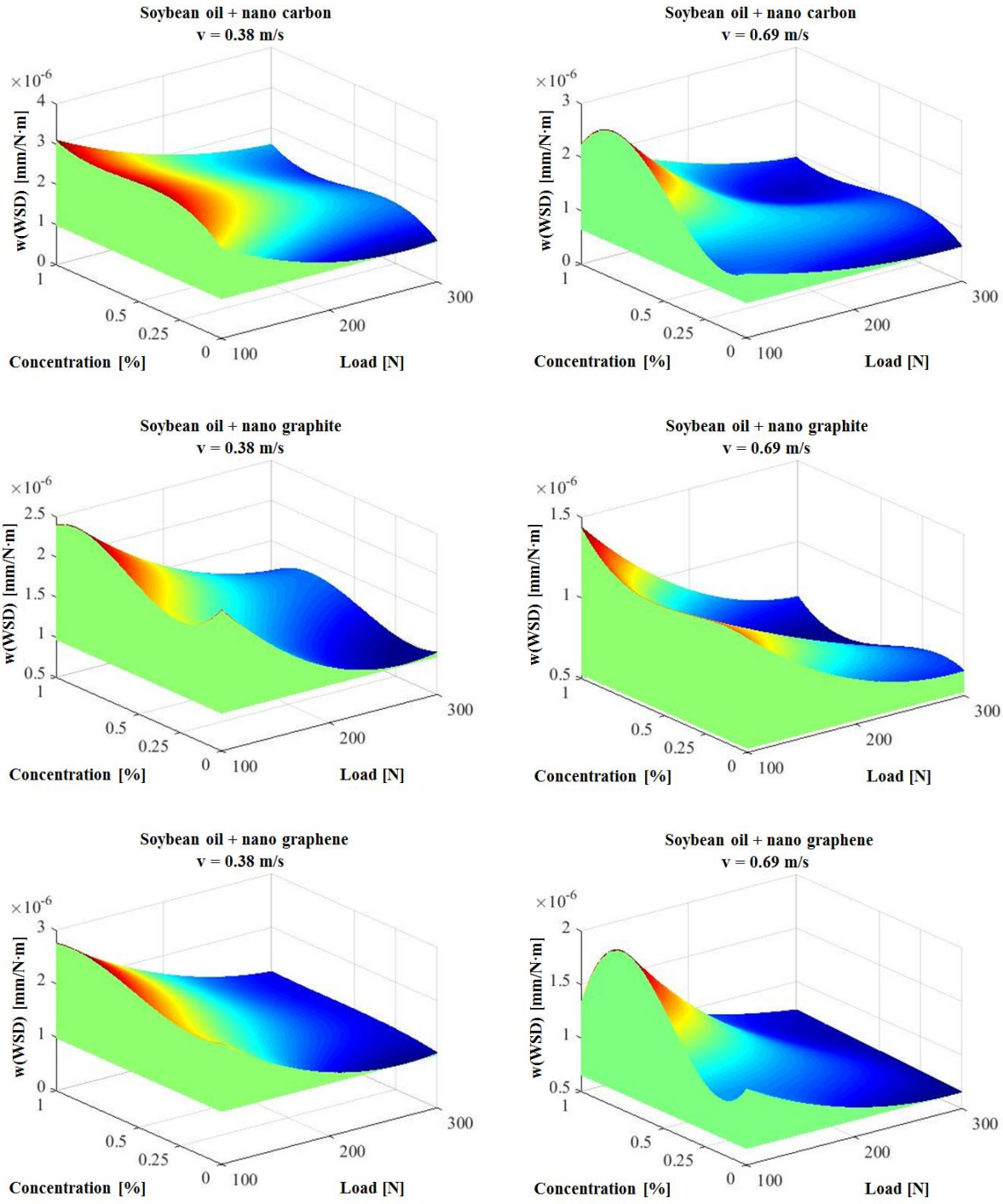

Fig. 4.26 w(WSD) maps for lubricants tested at extreme speed conditions

4.8. Conclusion

When comparing the results obtained by Abdullah [Abdullah, 2016], which tested according to ASTM, a diesel oil SAE15W-40 nano additioned with 0.5 vol% of 70 nm hBN, obtained by ultrasonography, it was observed that, for the test interval of 200 ... 500 N the WSD was lower for additivated oil, but this decrease is not clearly highlighted in the range of 200 to 400 N.

The tested nano additives increase w(WSD) with low values and uniform w(WSD) for different regimes (they lessen the influence of the test regime on this wear parameter), especially for graphene.

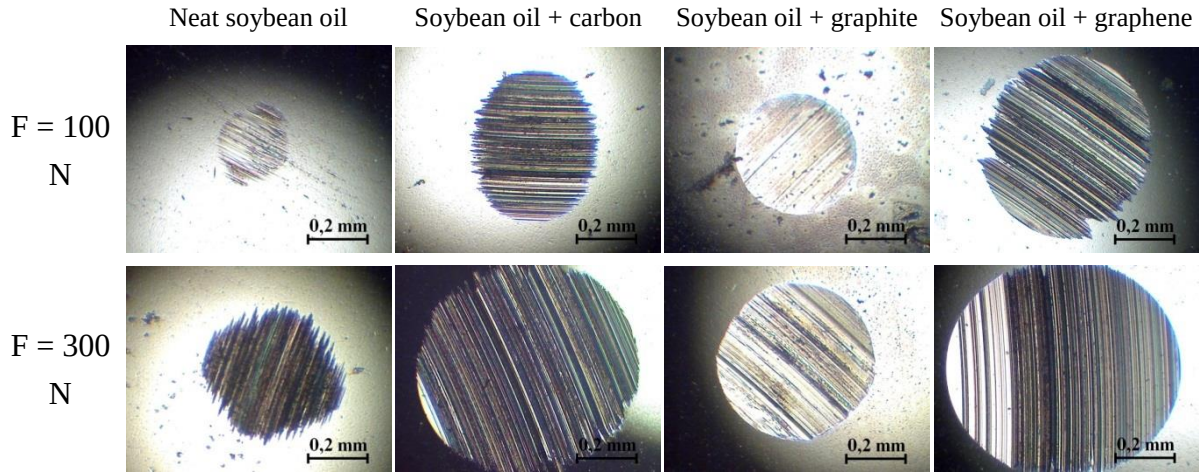

Fig. 4.27. Wear scar obtaind for lubricant soybean oil + 1% nano additive, v = 0.38 m/s

At v = 0.38 m/s, the COF value, as an average of the values obtained for two tests, can be considered in two areas: around 0.1 (mixed and/or boundary lubrication) and below 0.1, with EHD film). The smallest value was recorded for graphene in soybean oil, at the lightest load but for F = 200 ... 300 N the lowest values were obtained for non-additivated oil.

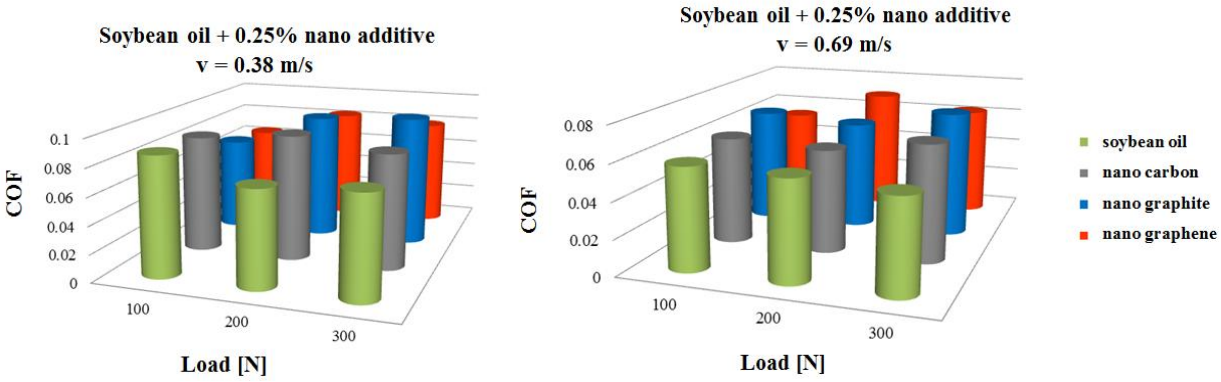

Fig. 4.28 The influence of additive in concentration of 0.25% on the friction coefficient

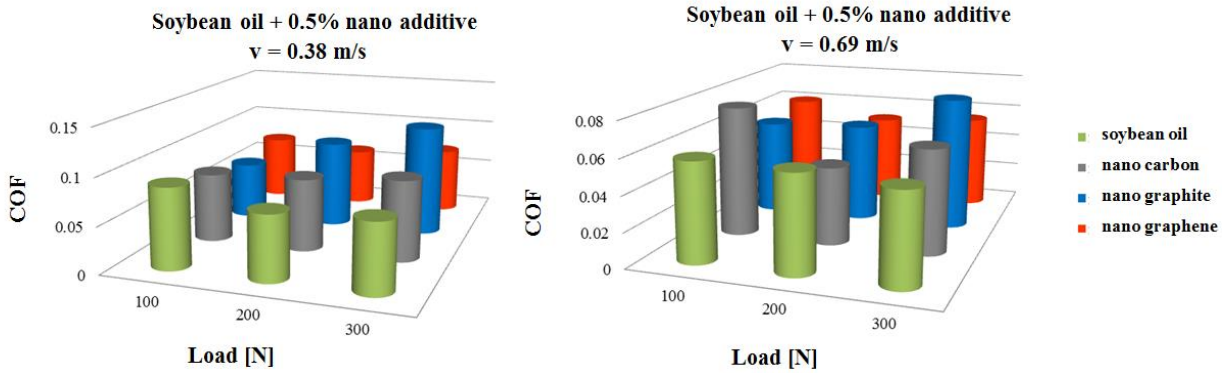

Fig. 4.29 The influence of additive in concentration of 0.5% on the friction coefficient

At v = 0.53 m/s the lowest values for COF were obtained for F = 100 N to 200 N and the additivated lubricants have lower friction as compared to the neat soybean oil. Nano lubricants with graphite have the highest value at F = 300 N.

At v = 0.69 m/s, COF values remain below 0.08. With the exception of graphite at F = 300 N, for the other additivated lubricants, the values are below the values obtained with the soybean oil. So at higher speeds, carbon-based additives begin to reduce friction.

At v = 0.38 m/s and 1% additive concentrations no clear COF decrease trend of COF is observed. At v = 0.53 m/s, for non-additivated oil, COF increases with the load, but remains characteristic of the full-film regime. At v = 0.69 m/s, the amorphous nano carbon had the most obvious tendency to decrease with the load. The same trend, but very poor, was obtained for graphene.

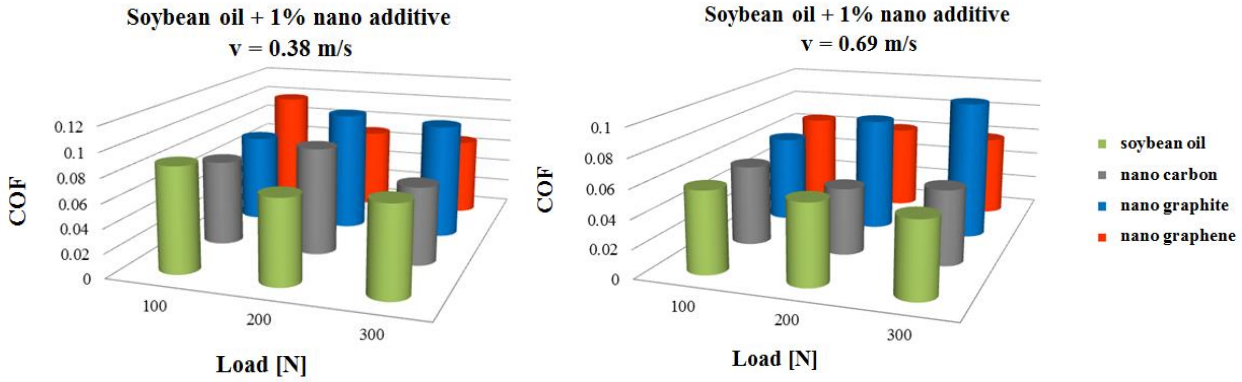

Fig. 4.30 Influence of additive in concentration of 1% on the friction coefficient

For the lubricant with nano graphite, the trend is to increase COF even to a mixed lubrication. This could be explained by the formation of micro agglomerations that cause large oscillations of COF and/or zonal, friction with the third body (the additive agglomerations).

Soybean oil without additives appears to be influenced by load growth. Considering COF analysis, but also the near values in the field of total film lubrication or to a boundary regime (COF = 0.1), the author considers the wear rate analysis to be relevant for the selection of one of the tested additives. For the best performance at wear, soybean oil is still in top.

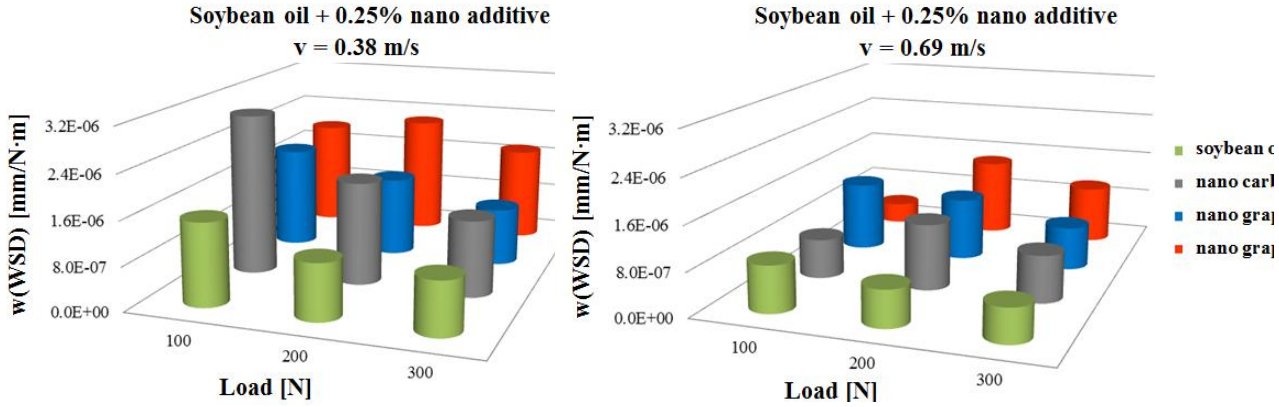

Fig. 4.31. Maps of the rate wear of WSD for lubricants additivated with 0.25% nano additive

At F = 300 N and v = 0.69 m/s (the most severely tested regime) the wear rate is comparable.

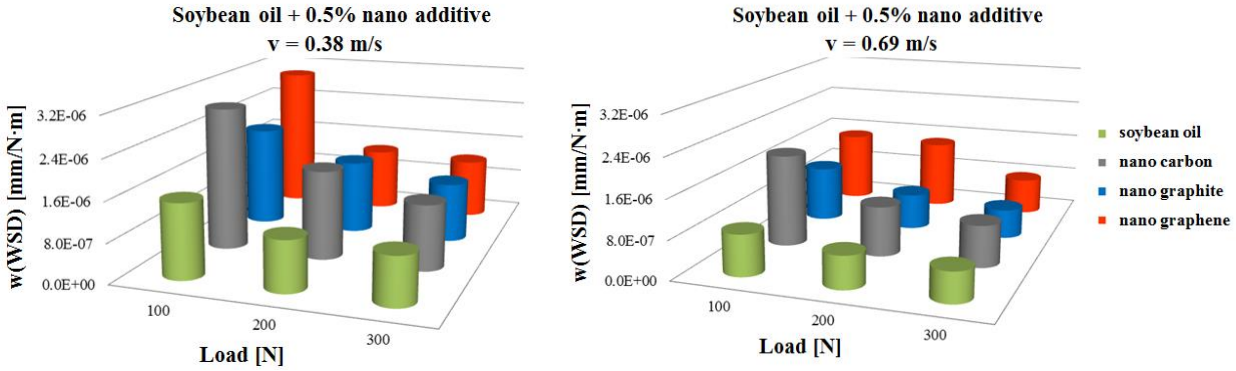

Fig. 4.32 Maps of the rate wear of WSD for lubricants additivated with 0.5% nano additive

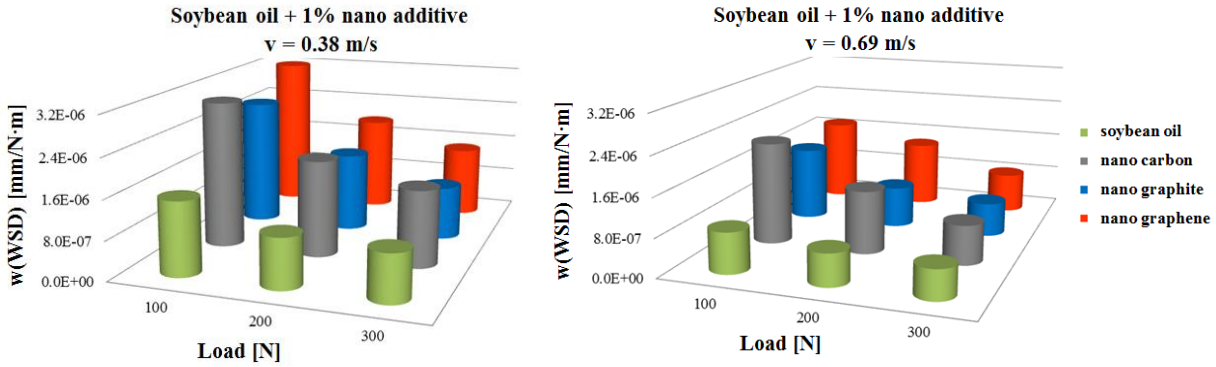

Fig. Maps of the rate wear of WSD for lubricants additivated with 1% nano additive

The downward trend of w(WSD) had a higher gradient for lubricants with1% nano additive, which would recommend further testing for more severe regimes, where additives are likely to better protect the surface of the contact.

Chapter 5
REOLOGICAL BEHAVIOR OF NANO ADDITIVATED SOYBEAN OIL

5.1. The purpose of the chapter

The rheology of vegetal oils and the factors that influence their viscosity are studied by specialists, the theoretical and experimental data being useful in solving design issues that require the use of these oils, either as lubricants, fuels or fluids, to comply with environmental and health regulations, but also as an alternative to exhausted oil products [Biresaw, 2013], [Brodnjak-Voncina, 2005], [Demirbas, 2009.], [Fernandez, 2013].

The purpose of this chapter is to study the rheological properties of non-additive soybean oil and lubricants formulated with carbon nanoparticles (amorphous carbon, graphite and graphene) in different concentrations. For these lubricants, the following rheological properties were determined:

- the rheological model of the oil, ie the law of variation of the tangential stresses depending on the speed gradient;

- the dependence of the rheological parameters on the temperature, for a certain value of the speed gradient.

5.2. Experimental test stand

The experimental test stand is a Brookfield CAP 2000+ viscometer, (Fig. 5.1). It is a rotational viscometer that measures the flow behavior and its viscosity of liquid and semi-solid materials, having the cone-shaped coupling geometry (Figure 5.2). The system is controlled by a specialized software, called CAPCALC 32, which has the ability to control the stand, to acquire and process data.

The calculation system has the ability to determine parameters of the rheological model of the analyzed lubricant for five rheological models: the Bingham model, the Casson model, the Herschel-Bulkley model, the power law model or the Ostwald de-Waele model:

$$\tau = m\dot{\gamma}^n \tag{5.1}$$

where m and k are material constants, k is called the consistency index [$m^{-1}.s^{n-2}$] and n – the flow index (non-dimensional) and the Newtonian model:

$$\tau = \eta\dot{\gamma} \tag{5.2}$$

Fig. 5.1. Brookfield Viscosimeter (Department of Machine Design and Tribology, Politehnica University of Bucharest)

Fig. 5.2 Working geometries

In viscous fluids, the deformation leads to increased internal friction forces, which dissipate some of their kinetic energy as heat. At low shear rates, in low-viscosity fluids, the phenomenon is minor, increasing the temperature of the fluid due to energy dissipation being negligible. High viscosity fluids can generate significant amounts of heat, which results in changes in fluid properties, including its viscosity.

The main cause of Fluid Deviation from the Newtonian behavior is the modification of the fluid structure under the action of shear stress.

The viscometer has the possibility to perform thermal determinations, namely the variation of the rheological parameters with the temperature, on the range of 5^0C to 75^0C.

5.3. Experimental methodology

In order to determine the rheological model for the analyzed lubricants, an "imposed gradient" type test was used, at a constant temperature, using a working geometry (cone 8) with the dimensions shown in Table 5.1.

Table 5.1. Geometry and cone viscosity measuring beach 8

Cone number	Cone radius, [mm]	Angle at the top of the cone, [^{0}]	Measured viscosity, [Pa·s]	Shear rate, [s^{-1}]
8	15.11	3	0.312 ... 3.12	200 … 2000

Tests were performed twice for the same fluid, characterized by the concentration and nature of the additive. In Fig. 5.3, two repeated tests for the same parameters are presented for a single lubricant (soybean oil with 1% graphene) to highlight the repeatability of the test methodology.

The proposed rheological model was the law of power (4), its parameters being determined by the regression analysis method.

To determine the variation of viscosity with temperature, similar tests of the "gradient speed " type were performed, but for a temperature range useful for the analyzed lubricants using the cone 8 as working geometry, at a shear rate of 1000 s^{-1}.

The experimental results on the temperature parameters were numerically processed with CurveExpert, starting from the Reynolds model, which is an exponential model:

$$\eta = \eta_0 e^{m\ (t-t_0)} \qquad (5.3)$$

where η– dynamic viscosity, η_0 – dynamic viscosity at the reference temperature of 20 °C (20,6...20,9 °C); m – temperature factor;t – temperature, in °C, t_0 – reference temperature (20,6...20,9) °C.

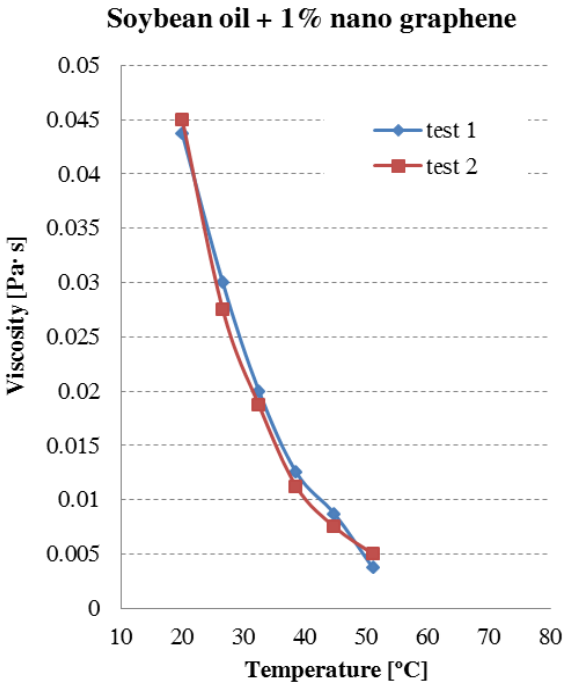

Fig. 5.3. Representation of the values obtained for two tests carried out with the same fluid and under the same measurement conditions

5.4. Results on viscosity dependence on shear rate

The property of the fluids to resist to irreversible change in position of the constituent volume elements, dissipating the mechanical energy as heat, is called viscosity.

For the analyzed lubricants, the following analyzes were performed:

–comparative graphs of neat soybean oil and additivated lubricants with black carbon and nano graphite, graphen in various concentrations;

–rheological parameters for the nano additive, in different concentrations;

–variation of viscosity with temperature, for the gradient of 2000 s^{-1} speed, comparatively purely additive;

–the parameters of the model for describing the viscosity dependence with temperature.

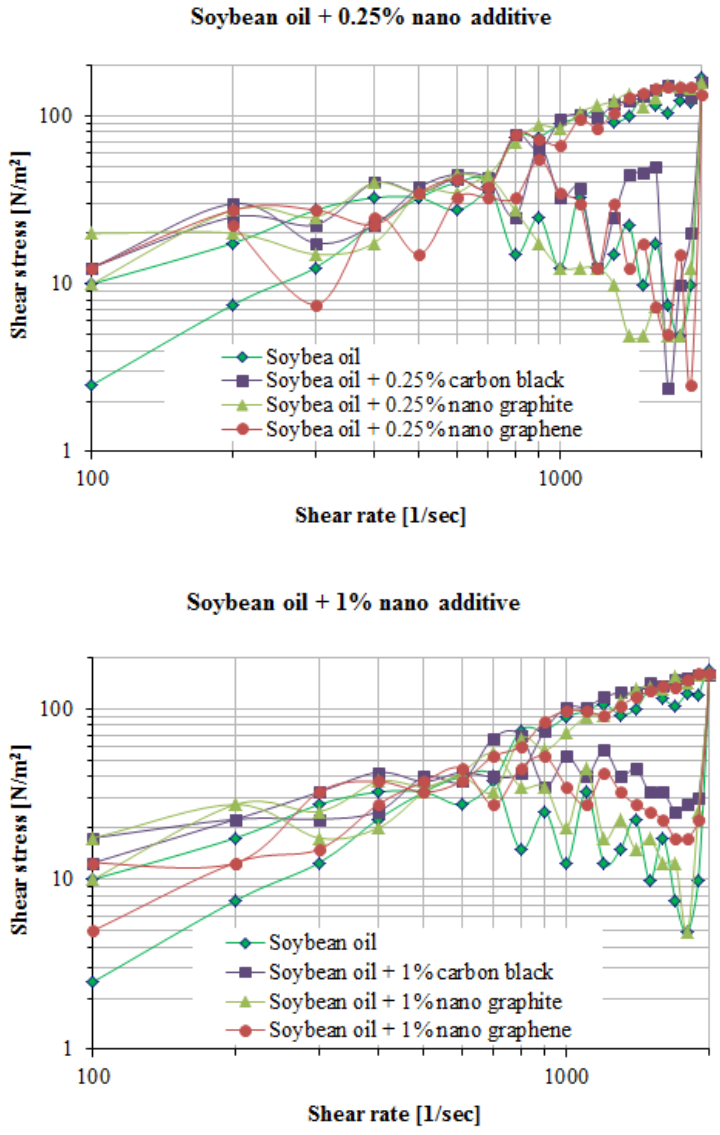

Fig. 5.4. Comparative reports for neat soybean oil and additivated soybean oil with different concentrations of nanoadditive.

1. From a rheological point of view, the soybean oil has an increased thixotropy in both neat and additivated state. It is interesting to note that, at low shear rates, below 600 s^{-1}, this thixotropy disappears.
2. The same phenomenon is noticed for the soybean oil, with the observation that thixotropy disappears at a shear rate of 700 s^{-1}.
3. For the soybean oil, the additivation with nano additives has a very limited influence on changing the thixotropic behavior, specific to non-additivated oil. So, lubricants formulated with nano additives also have a similar hysteresis to that exhibits by the neat soybean oil.

The variation of rheological parameters depending on the concentration and nature of the additive is shown in Fig. 5.5 for the consistency index and in Fig. 5.6 for the flow index.

Because of the pronounced hysteresis, the correlation coefficient is small.

Analyzing the graph in Fig. 5.5, it is observed that, with respect to the value for the soybean oil, it decreases with the concentration of nanocarbon and with the concentration of graphene, increases with the nanographite concentration, with the exception of the concentration of 0.25%. The slight increase in nanographite additivated lubricants can be attributed to the spatial graphite structure that prevents fluid flow. The other two additives, carbon and graphene, diminish this parameter, acting as friction modifiers between fluid molecules.

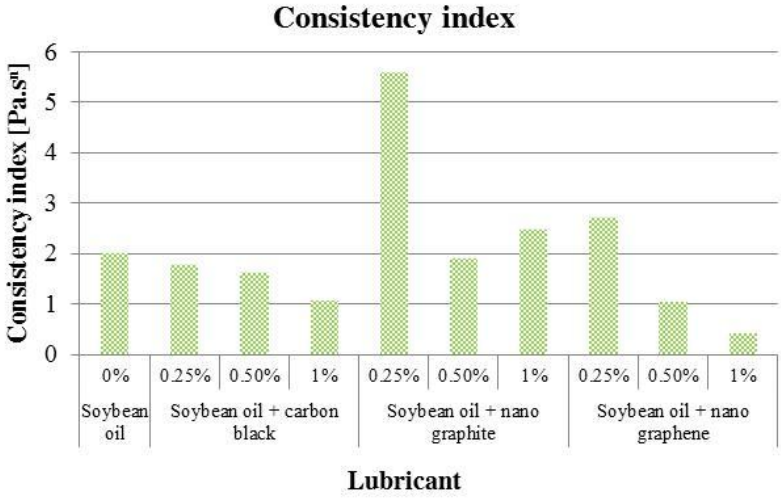

Fig. 5.5. Variation of the consistency index depending on the concentration of lubricant additive

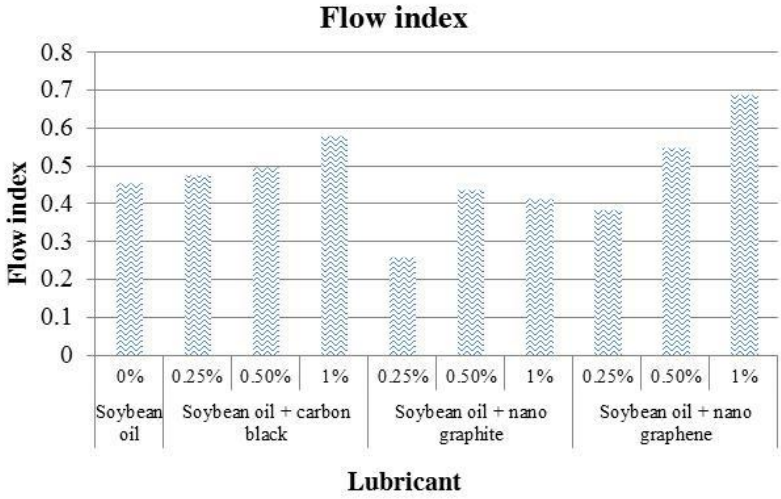

Fig. 5.6. Variation of the flow index depending on the concentration of lubricant addition

The author has divided the field of viscosity evolution depending on shear rate in two areas:

– an area with pronounced thixotropy (between 600 ... 700 s^{-1} and 2000 s^{-1}, for the tested oils),

– an area in which the fluid does not have an obvious dependence on the shear rate variation (100 s^{-1}...600...700 s^{-1}). The delimitation seems to depend more on the concentration of the additive and less on its nature (Fig. 5.7). The thixotropy is manifested at a lower shear rate (600 s-1) for lubricants with 1% nanoadditive.

Here are some conclusions.

- The rheological model that characterizes the behavior of the studied lubricants is the model of power law, but with a low correlation coefficient. This is due to the phenomenon of pronounced thixotropy for the neat soybean oil, but also for additivated lubricants.

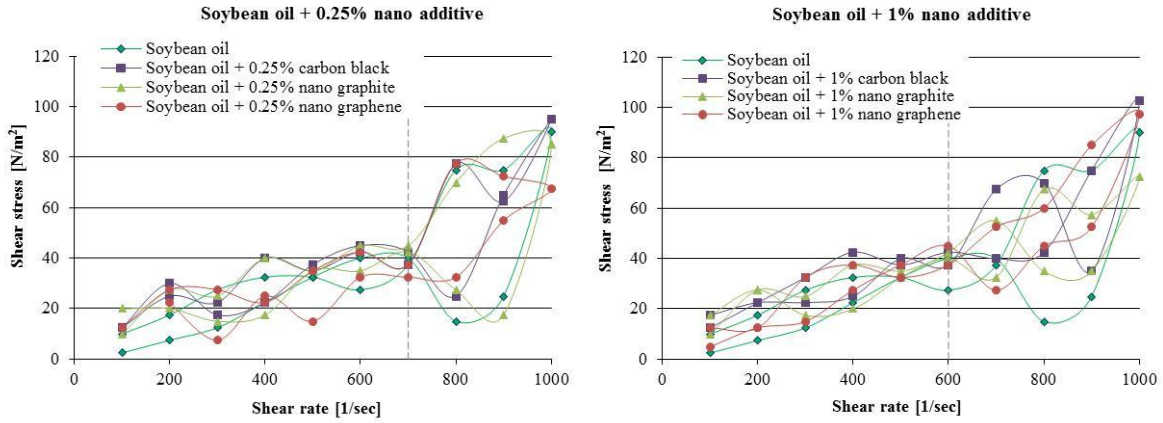

Fig. 5.7. Graphs for shear stress – shear rate, for the additive concentration of 0.25% and 1%.

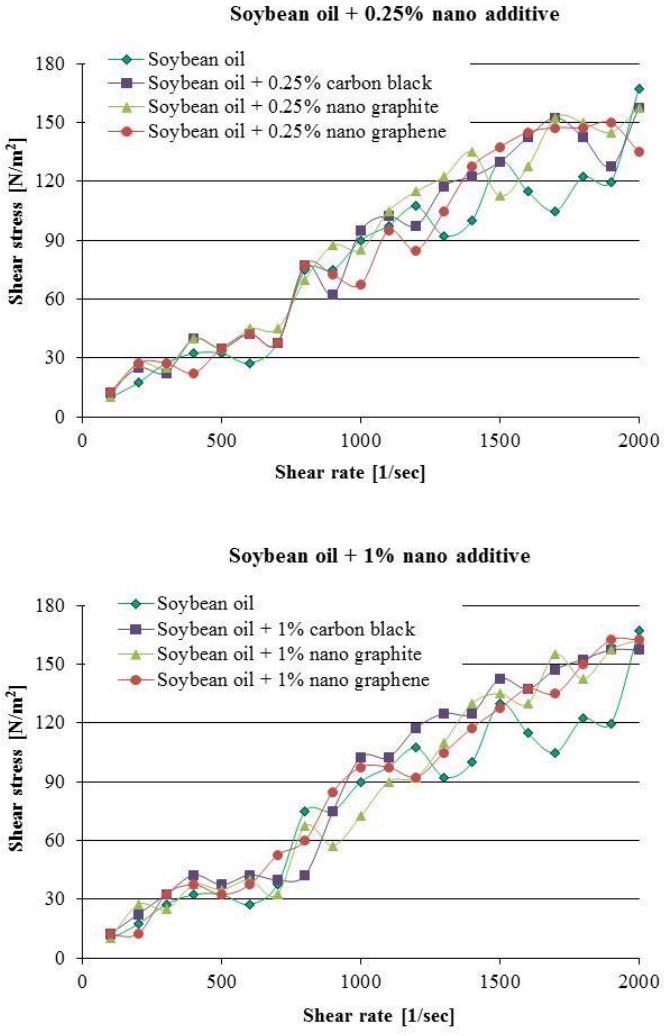

Fig. 5.8. Tension curve - Deformation velocity for increasing strain rate

- In the case of soybean oil, the increase in the nanoadditive concentration has the effect of lowering the consistency index and increasing the flow index with the decrease of the thixotropic degree.

Shear stress curve characteristics are:

– shear rate

– a large hysteresis,

– an interval of 100 ... 700 s^{-1} for which no hysteresis is observed,

– for the additives used in this study, the tendency is to increase the shear stress as compared to that of the beat soybean oil, for a shear rate of 100 s^{-1}, after which the obtained values fall into a smaller interval.

Increasing the shear rate has increased the shear stress, but the obtained curves by increasing the shear rate overlap or evolve in a narrow range, being almost insensitive to the addition of the nanoadditive and its concentration.

5.5 Dependence of dynaminc viscosity on temperature

To highlight that for the additive concentration range, as studied by the author, the concentration did not significantly influence the dependence of the dynamic viscosity on the temperature, curves were drawn for the same experimental conditions, but each graph was done for a particular additive (Fig. 5.9).

The addition of nano carbon maintains this dependence almost identical to that of neat soybean oil.

The addition of graphite reduces the dynamic viscosity of the formulated lubricants, but with the exception of results at 20 ° C, which are slightly broader (0.04 ... 0.047 Pa.s), the rest of the values are very close. The gradient of viscosity dependence on temperature is higher than that of the neat soybean oil.

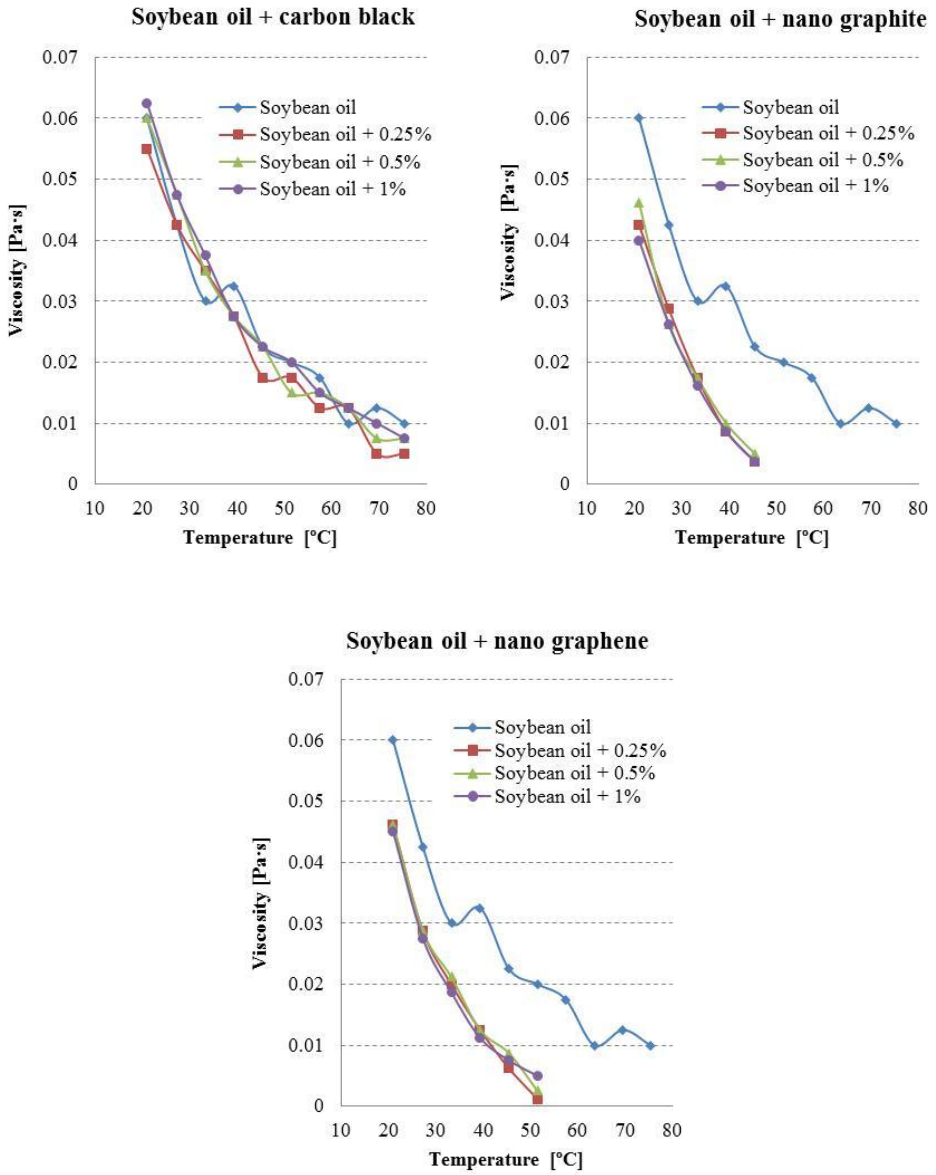

Fig. 5.9 The dependence of dynamic viscosity on the nature of the additive and on temperature

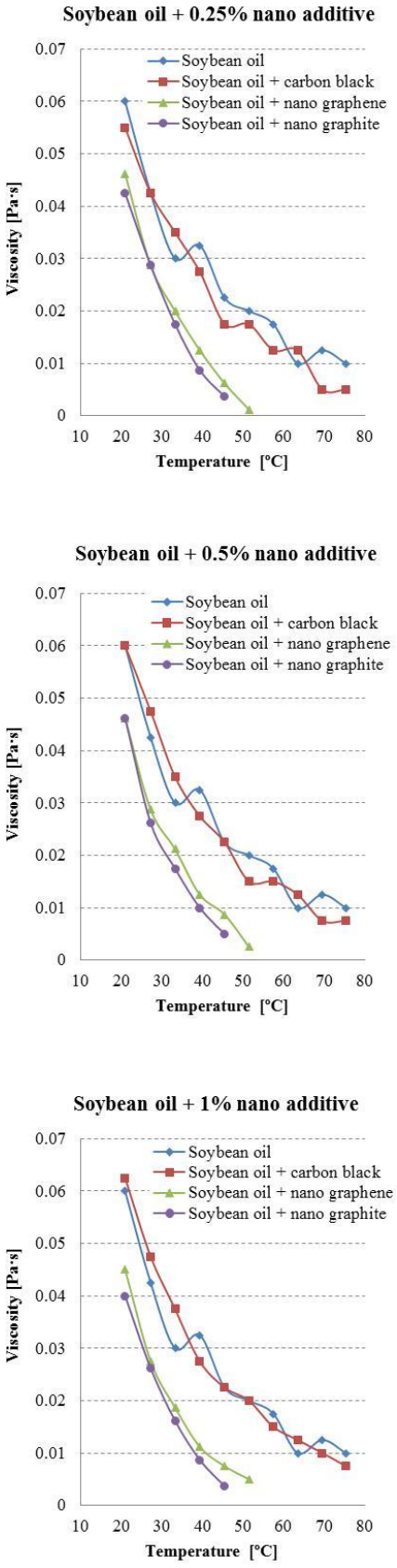

Fig. 5.10. Dependence of dynamic viscosity on temperature (at constant shear rate)

The dynamic viscosity decreases with the temperature rise. The values of the dynamic viscosity of the oils tend to become very close as the temperature increases [Şolea, 2013], [Wan Nik, 2005.], [Goodrum, 1982.], [Mustafa, 1999]. The increase in temperature tends to increase intermolecular motion and reduce the attraction forces among the oil molecules.

A similar study was conducted by Solea [Solea, 2013] but for lower shear rates (3.3...80 s^{-1}). The soybean oil had the lowest viscosity temperature curves of the tested oils (corn oil, rapeseed oil, corn oil).

Analyzing the graphs in Fig. 5.10 the following conclusions can be drawn concerning the influence of the nature of nanoadiatives on the dynamic viscosity temperature dependence.

The addition of nano carbon does not significantly alter the viscosity dependence on temperature, regardless of the concentration of the formulated lubricants, at least for the temperature range at which rheological tests have been performed and as compared to the neat soybean oil.

From the point of view of temperature viscosity dependence, the formulated lubricants can be grouped into two categories:

– soybean oil and soybean oil additivated with nano carbon

– additivated lubricants with nanographite and graphene.

For all nano additivated lubricants, the viscosity does not depend significantly on the concentration.

In graphene-added lubricants, the curves overlap with a greater slope than the neat soybean oil, with a slight scattering at 50 ° C.

5.6. Modeling the dependence of dynamic viscosity on temperature

For each formulated lubricant and for the neat soybean oil, the Reynolds viscosity variation constants were determined with temperature:

$$\eta = \eta_0 \cdot e^{a(t-t_0)} \tag{5.4}$$

where $\eta_0 \cdot$ is the dynamic viscosity at temperature $t_0 \cdot$ considered as the reference temperature. In this study, t_0 = 20^{0}C, a is the coefficient of dependence of the dynamic viscosity o temperature. Table 5.2 presents the synthesis of the results.

Table 5.2. Mathematical models for the dependence of dynamic temperature viscosity

Lubricant	$\eta = \eta_0 \cdot e^{a(t-t_0)}$	**Standard error**	**Correlation coefficient**	**Coefficient of Determination**
Non additivated soybean oil	$\eta_0 = 0.06$ Pa·s a = -0.04363...-0.03279	0.0035	0.975	0.951
1% carbon	$\eta_0 = 0.0625$ Pa·s a = -0.04363...-0.03279	0.0035	0.975	0.951
1% graphite	$\eta_0 = 0.04$ Pa·s a = -0.04014...-0.00085	0.0012	0.998	0.995
1% graphene	$\eta_0 = 0.0437$ Pa·s a = -0.07659...-0.00486	0.0016	0.993	0.987

* The variation range of a coefficient was calculated for 95% confidence.

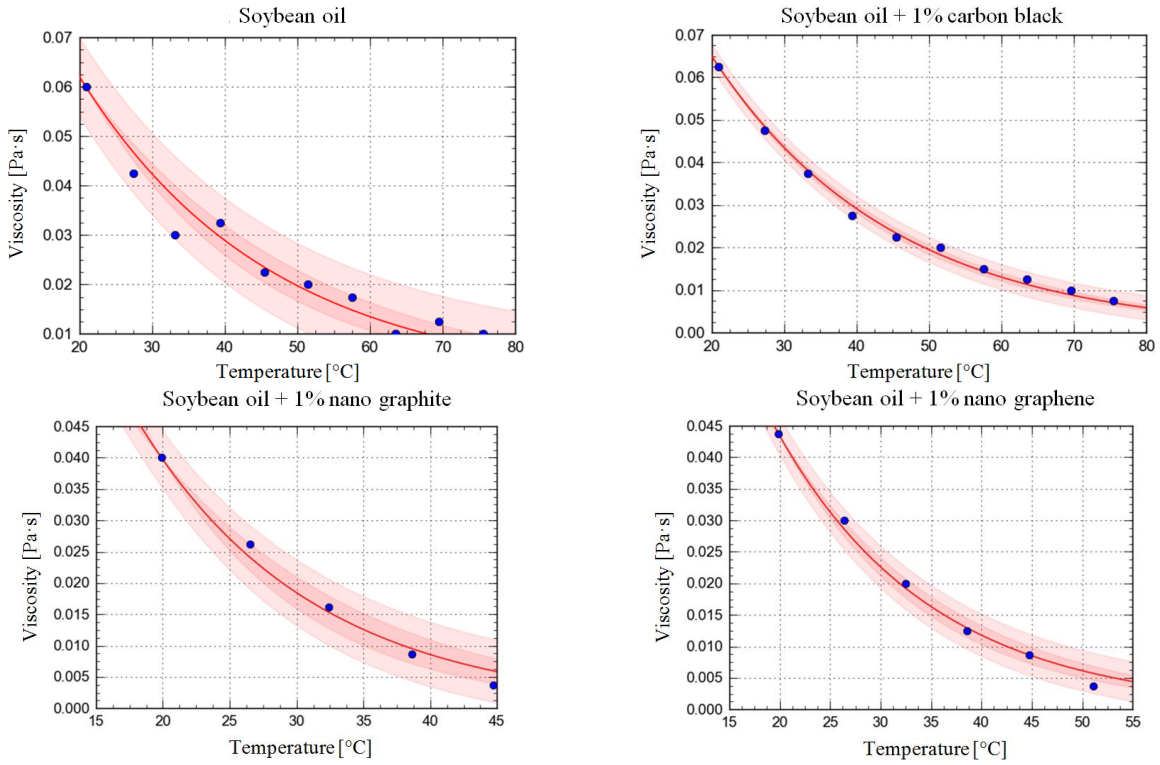

Fig. 5.11. Experimental data and the power law model for the neat soybean oil and 1% additive lubricants

A more complex mathematical function can be modeled to render experimental dependence in the form:

$$\eta = \eta_0 \cdot e^{a(t-t_0)} \cdot e^{b \cdot c} \tag{5.5}$$

where a is the coefficient of viscosity - temperature dependence and c - the concentration of the additive, in percent, c is a constant depending on the additive nature. Table 5.12 presents the determined relationships and the statistical parameters (standard error and correlation coefficient) and Fig. 5.12 graphically shows the surfaces of the determined functions and the experimentally determined values.

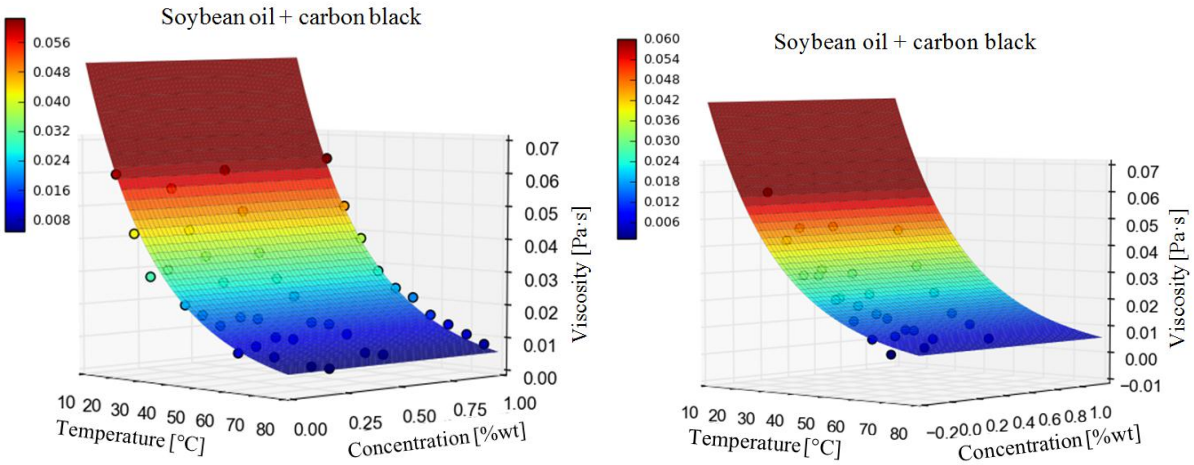

Fig. 5.12 3D representation of the mathematical models $\eta = \eta_0 \cdot e^{a(t-t_0)} \cdot e^{b \cdot c}$

Table 5.3. Mathematical models for dynamic viscosity temperature dependence and the additive concentration

Nanoadditive	$\eta = \eta_0 \cdot e^{a(t-t_0)} \cdot e^{b \cdot c}$	**Standard error**	**Correlation coefficient**
carbon	$\eta = \eta_0 \cdot e^{-0{,}040524(t-20{,}9)} \cdot e^{0{,}014402 \cdot c}$ $\eta_0 = 0.06$ Pa·s a = -0.042663...-0.038384 b = -0.039285...0.068089	0.0025 0.001057 0.0265	0.988
graphene	$\eta = \eta_0 \cdot e^{-0{,}040524(t-20{,}9)} \cdot e^{0{,}014402 \cdot c}$ $\eta_0 = 0.06$ Pa·s a = -0.042663...-0.038384 b = -0.039285...0.068089	0.0025 0.001057 0.02652	0.988
graphite	$\eta = \eta_0 \cdot e^{-0{,}0405(t-20{,}9)} \cdot e^{0{,}0144 \cdot c}$ $\eta_0 = 0.06$ Pa·s a = -0.042663...-0.038384 b = 0.014402...0.026520	0.0025 0.00105 0.02652	0.988

* The constants a and b were determined for a confidence interval of 95%. $\eta_0 = 0.06$ Pa·s for all models and it is the value of dynamic viscosity of the soybean oil at 20 °C.

The following conclusions may be written:

1. For soybean oil, both non-dditivated and additivated, it is found that the Reynolds model of viscosity variation with temperature approximates the experimental data satisfactorily, leading to correlation coefficients higher than 70%.

2. No clear variation of the thermal parameters (a and b)can be established depending on the additive concentration in the soybean oil.

5.7. Final conclusions on the results of rheology tests

The viscosity of the studied lubricants decreases with increasing the shear rate (Fig. 5.3 and 2.4).

All tested lubricants including the neat soybean oil have an increased thixotropy after a certain shear rate value, which does not depend on the nature of the nano additive, but on the additive's concentration.

The modeling of shear stress dependence – on shear rate following the law of power has a low correlation coefficient due to the hysteresis loop. If only the loading curve is considered, the dependence tends to be close to the linear one.

In terms of temperature viscosity dependence, the additives are separated in two groups

- nanocarbon that does not significantly affect this dependence, the nanographite,
- nanographene move down the curves of the dynamic viscosity dependence on temperature.

.

Chapter 6
The 2D and 3D parametric study of the texture of wear scars for soybean oil additivated with nano graphite

6.1. Introduction

From literature studies on the characterization of surface topography [Blunt, 2003], [Blunt, 2008], [Cotell, 2002], [Davim, 2004], [Dong, 1993], [Dong, 1994], [Leach, 2011], [McCormick, 2004], the following conclusions can be drawn:

– surface texture studies are statistical,

– there is no general methodology for characterizing the texture of the used (worn) surfaces, even for the new ones (not worn),

– the methodology depends on: the shape and size of triboelements, the available equipment and software, the set of parameters selected, the user experience and ingenuity.

For the analysis of the used surface quality, from the studied documentation ([Deleanu, 2009], [Pîrvu, 2017], [Demkin, 2010], [Fillon, 2007], [Georgescu, 2012], [Georgescu, 2016], [Stachowiak, 2004], [Stachowiak, 2001], [Stachowiak, 2004], [Stachowiak, 2005], the following directions of investigation are outlined.

– because there are few comparative studies for 2D and 3D analyzes in the literature, a comparison will be done between the values obtained for 2D and 3D parameters and a method of sampling the 2D records and the 3D investigation areas will be detailed,

– the study should correlate the evolution of the texture parameters with the exploitation parameters of the system (working regime, tribological parameters, acoustic emission etc.),

In this chapter, amplitude parameters and three functional parameters will be analyzed. In addition, characteristic shapes of the Abbott-Firestone curve will be discussed.

6.2. Amplitude parameters

Average arithmetic deviation of the profile, Ra, and of the surface, Sa [μm] [SPIP^{TM}, Version 6.7.2 (2017)]

Ra parameter is standardized [SR EN ISO 4287, 2003] and is the most commonly used. It was known in the form of AA (Arithmetic Average) in the United States, and CLA (Center Line Average) in the UK.

If a height z(x) of the profile, obtained by intersecting the measured surface with a reference plane, Ra is defined as the arithmetic mean of the absolute values of the ordinates z(x), measured from the mean line, within a basic length:

$$Ra = \frac{1}{M}\sum_{i=1}^{M}\left|z(x_i)\right| \tag{6.1}$$

where M is the number of points on the profile, by which it was meshed on the reference

length, and $z(x_i)$ is the height of the rated profile, at any position (x_i), i = 1...M.

For 3D records, the arithmetic mean of the absolute values of z (x, y) is defined within the limits of the measurement surface:

$$Sa = \frac{1}{M \cdot N} \sum_{j=1}^{N} \sum_{i=1}^{M} \left| z(x_i, y_j) \right| \tag{6.2}$$

where N is the number of profiles on the investigated surface, j=1...N, and M are the number of ecorde points on each line, i = 1...M.

The average square deviation of the profile/surface, Rq/Sq [μm], defined in ([SR EN ISO 4287, 2003], [SR EN ISO 25178-2, 2012]) as the quadratic mean of z(x) or z(x, y) ordinate values within the boundary of a base length or measuring surface and is a dispersion parameter of the height of the asperities]. For parameter 2D, the calculation relation is:

$$Rq = \sqrt{\frac{1}{M} \sum_{i=1}^{M} z^2(x_i)} \tag{6.3}$$

Blunt defines the mean square deviation of the surface as being [Blunt, 2002]:

$$Sq = \sqrt{\frac{1}{M \cdot N} \sum_{j=1}^{N} \sum_{i=1}^{M} z^2(x_i, y_j)} \tag{6.4}$$

where M is the number of points on a profile and N is the number of profiles on the investigated surface; z (x, y) is the set of gross state data obtained for the investigated surface.

The maximum profile/surface height, R/S, is the distance between the highest peak and the deepest valley in the investigated area [Blunt, 2003]. The maximum height of the profile or surface is denoted by Sz (according to ISO [SR EN ISO 2187, 2003]), St (according to ASME B46.1:2009) or Sy.

If working with unfiltered raw profiles relative to a reference line/surface:

$$Rt = (|Rp| + |Rv|) \tag{6.5}$$

$$St = (|Sp| + |Sv|) \tag{6.6}$$

The asymmetry factor of the evaluated profile/surface, or skewness, Rsk/Ssk, is a measure of the profile/surface deviation asymmetry from the mean/median plane. It is strongly influenced by isolated peaks or voids.

$$Rsk = \frac{1}{M \cdot Rq^3} \sum_{i=1}^{M} z^3(x_i) \tag{6.7}$$

$$Ssk = \frac{1}{M \cdot N \cdot Sq^3} \sum_{j=1}^{N} \sum_{i=1}^{M} z^3(x_i, y_j) \tag{6.8}$$

Physically, Ssk provides indications about the presence of sharp features on the profile or investigated microtopography.

The flattening factor of the assessed profile/surface (kurtosis), Rku/Sku, is a measure of the curvature of the flattening or "sharpness" of the surface heights distribution curve. These parameters provide information about the shape of the profile or the surface.

$$Rku = \frac{1}{M \cdot Rq^4} \sum_{i=1}^{M} z^4(x_i) \tag{6.9}$$

$$Sku = \frac{1}{M \cdot N \cdot Sq^4} \sum_{j=1}^{N} \sum_{i=1}^{M} z^4(x_i, y_j) \tag{6.10}$$

For a Gaussian surface with uniformly distributed peaks and valleys, the value of 2D and 3D parameters is 3. Physically, kurtosis indicates the peaks on a surface.

6.3. Functional parameters and Abbott-Firestone curve

According to [Blunt, 3002], [Blateyron, 2008], [Stout, 1994], [Botan, 2013], [Cotell, 2002], [SR EN ISO 25178-2, 2012], the functional parameters are defined by the load length curve (for 2D analysis) or the load area curve (for 3D analysis). In literature, the last one is also known as Abbott-Firestone curve and characterizes the bearing capacity of a surface.

These parameters are field parameters and must be taken into account that they are statistical ones.

The height of the peaks, Rpk/Spk, estimates the small peaks above the main plane of the surface. These peaks will be removed during the run-up period by deformation or removal as wear particles. In order to have as small as possible particles from the surface, a lower value for this parameter would be desirable. This parameter is used to evaluate the surface in the sense that small values mean unpeeled/unpeeling surfaces.

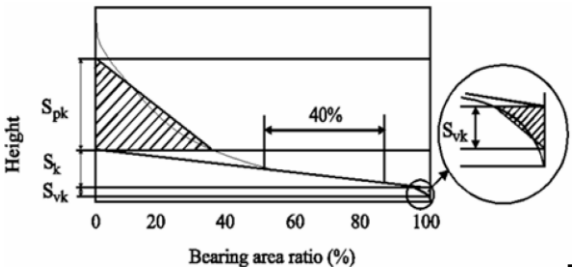

Fig. 6.1. 2D functional parameters

The relative height of the core of the surface, Rk/Sk, is the functional part of the surface. After the run-in period (after the peaks represented by Rpk/Spk are worn out), this part will take over the load during exploitation.

The reduced depth of the deepest valleys of the analyzed profile/area, Rvk/Svk, is an estimate of the valley depths that will retain the lubricant during exploatation.

Functional parameters

Regarding the functional parameters, Rpk, Rk and Rvk, respectively Spk, Sk and Svk, they were chosen for this analysis, considering that they could better reflect a correlation with the tribological parameters (coefficient of friction, wear and very probable acoustic emission), as shown in [Blunt, 3002], [Malburg, 2002], [Stout, 1994]. These parameters also have suggestive names: Rpk - "zone of asperity heights" or contact region (in this zone, in the wear process, the peaks of the asperities are deformed and/or detached in contact with the conjugate surface), Rk - the "core" of the texture, "the load bearing core" in service, Rvk - "the valley area" or "lubricant retention area".

6.4. Particular methodology for measuring surface texture parameters

For surface quality assessment, the NANOFOCUS μSCAN laser profile was used, from the "Ştefan cel Mare" University of Suceava. This is an optical non-contact profilometer for measurement of surface microtropography, with a measuring range of 150 mm x 200 mm, a vertical measurement range of 1.00 μm to 18 mm, a vertical resolution of 25 nm [NanoFocus AG μScan®]. SPIP program 6.7.2 [SPIP^{TM}, Version 6.7.2 (2017)] was used to process the results.

The 3D parameters were calculated for each wear scar on the three fixed balls and the average, maximum value and minimum value were calculated. The measurement step is the same for 3D and 2D: 5 μm. Line spacing for 3D measurements is also 5 μm. 2D parameters are the average of three measurements, that is, three profile lines, perpendicular to the sliding direction, on each ball. The linear profiles must be perpendicular to the sliding direction, so they are one of the axes of the selected ellipse.(the wear scar) 3D parameters are calculated for all z(x,y) values measured on the measuring area (wear scar).

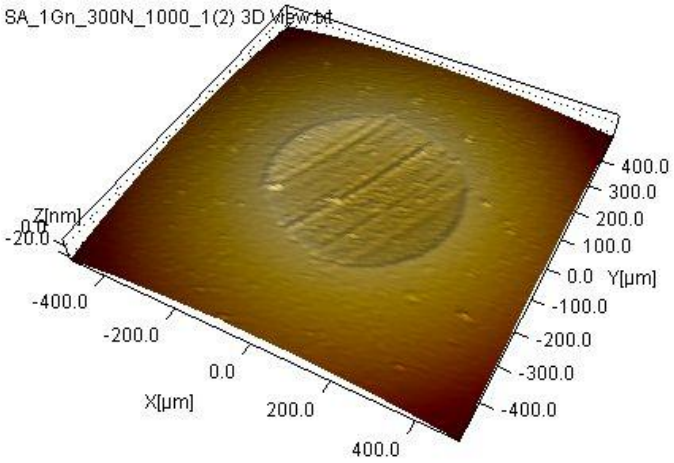

Fig. 6.2. Following wear, virtually reconstituted with SPIP on ball 3 of a test. Lubricant: soybean oil + 1% nano graphite
(Z scale is in microns, 200:1)
Test conditions: F = 300 N, v = 0.38 m/s

In this study, the following notations were introduced to evaluate the scattering of measured values for a texture parameter [Pîrvu, 2017], [Georgescu, 2012]. It will be exemplified by the roughness arithmetic parameter, Ra or Sa, depending on the measurement method (2D or 3D).

Each parameter on the measured area/line can be characterized by:

– the highest recorded value, Ra_{max} or Sa_{max};

– the minimum recorded value, Ra_{min} or Sa_{min};

– the average value of the parameter in several measurements, Ra_m or Sa_m:

$$Ra_m = \frac{1}{n}\sum_{i=1}^{n} Ra_i \tag{6.11}$$

$$Sa_m = \frac{1}{n}\sum_{i=1}^{n} Sa_i \tag{6.12}$$

where Ra_i is the value of the parameter Ra for the measurement (line) i, Sa_i is the value of the parameter Sa for the measurement i (on the investigated area), n being the number of measurements (in this study n = 3 for values 2D and n = 3 for those 3D);

- higher deviation above the calculated average for n measurements:

$$As = Ra_{max} - Ra_m \tag{6.13}$$

- lower deviation from the average calculated for n measurements:

$$Ai = Ra_{min} - Ra_m \tag{6.14}$$

- higher deviation above the calculated average, in percentage, for n measurements:

$$As(\%) = \frac{As}{Ra_m} \cdot 100 \quad [\%] \tag{6.15}$$

- lower deviation from the average calculated for n measurements:

$$Ai(\%) = \frac{Ai}{Ra_m} \cdot 100 \quad [\%] \tag{6.16}$$

The following case studies have been detailed in this chapter:

- a comparative study of the values obtained for the roughness parameters, 3D for the entire elliptical wear scar and 2D, for the longest line on the wear scar, perpendicular to the sliding direction,

- the study of the influence of graphite concentration and of test parameters (speed and force) on the 3D parameters of the wear scar surface, on the balls.

6.5. Comparative study of 2D and 3D parameters for worn surfaces of balls

Figure 6.3 shows a reconstructed (virtual) image obtained with the SPIP 6.7.2 program of the investigated area using the non-contact profilemeter, and Fig. 5.3 shows 3D amplitude and functional parameters for the non-worn (initial) surface of the ball.

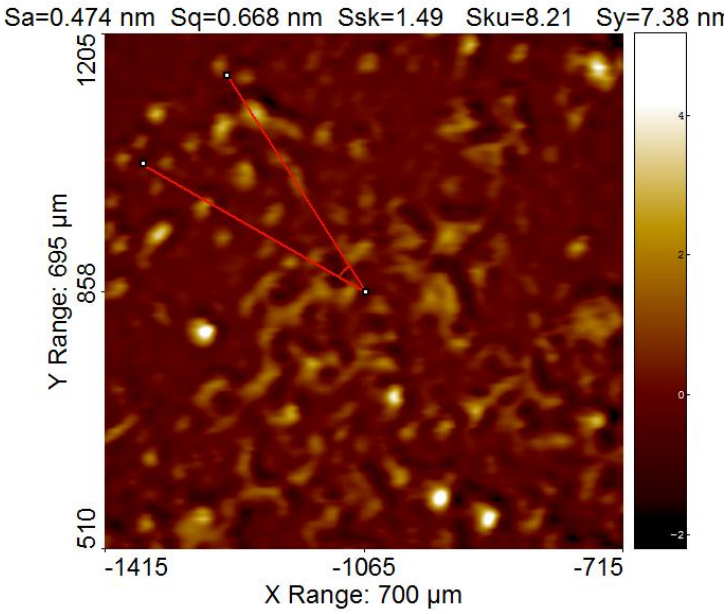

Fig. 6.3. Virtual image of the original surface of the ball

Table 6.1. Characteristic values for the surface of the balls

Sa [μm]	0.47396
Sq [μm]	0.66767
Ssk	1.4869
Sku	8.2139
St [μm]	7.3786
Sv [μm]	2.2138
Sp [μm]	5.1648
Spk [μm]	1.3671
Sk [μm]	1.0216
Svk [μm]	0.5582

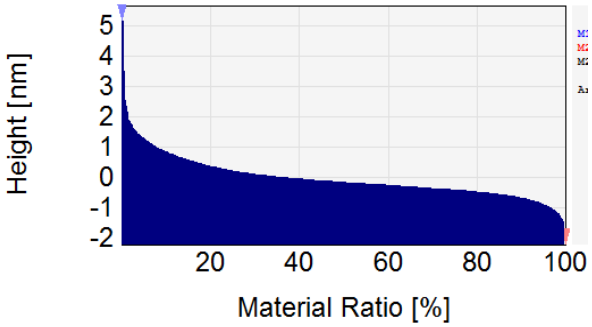

Fig. 6.4. The Abbott-Firestone curve for the unbroken surface of the ball

Taking into account the information in Figures 6.3 and 6.4 and Table 6.1, the characterization of the surface texture of the balls can be as follows:

- very high asperities (St = 7 μm)
- fine finished surface (Sa = 0.47 μm),
- plateau with bumps resulting from the technological peculiarities of obtaining the surface of the balls (Ssk = 1.48, Sku = 8.21),
- the Abbott-Firestone curve characteristic of fine-grained surfaces with low volume for retaining the lubricant (Svk = 0.55 μm), with high volume of material in the core of the profile, responsible for contact resistance and low values for Spk (Spk = 1.36 μm).

Analyzing the graphs in Fig. 6.5 and Table 6.2, the following observations can be done:

- generally, the average value of the same parameter is greater for 3D evaluation compared to the value obtained in 2D analysis, and the scatter range is lower for 3D than for 2D,
- for the parameters Ra, Sa, Rq, Sq, Rp, Sp and even Rsk, Ssk, there were obtained close average values, which means that these parameters are less sensitive to the measurement method,
- for the other analyzed amplitude parameters, the average 2D values are smaller than the 3D average values for the same parameter,
- the biggest difference was found between the mean values for Rt and St and, respectively, Rv and Sv. The values for Rp and Sp were close as average and spreading interval size, probably due to the uniform dispersion of the nano additive material.

Figures 6.5 shows comparisons of 2D and 3D parameters. The parameter set (F, v) was chosen only to give an example of the differences between the two types of wear measurements, after a test with soybean oil + 1% graphite. The rest of the graphs are given in the thesis).

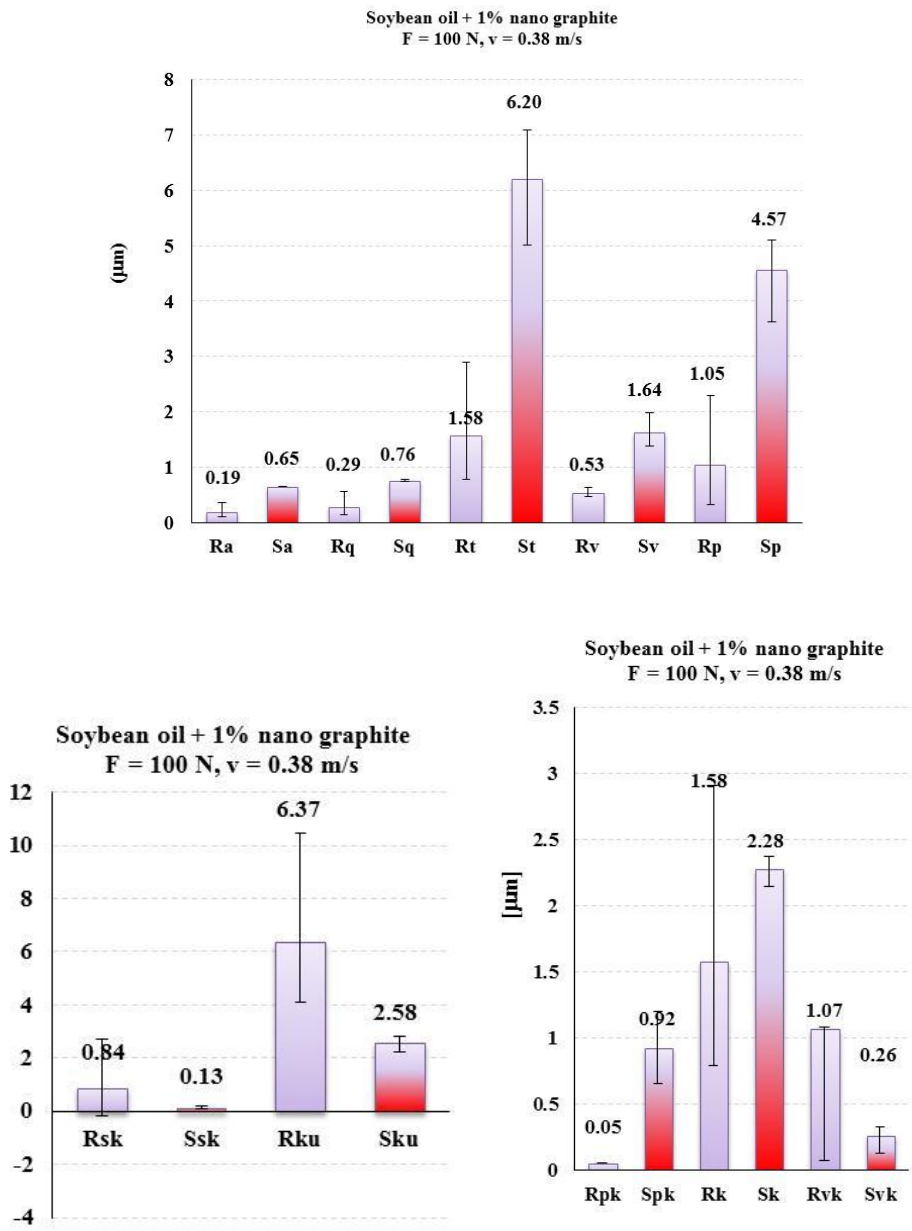

Fig. 6.5. Comparison of 3D and 2D parameter values as average and spread intervals

It can be seen from average values of the amplitude parameters that the ratio between 3D and 2D is between 2.5...3.5. This difference can be explained in this way. The 2D profile, although equal in length to one of the axes of the contact ellipse, perpendicular to the sliding direction, is not likely to contain extreme values of asperities. According to the EHD theory [Dowson, 1977], the maximum pressure in a point-to-point contact is at the entrance of the lubricant in contact. On many photos taken at the optical microscope, it can be noticed that the rougher texture is not on the axis of wear scars perpendicular to the direction of sliding, but between this line and the entrance in contact. The wear out of Fig. 6.6 is given to highlight this aspect. Another reason is that the 2D profiles are filtered with a reference length of 0.25 µm and the 3D profiles are analyzed on the raw profile only with a leveling of

the worn surface.

As in tribology extreme values of asperities are important in both dry and lubricated contact, it results that 3D measurements better reflect the surface quality and how the surface will behave during work.

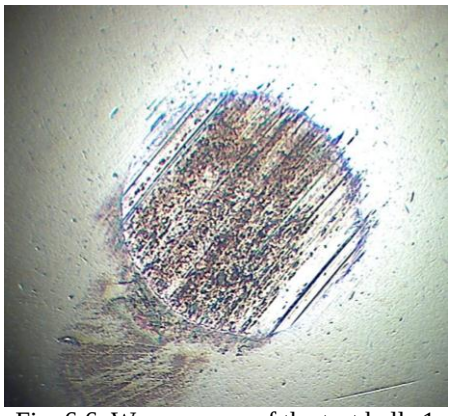

Fig. 6.6. Wear on one of the test balls 1 with soybean oil+1% graphite, F = 300 N and v = 0.69 m/s

Amplitude parameters

Figure 6.7 shows a comparison between the average values and the scattering intervals obtained for the 2D and 3D parameters, Ra and Sa, for the worn surfaces of the balls. All these graphs reflect the influence of the sliding velocity on the amplitude parameters of the surface texture. Considering the large number of data analyzed (Three 2D profiles, one on each wear scar and three wear scars on the 3 balls of a test set, for 3D parameters), it is considered that trends can be analyzed in the sense of comparing values and highlighting the benefits of 3D parameterization.

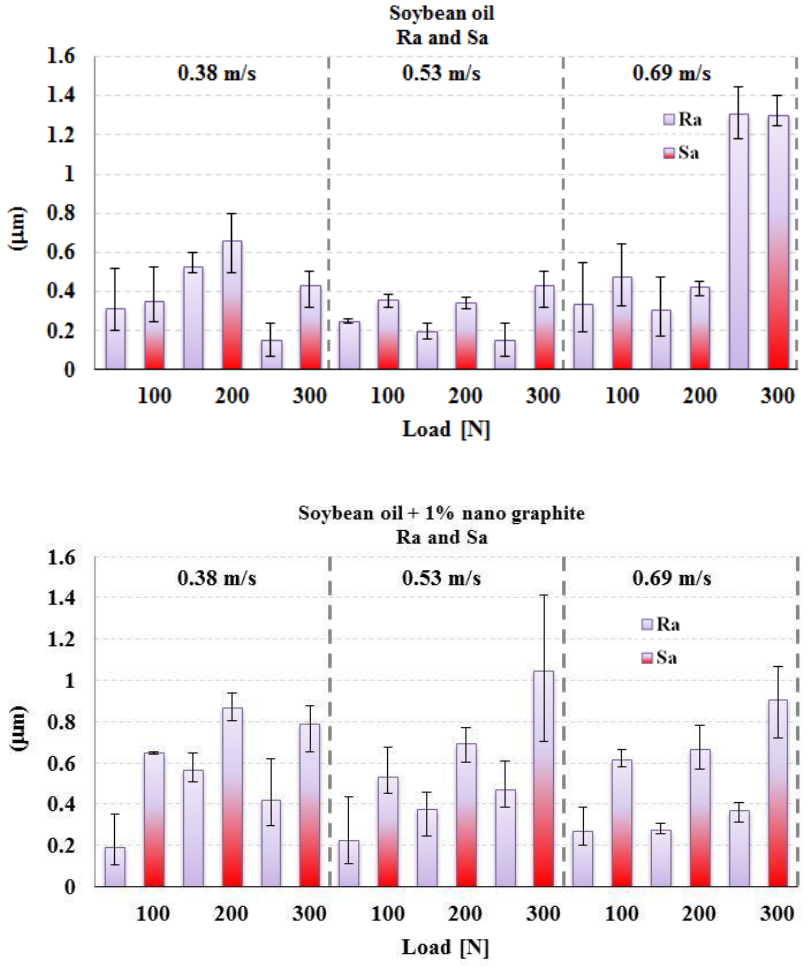

Fig. 6.7 Average values and scatter intervals obtained for 2D and 3D parameters

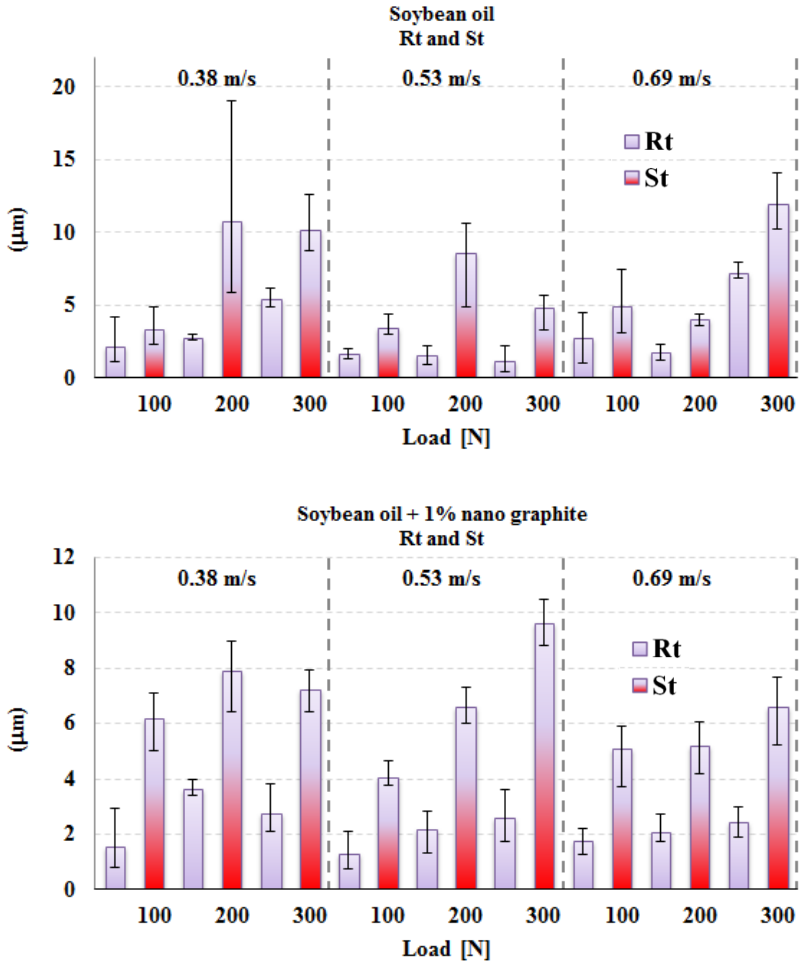

Fig. 6.8 Average values and scatter intervals obtained for 2D and 3D parameters

Qualitatively, the evolution trends of 2D and 3D parameters based on sliding speed are similar, but the values differ a lot.

Generally, the average 3D parameter is higher, but the scatter range is lower.

Figure 6.5 shows the following:

- as the sliding speed increases, the quality of the used surface improves;

- from the point of view of the allocated calculation time, given the dedicated program, for the investigator, it takes longer to select lines and calculate the average;

- large differences occur for Rku-Sku, Rz-Sz, Rv-Sv, Rp-Sp; the values obtained for 3D parameters are higher (almost all of them are at least twice as large);

- spreading intervals are smaller for 3D parameters.

This study examines the parameters of amplitude (Ra, Rq, Rt, Rsk, Rku and the "homologues" 3D (Sa, Sq, St, Ssk, Sku) and the functional ones (Rpk, Rk, Rvk, Spk, Sk, Svk). Why Ra (or Sa) parameter is not sufficient for surface quality assessment? Because in practice there may be surfaces with the same values of Ra (or Sa) (Fig. 6.7), but with very different characteristics, which will significantly affect their dry or lubricated behavior.

Ra or Sa does not provide information about the spatial structure and does not differentiate the valleys and the topography of the texture. Malburg [Malburg, 2008] also appreciated the surface quality with the ratio

$$\mathrm{Rt}/\mathrm{Ra} = \frac{\mathrm{Rt}}{\mathrm{Ra}} \tag{6.17}$$

for honed surfaces. This report should also be considered in this study of worn surfaces. A small value can indicate good surface quality and a continued operation of the system in good condition. A high value can characterize a surface with peaks and/or valleys (rare or not), but very high, which implies an aggressive wear process, at least in the area of the existence of the singular maximum. In this study, the author analyzed the Rt/Ra ratios and St/Sa ones, calculated with the average values obtained according to the methodology described above.

Tables 6.2 shows the average value and lower and upper deviation values, respectively, for each analyzed 3D and 2D parameter, for soybean oil + 1% graphite. This lubricant has been chosen for studying these wear scars because the tribological behavior of this lubricant was better as compared to other formulated lubricants in this research (see Chapter 4).

Table 6.2. Average values and spread intervals for 2D/3D amplitude parameters, for balls tested with soybean oil + 1% graphite

Para-meter	v = 0.38 m/s							Para-meter
	F = 100 N	F = 200 N	F = 300 N		F = 100 N	F = 200 N	F = 300 N	
Ra	$0.19^{+82.2\%}_{-45.6\%}$	$0.56^{+14.6\%}_{-10.2\%}$	$0.42^{+47.1\%}_{-29.8\%}$	**[µm]**	$0.65^{+0.9\%}_{-1.4\%}$	$0.87^{+7.5\%}_{-7.7\%}$	$0.79^{+11.1\%}_{-17.4\%}$	**Sa**
Rq	$0.28^{+94.5\%}_{-53.2\%}$	$0.72^{+9.8\%}_{-6.0\%}$	$0.53^{+48.0\%}_{-30.6\%}$	**[µm]**	$0.75^{+1.8\%}_{-2.4\%}$	$1.08^{+9.3\%}_{-9.3\%}$	$0.96^{+9.9\%}_{-13.7\%}$	**Sq**
Rp	$4.56^{+11.4\%}_{-20.8\%}$	$2.28^{+14.7\%}_{-13.6\%}$	$1.47^{+33.0\%}_{-24.6\%}$	**[µm]**	$4.56^{+11.4\%}_{-20.8\%}$	$4.97^{+24.6\%}_{-29.9\%}$	$4.70^{+12.5\%}_{-15.3\%}$	**Sp**
Rv	$1.38^{+21.6\%}_{-15.3\%}$	$1.34^{+7.3\%}_{-8.2\%}$	$1.27^{+44.4\%}_{-22.7\%}$	**[µm]**	$1.38^{+21.6\%}_{-15.3\%}$	$2.92^{+4.8\%}_{-5.7\%}$	$2.55^{+4.2\%}_{-4.1\%}$	**Sv**
Rt	$1.58^{+84.6\%}_{-50.5\%}$	$1.58^{+84.6\%}_{-50.5\%}$	$2.75^{+38.3\%}_{-23.3\%}$	**[µm]**	$6.20^{+14.4\%}_{-19.4\%}$	$7.90^{+13.4\%}_{-18.4\%}$	$7.26^{+9.6\%}_{-11.4\%}$	**St**
Rsk	$0.84^{+224.6\%}_{-123.1\%}$	$0.84^{+40.1\%}_{-52.1\%}$	$0.23^{+77.6\%}_{-74.9\%}$	-	$0.13^{+61.6\%}_{-34.2\%}$	$0.41^{+48.3\%}_{-58.1\%}$	$0.23^{+45.4\%}_{-38.5\%}$	**Ssk**
Rku	$6.37^{+64.3\%}_{-35.7\%}$	$3.81^{+34.1\%}_{-33.1\%}$	$3.28^{+9.0\%}_{-10.9\%}$	-	$2.58^{+8.6\%}_{-13.8\%}$	$3.26^{+14.0\%}_{-16.9\%}$	$2.90^{+28.0\%}_{-16.6\%}$	**Sku**
Rpk	$0.05^{+100\%}_{-200\%}$	$0.39^{+45.2\%}_{-72.7\%}$	$0.71^{+69.9\%}_{-51.1\%}$	**[µm]**	$0.92^{+30.6\%}_{-30.0\%}$	$1.47^{+24.6\%}_{-23.5\%}$	$1.04^{+8.1\%}_{-8.8\%}$	**Spk**
Rk	$1.58^{+84.6\%}_{-50.5\%}$	$3.62^{+9.6\%}_{-5.8\%}$	$1.29^{+46.6\%}_{-28.0\%}$	**[µm]**	$2.28^{+4.3\%}_{-6.1\%}$	$2.95^{+6.3\%}_{-4.8\%}$	$2.74^{+13.2\%}_{-24.2\%}$	**Sk**
Rvk	$1.07^{+188.8\%}_{-100\%}$	$0.01^{+88.8\%}_{-22\%}$	$0.43^{+64.9\%}_{-35\%}$	**[µm]**	$0.26^{+27.6\%}_{-49.6\%}$	$0.59^{+7.2\%}_{-3.8\%}$	$0.55^{+20.5\%}_{-26.5\%}$	**Svk**
Rt/Ra	**8.15**	**2.82**	**6.54**	**-**	**9.53**	**9.08**	**9.19**	**St/Sa**

For the sampling method used in this study, the St/Sa ratio is two to three times higher than Rt/Ra (Tables 6.2). It follows that 3D surface quality evaluation can highlight the existence of extreme values with greater probability. There is a decrease in this ratio

with increased speed, more pronounced for St/Sa. At higher speeds, worn surfaces are of better quality than those obtained for lower test speeds (in the present study, v = 0.38 m/s), which a designer is interested in when selecting the working tribosystem, especially in the case of the regime with repeated starts and stopps.

Rq = 3
Rsk = 0
Rku = 3

a) Gaussian surface

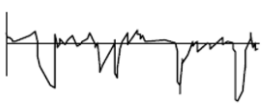

Rq = 12
Rsk = -1
Rku = 8

b) Surface with deep and narrow valleys

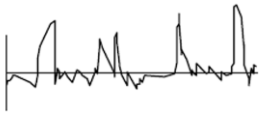

Rq = 12
Rsk = 1
Rku = 8

c) Surface with tall and narrow peaks

Rq = 4
Rsk = 0
Rku = 1.5

d) Surface with valleys and wide peaks, with relatively high slope

Rq = 4
Rsk = 0
Rku = 10

e) Surface with peaks and rare valleys but with extreme values

Fig. 6.9. Surface types and amplitude parameters

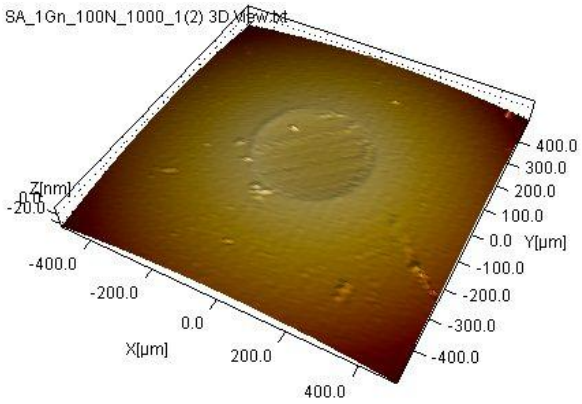

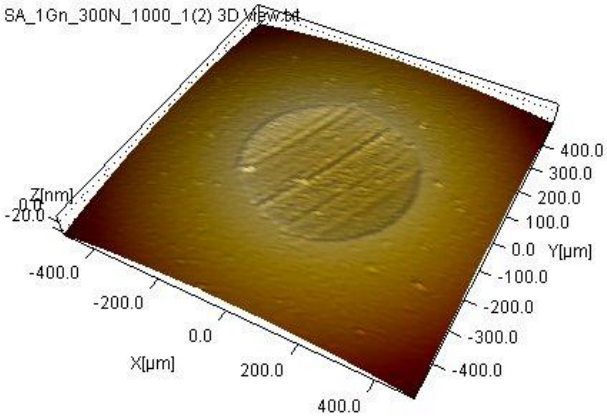

Rq = 0.166 µm, Rsk = -0.01, Rku = 4.55
F = 100 N

Rq = 0.166 µm, Rsk = 0.224, Rku = 3.58
F = 300 N

F. 6.10 Soybean lubricant +1% graphite, v = 0.38 m/s, (for 3D images, Z scale is in microns, 200:1)

To highlight the importance of studies based on a set of texture parameters, Figure 6.9 schematically presents different profiles, characterized by the set (Rq, Rsk, Rku). Therefore, in this study, the values of these amplitude parameters are analyzed only for 3D (Sq, Ssk, Sku).

In international standards, it is recommended for well-processed surfaces that these deviations are within ± 16% for 2D parameters, but these are worn surfaces. The tables show that this range would only be met for a few 3D parameters (Sa, Sq and St - except for the original surface).

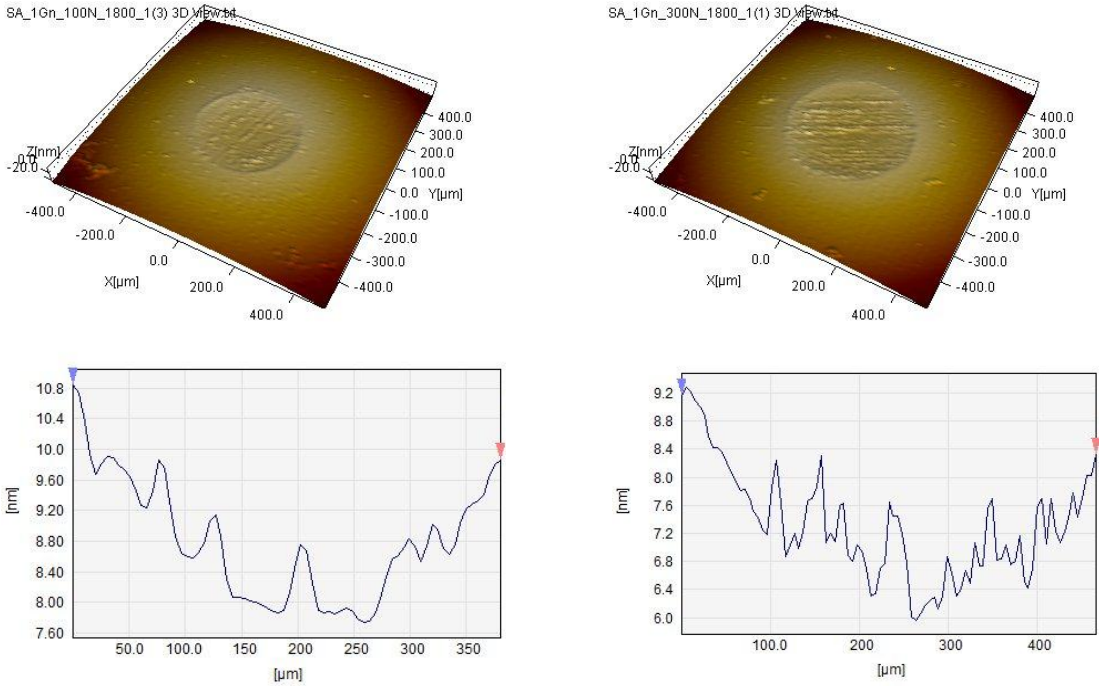

Rq = 0.27 µm, Rsk = -0.32, Rku = 6.089, F = 100 N Rq = 0.39 µm, Rsk = 0.6, Rku = 3.48, F = 300 N

Fig. 6. 11 Wear scars for v = 0.69 m/s. 3D virtual images are reconstituted from data measurements and their cross sections, (for 3D images, Z scale is in microns, 200:1), 2D profiles are taken on the scar axis perpendicular to the sliding direction

Analyzing the values for the pair (Rsk, Rku) or (Ssk, Sku), it is observed that Rsk (and Sku) are positive and Rku has values in the range 2 ... 3. It results that the vast majority of wear scars are surfaces with tall and narrow peaks, resulting from abrasive wear, the traces being visible also on the images obtained with the optical microscope and on the virtual images that reconstruct the surface with the help of the profiling software, SPIP 6.7.2.

Figures 6.10 and 6.11 exemplify these conclusions only for one ball of a test, but they are supported by the data in Table 6.2. Analyzing the data from Tables 6.2, it can be seen that for all measurements, St is higher than Rt, which means that the maximum values were not found on the axis of the ellipse perpendicular to the sliding direction. This is logical because in a circular or almost circular contact, the maximum contact pressure is towards the front of the contact. So, a 3D study will also include the area of maximum contact pressure that will most likely affect the surface texture quality to a greater extent. For some test regimes, i.e. (F=100 N, v=0.38 m/s), lower values were obtained than those obtained on the initial surfaces of the balls, which implies that the test regime acts as a running-in process, improving the surface quality.

6.6. Influence of additive concentration and test regime on amplitude parameters

In the following graphs, the null concentration corresponds to the neat soybean oil.

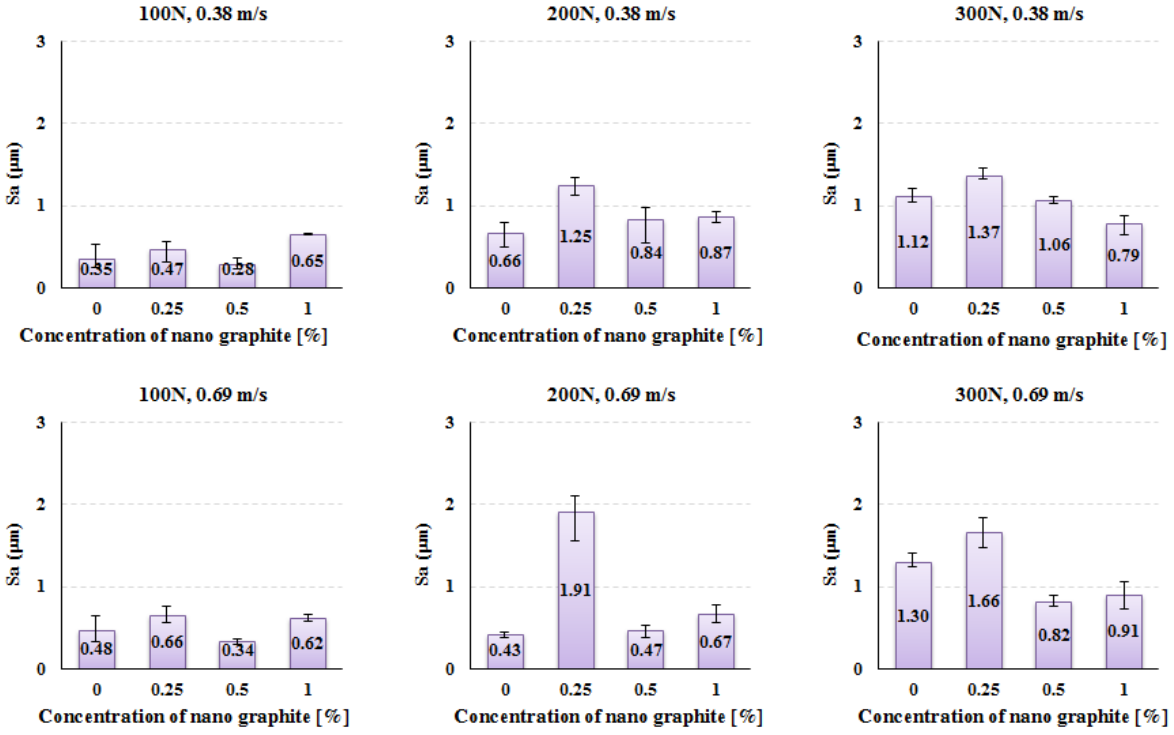

Fig. 6.12 Parameter Sa as a function of additive concentration, sliding speed and load, 0 is taken for the non-additivated soybean oil

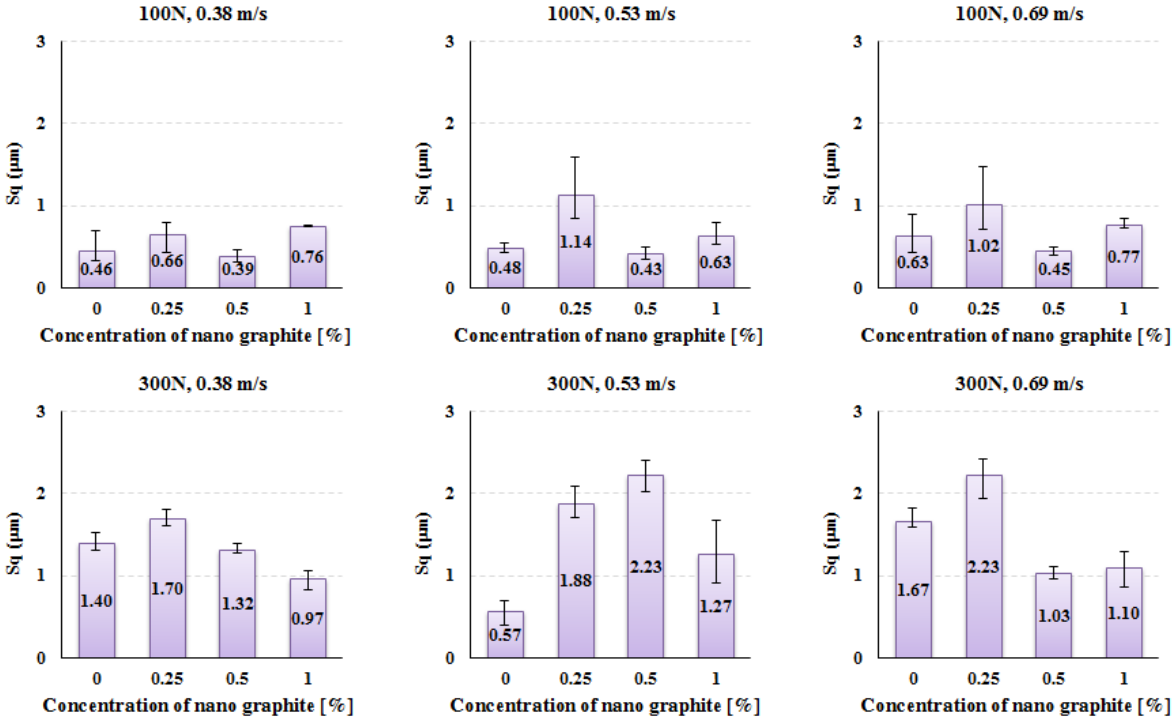

Fig. 6.13 Parameter Sq as a function of additive concentration, sliding speed anf load, 0 is taken for the non-additivated soybean oil

For the graphite concentration of 0.25%, the value of Sa is the highest, except for F = 300 N and v = 0.69 m/s. The conclusion is that a small concentration of nano additive is not

beneficial to keep amplitude parameters at low values. For the highest concentration (1% graphite), it decreased, but not below the value obtained on the scars of neat soybean oil.

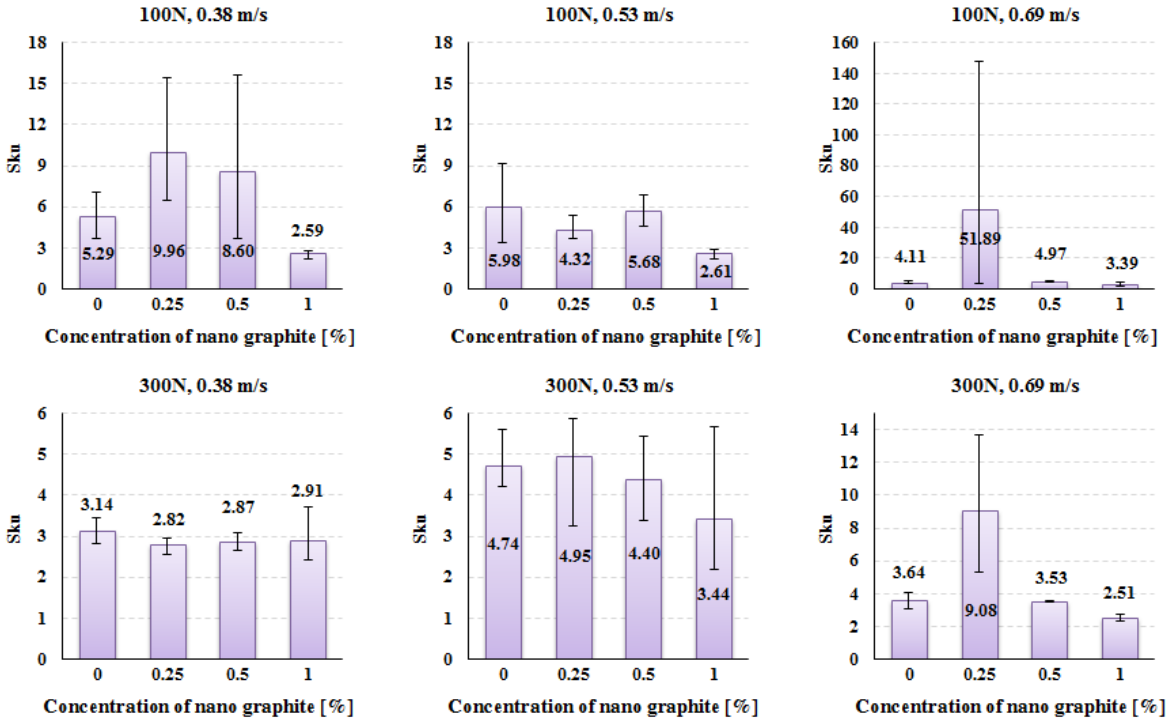

Fig. 6.14. Parameter Sku as a function of additive concentration, sliding speed anf load, 0 is taken for the non-additivated soybean oil

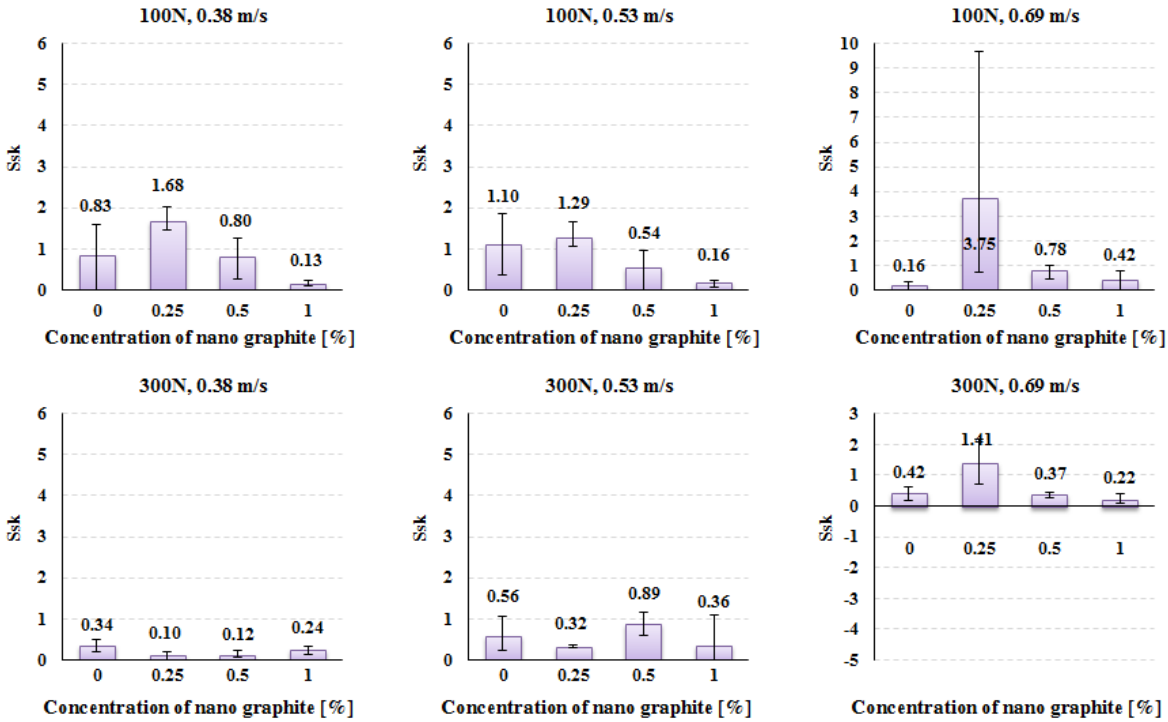

Fig. 6.15. Parameter Ssk as a function of additive concentration, sliding speed anf load, 0 is taken for the non-additivated soybean oil

For these worn surfaces, the dependence of type $Sq = a \cdot Sa$ can not be observed, as exemplified by the different altitude of the graphs for Sa and Sq, in the regimes (F = 300 N, v

= 0.53 m/s), (F = 200 N, v = 0.69 m/s). The average values for Sku are between 2.40 and 9.96 (with two very high values, 33.42 and 51.89). Thus, this is a rough surface with high and narrow peaks typical of surfaces with abrasive wear, Ssk ranging from 0 (some negative values close to zero) and 3.75.

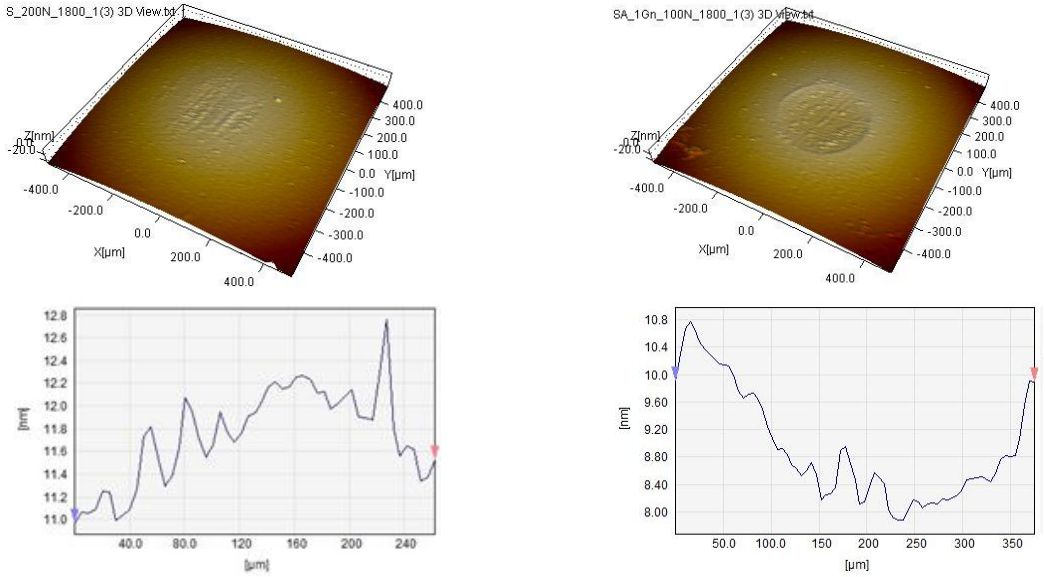

F = 200 N, v = 0.69 m/s, non-additivated soybean oil
Sku = 33.42, Ssk = -0.69

F = 100 N, v = 0,69 m/s, soybean oil + 0.25% graphite
Sku = 51.89, Ssk = 3.75

Fig. 6.16. Extreme values for Sku

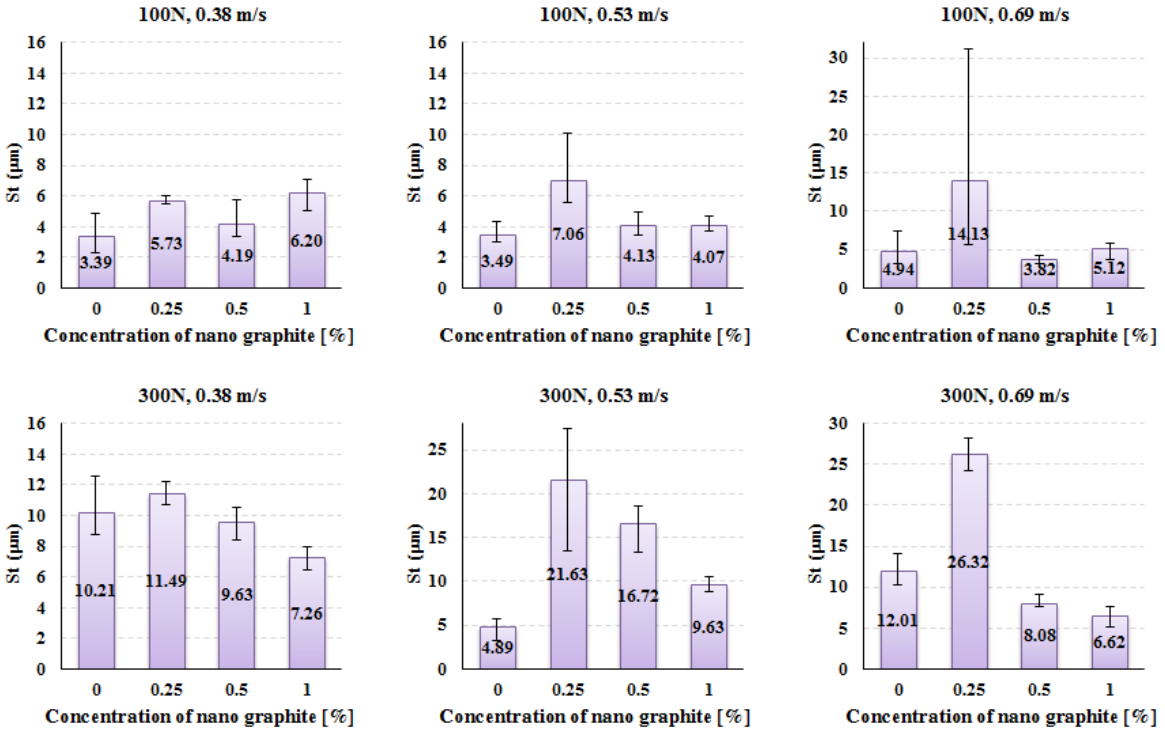

Fig. 6.17 Parameter St as a function of additive concentration, sliding speed anf load, 0 is taken for the non-additivated soybean oil

The highest values were obtained for the 0.25% nano graphite lubricant, which means that the addition of the additive in a too low concentration does not protect the surface. There may be

micro-zones in contact where these intermediate nanoparticles exist and take up a part of the load but, when the particles are dispersed, the contact becomes directly among the asperities and the friction and wear processes are more intense than with the oil without additives.

6.7. Influence of additive concentration and test regime on functional parameters

In Figure 6, the Abbott-Firestone 3D curves are given, and under each curve there is a trace of wear, as obtained with the optical microscope.

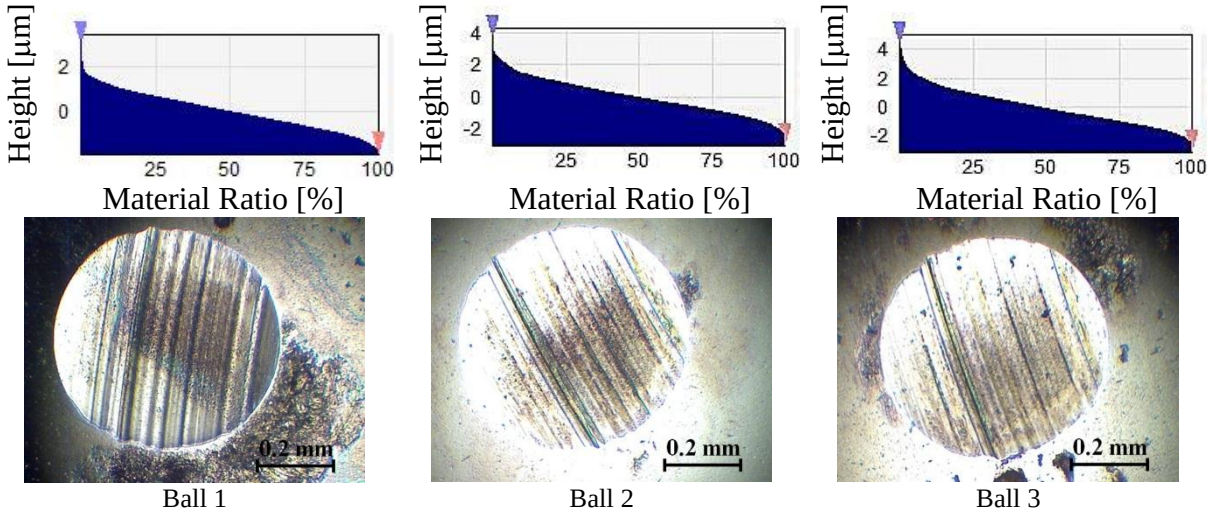

Soybean oil + 1% nano graphite, test conditions: F = 300 N, v = 0.69 m/s

Fig. 6.18. Abbott-Firestone curves (3D) and the images of the worns scars

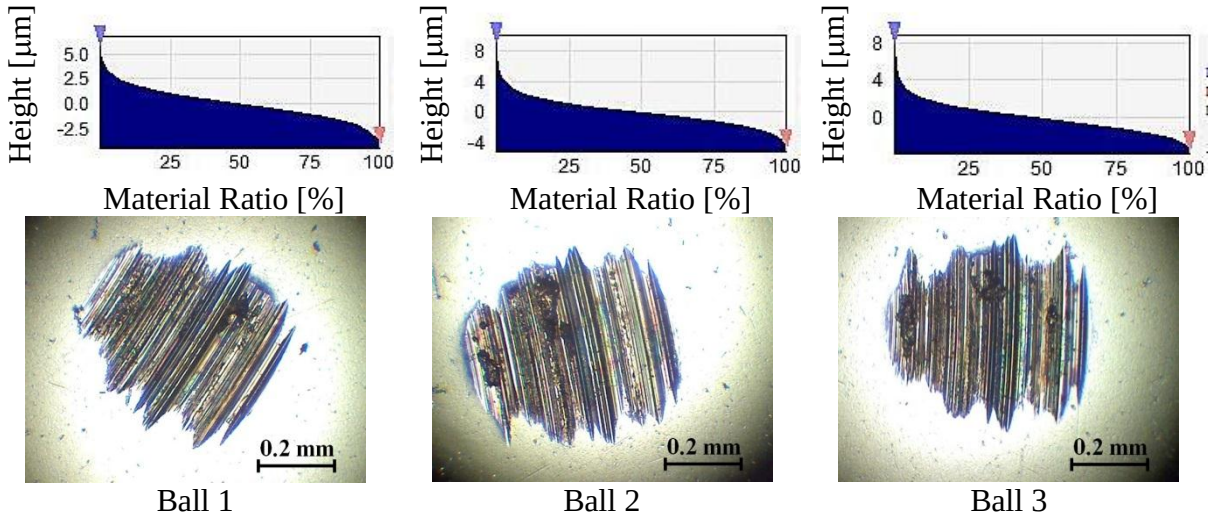

Fig. 6.19. Abbott-Firestone curves (3D) and the images of the worns scars. Soybean oil, test conditions: F = 300 N, v = 0.69 m/s

A significant change of Svk is observed for the low graphite concentration (0.25%), for loads of 200 N and 300 N, at higher slidind speeds v = 0.53 m/s and v = 0.69 m/s.

Where Spk is smaller than Spk of the initial surface, the remaining Sk and Svk values are similar to those of the original surface; it is estimated that there was an abrasive running-in wear, ie only the peaks of the asperities were flattened or cut, without deterioration by wear of the entire profile.

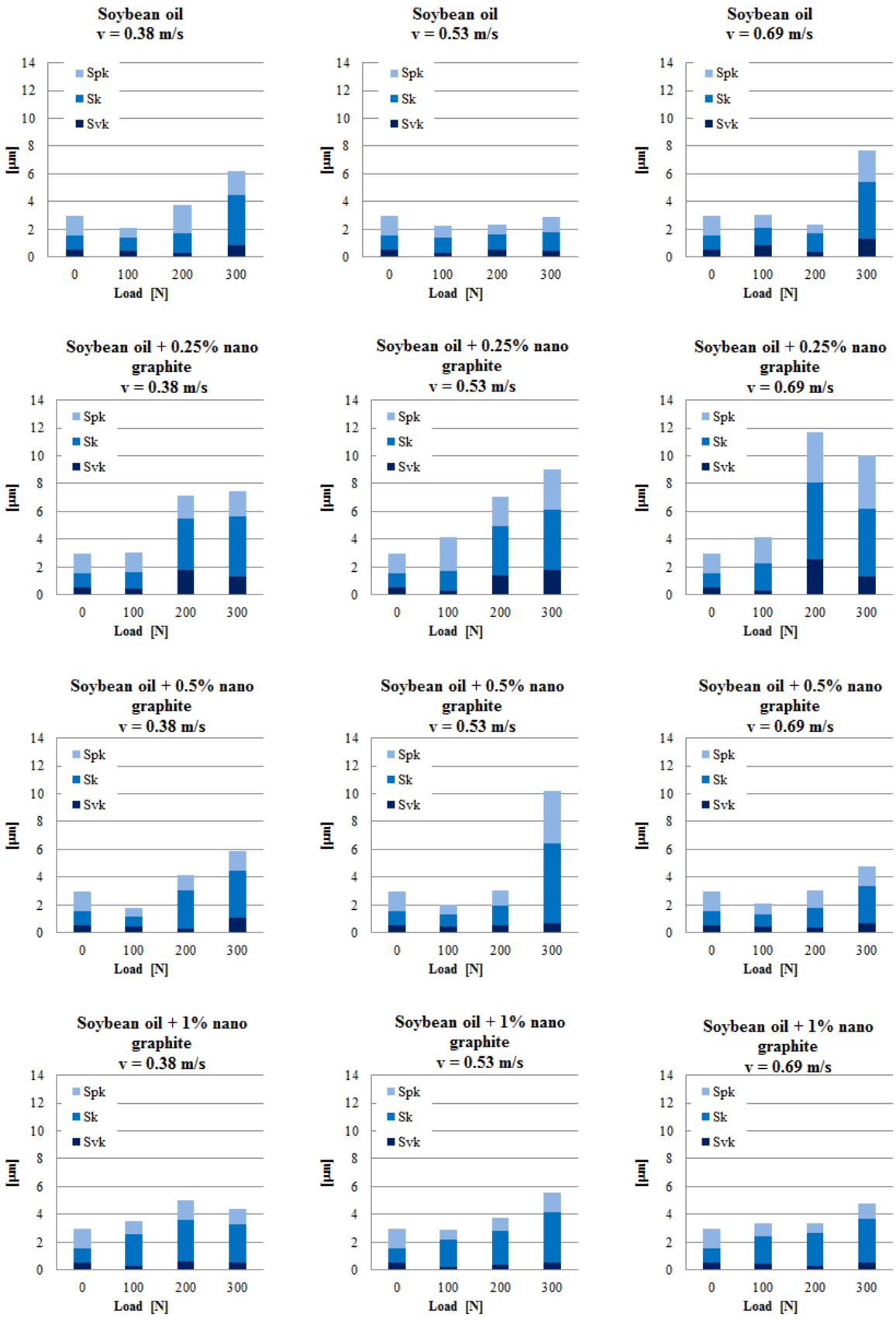

Fig. 6.20. Sum of functional parameters (Svk+Sk+Spk), depending on the nano additive concentration, load, and velocity (0 represents the non-worn initial surface of the ball)

If $(Spk+Sk+Svk)_{initial} < (Spk+Sk+Svk)_{worn}$, it can be imagined that the abrasive wear has remodel the whole profile. Such values were obtained for the soybean oil, only at v = 0.53 m/s and (F = 100 N, v = 0.38 m/s), for the lubricant with 0.5% graphite, also under light conditions F = 100 N). The lubricant with 1% nano additive generally maintains the sum of the parameters for the light regimes and slightly increases it for F = 300 N, meaning that the additive protects the surface. through the friction process with the third body.

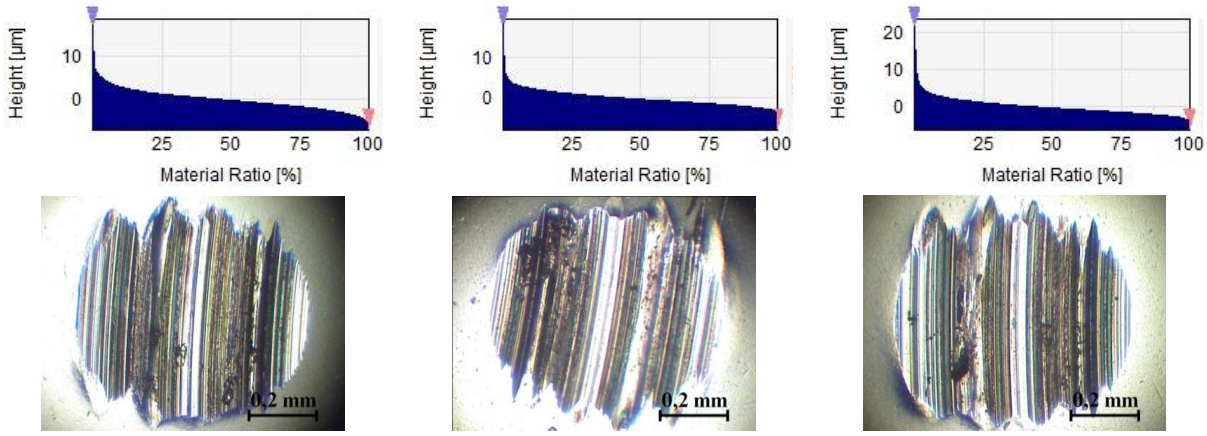

Ball 1 Ball 2 Ball 3

Fig. 6.21. Significant modification of Svk
Lubricant: soybean oil + 0.25% nano graphite, F = 300N, v = 0.69 m/s

From the graphs showing the functional parameters according to the test regime for the nano additivated lubricant, it is observed that the highest values were measured on scars resulting from the lowest additive concentration of 0.25% (with the exception of a large value associated with the concentration of 0.5%, at F = 300 N and v = 0.53 m/s), which is also observed in Fig. 6.20. Wear scars are deep, sharp, and one may see the resulting smears as a process of adhesive wear. Abbot curves are very sharp at the top of the profile, although the slope of the profile strength zone is not substantially altered. It is typical for an abrasive wear process.

For the lubricant with 1% graphite, less scratched traces were obtained, the distribution of the material remained more favorable to support the load (see Abbott-Firestone curves in Figure 6.18) and the values of the functional parameters are better in the sense that they have lower values and the distribution of the material is better (Sk is higher than Spk, which means that the roughness is not sharp and favorable to more intense abrasive wear).

6.8. Maps of roughness parameters

The same trend is observed for Sa and St, although a parameter is calculated from the reference line (Sa) and the other one is a singular value (St) from a raw texture investigation.

Between 0.5...1% graphite in soybean oil, the test regimes do not generate high St values, very high asperities were noticed for nano addiativated oil at low concentrations, especially for F = 200 N and F = 300 N. The conclusion is that at a higher concentration, the nano-additive begins to fulfill its role of surface protection and damping, reducing the generation of isolated, but high peaks.

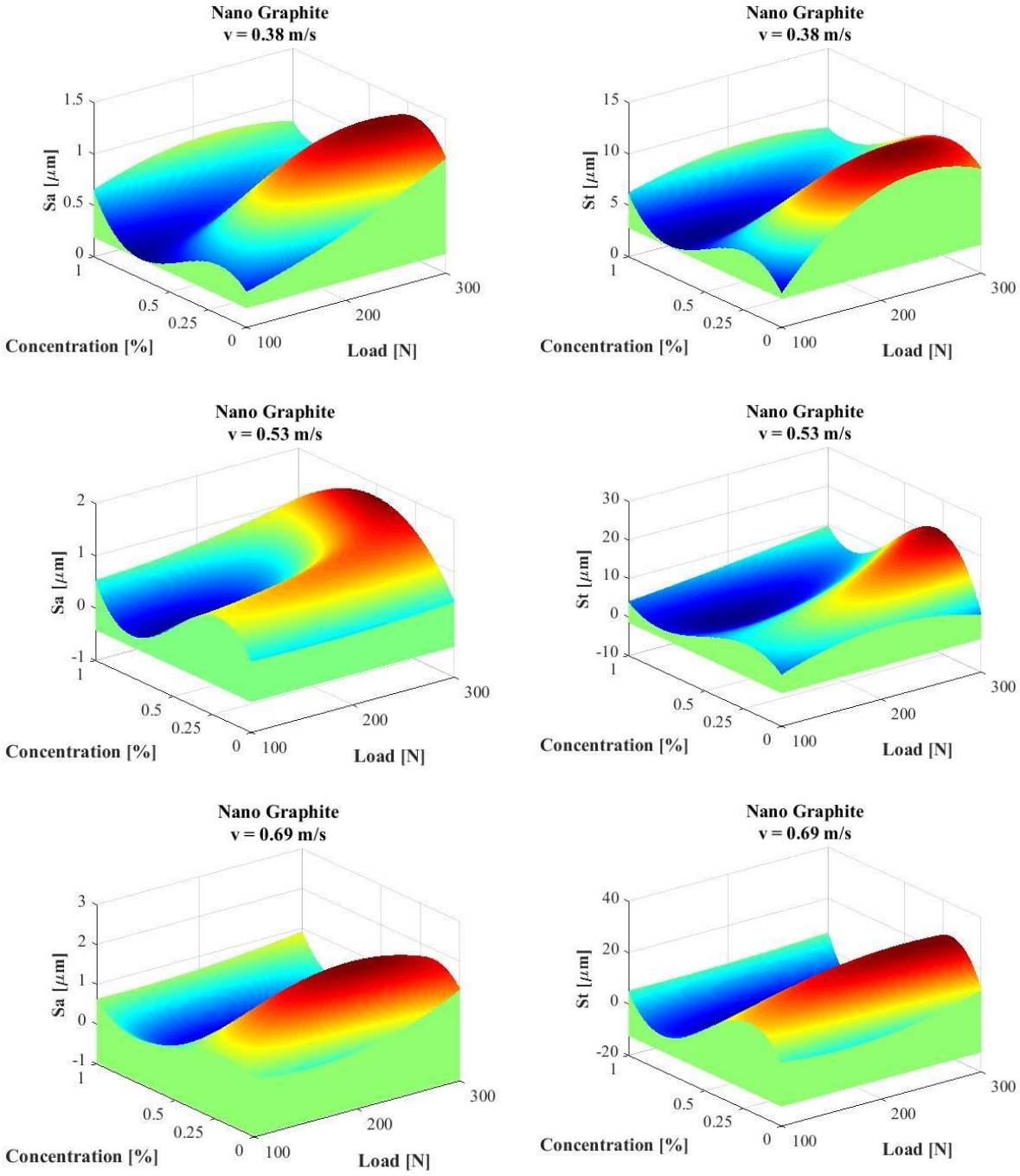

Fig. 6.22. Maps for Sa and St parameters

6.9. Conclusion

The evaluation of the surface quality, whether worn or not, using 3D parameters is closer to reality, the finer the step and the larger investigation area (or the result of an average of 3-5 measurements on the studied surface), in the case of an analysis 3D.

In the case of worn surfaces, the engineer is very interested in the values for Ssk, Sku, St, Sp and Sv, because the high peaks affect the tribological parameters, especially in the case of lubricated contacts with low values of dynamic viscosity fluids because high peaks disrupt

the film and are prone to generate mixt lubrication regime.

A comparative study was carried out between the 2D and 3D parameters for the wear traces obtained on the bead tested with soybean oil lubricated with nanotube, which showed that the use of the set 3D parameter set reflects the change in surface quality under the sampling of the investigative methodology proposed by the author.

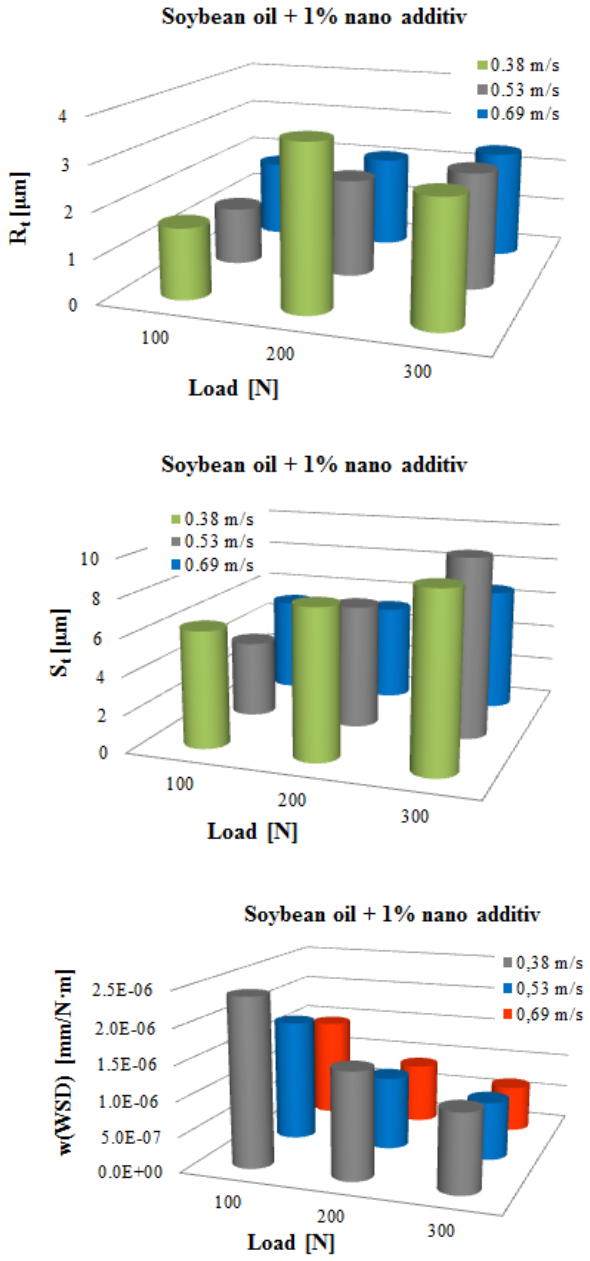

Fig. 6.23 Comparison between 2D/3D parameters and the wear rate of WSD

The surface quality was evaluated by a dimensional parameter St/Sa, which brings together an averaging parameter (Sa) and an extreme parameter (St), which justifies why single elements, such as very rare and very high asperities, have a great influence on the tribological behavior, especially for lubricated contacts.

In the case of studying the wear scars produced in lubrication with soybean oil + nano

graphite, for the three tested forces and speeds, the parameters describing the texture of the worn surfaces are not linked to a direct proportionality to load and speed, at least for the studied ranges.

Analysis of parameter λ for the performed tests

In the process of assessing the thickness of the lubricant film it was considered that the contact surfaces lubricated under the elastohydrodynamic regime were perfectly smooth. In practice, these surfaces are characterized by roughness.

Depending on the height of the asperities of the two surfaces in contact, the separation of surfaces through a lubricant film of minimum thickness, h_{min}, may be complete or partial. Thus, for estimating the separation of the two surfaces in contact by the lubricant film, and emplicitly, for evaluating the lubrication regime, specialists use the λ parameter:

$$\lambda = \frac{h_{min}}{\sqrt{R_{q1}^2 + R_{q2}^2}} = \frac{h_{min}}{1.15 \cdot \sqrt{Ra_1^2 + Ra_2^2}} \tag{6.18}$$

where h_{min} – the minimum thickness of the lubricant film, [m]; Rq_1, Rq_2 – the average square deviations of the heights of the roughness of the two surfaces in contact, [μm]:

It is admitted that for $\lambda<1$, the lubrication regime is mixed for $1\leq\lambda\leq3$, the lubrication regime is partly EHD and if $\lambda > 3$, the lubrication regime is full lubricant film [Olaru, 2002], [Stachowiak, 2005].

It is also noted that all theoretical values of the minimum film thickness of the lubricant are comparable to the measured initial roughness value of the contact balls (Sa = 0.4 μm and Ra = 0.12 μm, see Table 6.1) for all analyzed lubricants and for all considered axial loads. For this reason, all calculated values of the lubrication parameter λ are between 0.64 and 0.041, resulting that the lubrication regime is mixed or, at best, a boundary regime due to the nature of the soybean oil.

Table 6.3. Maximum and minimum values for λ, for the range of tested parameters

	Lubricant	Test conditions	h_{min}	λ(Ra)
20°C	soybean oil + 1% carbon	F = 100 N, v = 0.69 m/s	$4.19 \cdot 10^{-8}$ m	0.64
	soybean oil + 1% graphite	F = 300 N, v = 0.38 m/s	$1.8 \cdot 10^{-8}$ m	0.277
45°C	soybean oil soybean oil + 0.5 carbon soybean oil + 1% carbon	F = 100 N, v = 0.69 m/s	$1.9 \cdot 10^{-8}$ m	0.292
	soybean oil + 0.25% graphite soybean oil + 1% graphite	F = 300 N, v = 0.38 m/s	$0.27 \cdot 10^{-8}$ m	0.041

If Sa is entered in the parameter calculation, , λ(Sa) the values of the working regimes are changing. Taking into account the comparison made between 2D and 3D measurements

and the vast majority of data in this chapter, Sa≈3Ra, a new evaluation of the working regime can be proposed based on the 3D parameter, Sa, according to the table below.

Table 6.4

Regime	**Ra**	**Sa**
mixed regime	$\lambda < 1$	$\lambda < 0.3$
boundary and mixed mode	$1 \leq \lambda \leq 3$	$0.3 \leq \lambda \leq 1$
fluid film lubrication (EHL)	$\lambda > 3$	$\lambda > 1$

Because $\lambda < 1$, the regime is mixt for all considered lubricants, which means that the surfaces come into contact, deformations occur in the asperities and abrasive wear processes develop.

Conclusions based on the evaluation of the theoretical lubrication regimes and parameter λ

The lubrication parameter λ has been calculated for all tested lubricants and for all rated axial loads and dynamic viscosities. All values obtained were less than 1, the lubrication regime being a boundary or mixt one.

In Chapter 2, the minimum theoretical thickness of the lubricant film was calculated for all tested lubricants and tested regimes and for all determined dynamic viscosity. The obtained thicknesses of the lubricant film for the four classes of lubricants are very close and comparable to the roughness value Ra of the contact surfaces, thus, with high probability, lubrication is a mixt or partial EHL.

Worn surfaces must be characterized by a set of parameters.

Same qualitative conclusions could be drawn from an analysis of the longest profile on the wear scar, recorded perpendicular to the sliding direction. But values are different from those obtained by a 3D analysis on the entire wear scar.

As the recent designed instruments, like that used in this analysis (profilometer Laser NANOFOCUS μSCAN), are more performant, an analysis on the entire wear scars on the balls from the four ball tester are more suitable to characterize the surface quality after tests and to rank the lubricant capacity of an oil depending on a set of parameters, including amplitude parameters, spatial parameters and functional ones.

This conclusion has to be related only to the experiments the author has done and included in this study.

As far as the author knows from the available specialised literature, it is for the first time that all the surface of the wear scar generated on the four ball machine is investigated and the conclusion is that from the tribological point of view, the 3D parameters reflect better the surface quality evolution after testing.

Chapter 7
CONCLUSIONS AND PERSONAL CONTRIBUTIONS

7.1. Final conclusions

Biodegradable lubricants based on vegetable oils are of particular interest due to some predominantly economic advantages over biodegradable lubricants based on polyglycols or synthetic ester oils.

Both the relatively inexhaustible source and the nontoxicity and rapid biodegradability of vegetable oils are their main advantages.

The research in this PhD thesis focused on the rheological and tribological study of soybean oil and additives based on carbon nano materials (black carbon, nano graphite, nano graphene).

The study highlighted that the evaluation of a lubricant, especially additive, should be done according to several criteria. In this paper two interconditioned behaviors were studied: tribological behavior and rheology behavior.

The rheology behavior was analyzed for the three classes of nano additivated lubricants and non-additivated soybean oil.

The author determined the dependence of dynamic viscosity on the shear rate and temperature and modeled after the law of power the experimental data obtained. This model best approximates the dependence of dynamic viscosity on shear rate and temperature.

The author formulated a mathematical model, also after the law of power, which introduces the concentration of nano additive in relation:

$$\eta = \eta_0 \cdot e^{a(t-t_0)} \cdot e^{b \cdot c}$$

where η_0 is the dynamic viscosity at temperature t_0 (η_0 is considered for 20 °C, considered as the reference temperature). In this study, a is the coefficient of dependence of the dynamic viscosity on temperature (being a constant of the material), c is the massic concentration of the additive and b is a constant dependent on the nature of the additive.

Analyzing the values of material constants as the author has found, it is shown that the additive concentration dependence is poor for these modifiers of friction and wear. Nano carbon did not change the viscosity, but the other two additives lowered the viscosity-temperature curve, regardless of concentration.

It was found that tested nano additives may be grouped into two categories, according to the influence of their nature:

- the additive that did not significantly modified the viscosity of soybean oil and the shear stress - shear rate curve is the black carbon,

- additives that have reduced the dynamic viscosity over the studied temperature range: graphite and graphene, these additives lowering the dynamic viscosity curves with temperature.

This decrease in viscosity, induced by these nano additives, has led to a particular tribological behavior of the lubricants.

All nano additivated lubricants have an accentuated thixotropy after a certain value of shear rate , 600 ... 700 s^{-1} and up to 2000 s^{-1}, the extreme value for which determinations have been made. Between 100 s^{-1} and 600 ... 700 s^{-1}, the loading and decreasing hysteresis is not significant, the shear stress dependence on the shear rate being almost linear, characteristic for fluids closer to newtonian behavior.

The modeling of shear stress - sgear rate dependance following the law of power has a low correlation coefficient due to the hysteresis loop. If only the loading curve is considered, dependence tends to be close to the linear one.

The tribological behavior of the three classes of lubricants andthe non-additivated soybean oil was analyzed using the four-ball tribosteter.

Analyzing the tribological characteristics, friction coefficient, wear scar diameter (WSD) and the wear rate of WSD (w(WSD)), determined by testing on the triboteter with four balls, the best tribological behavior is the nano graphite and black carbon lubricants in the concentration of 1.0 % wt.

Changing the tribological behavior with this type of additive is not significant, at least on the range of parameters studied for speed, load and concentration, but from the tribological parameter maps the tendency of nano additivated lubricants to behave better at more severe regimes is observed.

From a tribological point of view, degummed soybean oil can be used as the basic raw materials of biodegradable lubricants, and research on oxidation stability.

7.2. Personal contributions

Vegetable oils have been analyzed in the literature, but the reported results for non-additivated or additivated oils are still inconclusive and the applications of these oils rely more on market inertia or on the practical experience of users.

Considering that the purpose of this research study was to assess the tribological and rheological impact of carbon nanoparticles (black carbon, graphite and graphene) in soybean oil, the author made the following:

- analytical study of recent documentation on non-additivated and additivated vegetable oils for lubrication applications,
- identify lubrication regimes and determine the minimum thickness of the lubricant film for the studied lubricants to establish test regimes and explain the experimental values obtained.

- developing an own methodology for the evaluation of vegetable oil based lubricants through a set of tribological and rheological tests,
- laboratory formulation of lubricants to ensure dispersion of nanoadiatives,
- a rheological study of formulated lubricants,
    - the experimental determination of the viscosity dependence on the shear rate for formulated and tested lubricants, the modeling of this dependence by power functions,
    - determining the dependence of the dynamic temperature viscosity on formulated lubricants and modeling this dependence using the Reynolds equation.
- a complex tribological study on lubricants formulated by four variables: the nature of the additive, its concentration, speed and load), ensuring, by doubling the tests at the same parameters, a good repeatability,
    - determination of tribological parameters (COF, WSD and w(WSD)),
    - interpretation of information from experimental data to determine the influence of soybean oil additive
    - the mapping of COF, w(WSD) and their use for tribological behavior assessment,
    - a non-destructive investigation to evaluate the texture of WSD using the 3D parameters of surface texture in relation to concentration and load. From the literature studied, the author observed that the evaluation of the texture of the worn surfaces is rare and when it is made it is based on a single parameter, usually Ra, but which does not sufficiently describe the nature of the worn surfaces. In the study, the author used a set of parameters, amplitude parameters and functional parameters to characterize the worn surfaces. The author studied the material distribution curves (Abbott-Firestone curves) on the worn profile and observed that at low concentrations the surface quality is worse compared to the worn surfaces, when using the soybean + 1% nanographite,
- data interpretation and dissemination through scientific articles published and sustained at international conferences (see the list in the end of this document),
- in terms of research competencies, during the elaboration of the thesis, the author learned to use the software necessary to manage the information from experimental data using the following: MathLab, SPIP (SPIP^{TM}, Version 6.7.2), Excel, CurveExpert, dedicated software of the four-ball machine, the software that serves the NanoPhot 2 microscope, the NanoFocus AG μScan® profilometer software, the Brokfield CAP 2000+ Viscometer software, the CAPCALC 32,

- calibrating a real-time frictional force monitoring system on the four-ball machine.

Future research directions

Based on the obtained results, this research may be continued in the following directions:

- extending the load and speed test ranges,
- the study of seizure capability and the influence of nanoditives, because on the wear and COF maps there was a tendency to reduce the influence of load for the nano additivated lubricants and, at high loads, it is likely that the additive will increase the load to seizure and it will reduce the slope of the seizure curve,
- the use of other methods of investigation to explain the particular rheological and tribological behavior of these additivated lubricants, especially for those that reduced the viscosity, as it was proved for soybean oil with graphene and graphite,
- complex additivation of soybean oil (by testing a set of additives, including viscosity modifiers and oxidation inhibitors).

References

1. Abdullah, M. I. H.C., bin Abdollah, M. F. (2016). Tamaldin N., Amiruddin, H., Nuri, N. R. M., Effect of hexagonal boron nitride nanoparticles as an additive on the extreme pressure properties of engine oil. *Industrial Lubrication and Tribology*, 68(4), pp. 441-445.

2. Adhvaryu, A., Erhan S. Z., Perez J. M. (2004). Tribological studies of thermally and chemically modified vegetable oils for use as environmentally friendly lubricants, *Wear*, 257(3-4), pp. 359–367.

3. Akbulut, M. (2012). Nanoparticle-Based Lubrication Systems, *Journal of Powder Metallurgy and Mining*, 1, p. 101.

4. Alves, S. M. A, Barros, B. S., Trajano, M. F., Ribeiro, K. S. B., Moura, E. (2013). Tribological behavior of vegetable oil-based lubricants with nanoparticles of oxides in boundary lubrication conditions, *Tribology International*, 65, pp. 28–36.

5. Bakunin, V. N., Suslov, A. Yu., Kuzmina, G. N. Parenago O.P. (2004). Synthesis and application of inorganic nanoparticles as lubricant components – a review, *Journal of Nanoparticle Research*, 6. pp. 273–284.

6. Berman, D., Erdemir A., Zinovev, A.V., Sumant A. V. (2015). Nanoscale friction properties of graphene and graphene oxide, *Diamond & Related Materials*, 54, pp. 91–96.

7. Berman, D., Erdemir, A., Sumant A. V. (2013). Few layer graphene to reduce wear and friction, on sliding steel surfaces, *Carbon*, 54, pp. 454–459.

8. Biresaw G., Bantchev G. (2008). Effect of chemical structure on film-forming properties of seed oils. *Journal of Synthetic Lubrication*, 25, pp. 159–83.

9. Biresaw, G., Mittal, K. L. (2008). *Surfactants in tribology*, CRC Press, Francis & Taylor Group.

10. Biresaw, G., Bantchev, G. B. (2013). Pressure viscosity coefficient of vegetable oils. *Tribology Letters*, 49, pp. 501-512.

11. Blateyron, F., (2008). 3D parameters and new filtration techniques. www.digitalsurf.fr/pressreleases/2008-06-unm-prize.pdf.

12. Blunt, L., Jiang, X. (2003). Advanced techniques for assessment surface topography, London, Butterworth-Heinemann.

13. Botan, M., Pirvu, C., Georgescu, C., Deleanu L. (2013). Influence of Feed Speed on Surface Quality of Several Building Stones, paper 777, Proceedings from *5th World Tribology Congress (WTC 2013*), p. 1958, Torino, Italy, 8-13 September 2013, Curran Associates, Inc.

14. Bowden, F.P., Tabor, D., (1956). *Friction and Lubrication*, London, Methuen.

15. Brodnjak-Voncina, D., Kodba, Z. C., Novic, M. (2005). Multivariate data analysis in classification of vegetable oils characterized by the content of fatty acids, *Chemometrics and Inteligent Laboratory Systems*, 75, pp. 31-43.

16. Cameron, A., (1983). *Basic Lubrication Theory*, Third Edition, Ellis Horwood Ltd.

17. Campanella, A., Rustoy, E., Baldessari A., Baltanas M. (2010). Lubricants from chemically modified vegetable oils. *Bioresource Technology*, 101, pp. 245-254.

18. Cazamir D. (2017). Studiul influenței aditivării uleiului de rapiță cu dioxid de titan (TiO_2), disertație, Universitatea Dunarea de Jos, Galati, 2017.

19. Cermak, S. C., Biresaw, G., Isbell, T. A., Evangelista, R. L., Vaughn, S. F., Murray, R. (2013) New crop oils—Properties as potential lubricants. *Industrial Crops and Products*, 44, pp. 232–239.

20. Chang, L., Friedrich, K. (2010). Enhancement effect of nanoparticles on the sliding wear of short fiber-reinforced polymer composites: a critical discussion of wear mechanisms, *Tribology International*, 43, pp. 2355–2364.

21. Cheenkachorn, K. (2013). A study of wear properties of different soybean oils, The Mediterranean Green Energy Forum 2013, MGEF-13, *Energy Procedia*, 42, pp. 633-639.

22. Chinas-Castillo, F., Spikes, H. (2003) Mechanism of action of colloidal solid dispersions, *Journal of Tribology*, pp. 125-552.

23. Cotell, C.M., Sprague, J.A., Smidt, F. A. Jr. (2002). *ASM Handbook volume 5 – Surface Engineering*, ASM International, USA.

24. Crețu, S. (2014). Four balls test on steel balls versus balls with phosphate treatment.

25. Cristea, G. C., Dima, C., Georgescu, C., Dima, D., Solea, L., Deleanu, L. (2017). Evaluating lubrication

capability of soybean oil with nano carbon additive, *15th International Conference on Tribology*, Kragujevac, Serbia, 17 – 19 May 2017.

26. Cristea, G. C., Dima, C., Dima, D., Georgescu, C., Deleanu, L. (2017). Nano graphite as additive in soybean oil, MATE C Web Conf., vol. 112, *21st Innovative Manufacturing Engineering & Energy International Conference – IManE&E 2017*, https://doi.org/10.1051/matecconf/201711204023, 2017,

27. Czichos, H., Saito, T., Smith, L. (2006). *Springer Handbook of Materials Measurement Methods*, Berlin, Springer Science-Business Media.

28. Czichos, H. (1978). *Tribology – A system approach to the science and technology of friction, lubrication and wear*, New-York,Elsevier Scientific Publishing Company.

29. D'Agostino, V. (2002). *Fondamenti di tribologia*, vol. I, CUEN, Napoli.

30. Deleanu, L., Cantaragiu, A., Bîrsan, I. G., Podaru, G., Georgescu, C. (2011). Evaluation of the spread range of 3D parameters for coated surfaces. *Tribology in Industry*, 33(2), pp. 72-78.

31. Demirbas, A. (2009). Political, economic and environmental impacts of biofuels: A review, *Applied Energy*, 86, pp. S108-S117, 2009.

32. Dong W.P., Sullivan, P.J., Stout K. J. (1994). Comprehensive study of parameters for characterising three-dimensional surface topography. III: Parameters for characterising amplitude and some functional properties, *Wear*, 178(1-2), pp. 29-43.

33. Dowson, D., Higginson, G., R. (1977). *elasto-hydrodynamic lubrication*, Oxford, Pergamon Press.

34. Erhan, S. Z., Sharma, B. K., Perez, J. M. (2006). Oxidation and low temperature stability of vegetable oil-based lubricants, *Industrial Crops and Products*, 24, pp. 292–299

35. Erhan, S.Z. (2005). Industrial Uses of Vegetable Oils, Peoria, Illinois, AOCS Press,.

36. Eswaraiah, V, Sankaranarayanan, V, Ramaprabhu, S. (2011). Graphene-based engine oil nanofluids for tribological applications. *ACS Appl Mater Interfaces*, 3(11), pp. 4221-4227.

37. Fang J. H. et al., "Friction and Wear Performances of Magnesium Alloy against Steel under Lubrication of Soybean Oil with S-Containing Additive", Applied Mechanics and Materials, Vol. 538, pp. 19-23, 2014

38. Fernandez, I., Ortiz, A., Delgado, F., Renedo, C., Perez, S. (2013). Comparative evaluation of alternative fluids for power transformers, *Electric Power Systems Research*, 98, pp. 58-69.

39. Fessenbecker, A., Roehrs, I. Pegnoglou, R. (1996). Additives for environmentally acceptable lubricants, *NLGI Spokesman*, 60(6), pp. 9-25.

40. Fox, N. J., Stachowiak, G. W. (2007). Vegetable oil-based lubricants - A review of oxidation, Tribology International, 40, pp. 1035-1046,.

41. Frêne, J., Nicolas, D., Deguerece, B., Berthe, D., Godet, M. (1990). *Lubrification hydrodynamique. Paliers et butées*, Paris, Edition Eyrolles.

42. Friedrich, K., Schlarb A. K. (2008). *Tribology of polymeric nanocomposites – friction and wear of bulk materials and coatings*, Tribology and Interface Engineering Series, 55, Part I: Bulk Composites with Spherical Nanoparticles, Amsterdam, Elsevier, pp. 17-148.

43. Georgescu, C., Cristea, G. C., Dima, C., Deleanu, L. (2017). Evaluating lubricating capacity of vegetal oils using AbbottFirestone curve, 13th International Conference on Tribology, *ROTRIB'16 IOP Publishing IOP Conf. Series: Materials Science and Engineering* 174 012057, http://iopscience.iop.org/article/10.1088/1757-899X/174/1/012057/pdf

44. Georgescu, C., Solea L. C., Cristea G.C., Deleanu L. (2015). On the lubrication capability of rapeseed oil, paper 5533, *Recent Advances in Mechanics and Materials in Design*, *M2D'2015*, 26-30 July 2015, Ponta Delgada, Azores, Portugal.

45. Georgescu, C., (2012). *Stratul superficial în procesele de frecare şi uzură ale unor materiale compozite cu matrice de polibutilentereftalat*, teză de doctorat, Universitatea "Dunărea de Jos". Galați.

46. Georgescu, C. (2015). *Utilizarea uleiurilor vegetale pentru obţinerea lubrifianţilor ecologici, raport postdoctorat*, Universitatea "Dunărea de Jos". Galați.

47. Gold, P.W. (2002). *Basics of Tribology* (Lectures Notes), Institut für Maschinenelmente (IME) der RWTH-Aachen.

48. Gu K., Chen B., Chen Y., (2013), Preparation and tribological properties of lanthanum-doped TiO_2 nanoparticles in rapeseed oil, Journal of Rare Earths, 31 (6), 589–594

49. Hamrock, B.J., Schmid, S.R., Jacobson, B.O. (2004). *Fundamentals of fluid film lubrication*, Second Edition, New York, Marcel Dekker Inc.

50. Holmberg, K., Andersson, P., Erdemir, A. (2012). Global Impact of Friction on Energy Consumption, Economy and Environment. *Tribology International*, 47, pp. 221–234.

51. Holmberg, K. (19.8.2005). Quality of reporting empirical results in tribology, IRG-OECD: New Wear Unit / Documents.

52. Honary, L.A.T., Richter, E. (2011). Biobased Lubricants and Greases. Technology and Products, John Wiley and Sons, Ltd, Publication, Chichester, UK.

53. Hwang, Y., Lee, C, Choi, Y, et al. (2011). Effect of the size and morphology of particles dispersed in nanooil on friction performance between rotating discs. *Journal of Mechanical Science and Technology*, 25(11), pp. 2853-2857.

54. Ibrahim A. et al. (2015). Comparison between sunflower oil and soybean oil as gear lubricant, *Applied Mechanics and Materials*, 699, pp. 443-448.

55. Ilie, F., Covaliu, C. (2016). Tribological properties of the lubricant containing titanium dioxide nanoparticles as an additive, *Lubricants*, 4, pp. 12.

56. Iliuc, I. (1980). *Tribology of thin layers*, North Holland.

57. James, W. (2006). The National Ag-Based Lubricants Center & Transportation Sustainability, http://www.intrans.iastate.edu/mtc/documents/tsPresentations/2006seminar/james_mar31.pdf

58. Jayadasa N.H., Nair K. P., Ajithkumar G. (2007). Tribological evaluation of coconut oil as an environment-friendly lubricant, *Tribology International*, 40, pp. 350–354.

59. Joly-Pottuz, L., et al. (2008). Anti-wear and friction reducing mechanisms of carbon nano-onions as lubricant additives. Tribology Letters, 30(1), pp. 69-80.

60. Kosmert, T., Abramovic, H., Klofutar, C. (2000). The reological properties of Slovenian wines, *Journal of Food Engineering*, 46, pp. 165-171.

61. Kreivaitis, R., Gumbyte, M., Kazancev, K., Padgurskas, J., Makareviciene, V. (2013). A comparison of pure and natural antioxidant modified rapeseed oil storage properties, *Industrial Crops and Products*, 43, pp. 511-516.

62. Lahouij, I., Bucholz, E. W., Vacher, B., Sinnott, S. B., Martin, J. M., Dassenoy, F. (2012). Lubrication mechanisms of hollow-core inorganic fullerene-like nanoparticles: coupling experimental and computational works. *Nanotechnology*, 23, pp. 3757-01.

63. Lansdown, A. R. (2004). *Lubrication and lubricant selection. a practical guide*, Third Edition, London, Professional Engineering Publishing Limited.

64. Leach, R. (2011). *Optical measurement of surface topography*, Berlin, Heidelberg, Springer.

65. Lee, K., Hwang, Y., Cheong, S., Choi, Y., Kwon, L., Lee, J. et al. (2009). Understanding the role of nanoparticles in nano-oil lubrication, *Tribology Letters*, pp. 35-127.

66. Lee, Y.-H., Lee J.-H., (2010). Scalable growth of free-standing graphene wafers with copper(Cu) catalyst on SiO_2/$SiSiO_2$/Si substrate: Thermal conductivity of the wafers. Appl. Phys. Lett. 96 083101.

67. Lin, J, Wang, L, Chen, G. (2011). Modification of graphene platelets and their tribological properties as a lubricant additive. *Tribology Letters*, 41(1), pp. 209-215.

68. Liu, G., Li, X., Qin, B., Xing, D., Guo, Y., Fan, R. (2004). Investigation of the mending effect and mechanism of copper nano-particles on a tribologically stressed surface, *Tribology Letters*, 17, p. 961.

69. Liu, Z., Sharma, B.K., Erhan, S.Z., Biswas, A., Wang, R., Schuman, T. P. (2015). Oxidation and low temperature stability of polymerized soybean oil-based lubricants, Thermochimica Acta, 601, pp. 9–16.

70. Malburg, M. C. (2002). *Cylinder Bore Surface Texture Analysis*, Digital Metrology Solutions Inc., http://www.digitalmetrology.com/Papers/CylinderBoreNoBkgd.pdf

71. Martin, J. M., Ohmae, N., (2008), *Nanolubricants*. Tribology Series, Wiley.

72. McCormick, H., Duho, K. (2004). A brief history of the development of 2-d surface finish characterization and more recent developments in 3-d surface finish characterization, Contract DAAE07-C-L130 issued by the U.S. Army TACOM, Warren, MI., http://www.c-kengineering.com/images/pdf/product/surface%20finish/see%203di/3-D%20Surface%20Measurement.pdf

73. Miller, M. (2008). *Chapter 18, Additives for bioderived and biodegradable lubricants*. In Rudnick L. R., Erhan S. Z. (eds), Lubricant Additive Chemistry and Applications, 2nd Edition. CRC Press. Boca Raton, Florida.

74. Mobarak, H. M., Mohamad, E. N., Masjuki, H. H., Kalam, M. A., Al Mahmud, K.A.H. (2014). The prospects of biolubricants as alternatives in automotive applications, *Renewable and Sustainable Energy Reviews*, 33, pp. 34-43,.

75. Murilo, F., Luna, T., Rocha, B. S., Rola, Jr. E. M., Albuquerque, M. C. G., Azevedo, D. C. S., Cavalcante, Jr. C. L. (2011). Assessment of biodegradability and oxidation stability of mineral, vegetable and synthetic oil samples, *Industrial Crops and Products*, 33, pp. 579–583.

76. Mustafa, E.T., Gerpen, J.H.V, (1999). The Kinematic viscosity of biodiesel and its blends with diesel fuel, *J. Am. Oil Chem. Soc.*, 76, pp. 1511-1513,

77. Nagendramma, P., Kaul, S. (2012). Development of ecofriendly/biodegradable lubricants: An overview. *Renewable and Sustainable Energy Reviews*, 16, pp. 764–774.

78. Norrby, T., (2003). Environmentally adapted lubricants – where are the opportunities?. *Industrial Lubrication and Tribology*, 55(6), pp. 268-274.

79. Novoselov, K. S. et al. (2004). Electric Field Effect in Atomically Thin Carbon Films, *Science*, 306, 666.

80. Olaru, D. (2002). Fundamente de lubrificaţie, Iaşi, Editura Gh. Asachi.

81. Ossia, C. V., Han, H. G., Kong, H. (2010). Tribological evaluation of selected biodegradable oils with long chain fatty acids, *Industrial Lubrication and Tribology*, 62(1), pp. 26-31.

82. Padgurskas, J., Rukuiza R., Prosycevas I., Kreivaitis, R. (2013). Tribological properties of lubricant additives of Fe, Cu and Co nanoparticles, *Tribology International*, 60, pp. 224–232.

83. Paleu, V. (2002). *Cercetări teoretice şi experimentale privind dinamica şi fiabilitatea rulmenţilor hibrizi*, Teză de doctorat, Universitatea Tehnică "Gheorghe Asachi" Iaşi, http://vpaleu.tripod.com - accesat iulie 2014

84. Paredes X, Comunas M. J. P., A. S. Pensado, J.-P. Bazile, C. Boned, Fernández J., (2014). High pressure viscosity characterization of four vegetable and mineral hydraulic oils, *Industrial Crops and Products*, 54, pp. 281–290.

85. Pascovici, M. D., Cicone, T. (2001). *Elemente de tribologie*, Bucureşti, Editura Bren.

86. Pierson, H. O. (1993). *Handbook of carbon, graphite, diamond and fullerenes properties, Processing and applications*, Noyes Publications, New Jersey.

87. Pirvu C., Maftei L., Georgescu C., Deleanu L. (2017). Maps of 3D Parameters for Worn Surfaces of Composites PA + Glass Beads Sliding on Steel, *Industrial Lubrication and Tribology*, 69(1), pp. 42-51.

88. Quinchia, L. A., Delgado, M. Reddyhoff, A. T., Gallegos, C., Spikes, H. A., (2014). Tribological studies of potential vegetable oil-based lubricants containing environmentally friendly viscosity modifiers, *Tribology International*, 69, pp. 110–117.

89. Rîpă, M., Tomescu (Deleanu), L. (4004). Elemente de tribologie, Galaţi, Ed. Fundaţiei Universitare "Dunărea de Jos".

90. Rîpă, M., Deleanu, L. (2008). *Deteriorări în tribosisteme,* Galaţi, Ed. Zigotto.

91. Rudnick, L. R., Erhan, S. Z. (eds) (2006). Natural oils as lubricants. in Synthetics, mineral oils, and bio-based lubricants: chemistry and technology. Rudnick, L. R., Erhan, S. Z. (eds). New York: CRC/Taylor & Francis Group.

92. Rudnik L.R. (ed) (2009). *Lubricant additives. Chemistry and applications*, Second Edition, CRC Press, Taylor & Frances Group.

93. Solea L., C., (2013). Contribuţii la studiul comportării reologice şi tribologice a unor lubrifianţi biodegradabili pe bază de uleiuri vegetale, Teză de doctorat, Universitatea "Dunărea de Jos", Galaţi.

94. Spânu C., Rîpă M., Ciortan S., (2008). Study of wear evolution for a hydraulic oil using a four ball tester, The Annals of University "Dunarea de Jos" of Galati, Fascicle VIII, Tribology, pp. 186-189

95. Stachowiak, G.W., Batchelor, A.W. (2005). *Engineering tribology*, Butterworth-Heinemann, Team Lrn.

96. Ştefănescu, I., Deleanu, L., Rîpă, M., (2008). *Lubrifiere şi lubrifianţi*, Galaţi, Europlus.

97. Stout, K. J., Sullivan, P. J., Dong, W. P., Mainsah, E., Luo, N., Mathia, T., Zahouani, H. (1994). The development of methods for the characterisation of roughness in three dimensions, Publication no. EUR 15178 EN of the Commission of the European Communities: Brussels-Luxembourg.

98. Syahrullai, S., Ani, F. H., Golshkouh, I., (2013). Wear resistance characteristic of vegetable oil, *The 2nd International Conference on Sustainable Materials Engineering*, Penang, Malaysia, 26-27 March, 44-47.

99. Taheri, R.; Kosasih, B.; Zhu, H.; Tieu, A. K. (2017). Surface film adsorption and lubricity of soybean oil in-water emulsion and triblock copolymer aqueous solution: a comparative study. Lubricants, 5, 1.

100. Tang, Z., Li, S. (2014). A review of recent developments of friction modifiers for liquid lubricants (2007–present), *Current Opinion in Solid State and Materials Science*, 18, pp. 119–139.

101. Tevet, O., von-Huth, P., Popovitz-Biro, R., Rosentsveig, R., Wagner, H. D., Tenne, R., (2011). Friction mechanism of individual multilayered nanoparticles. Proc Natl Acad Sci USA, 108, p. 19901.

102. Ting C., Chen C., (2011). Viscosity and working efficiency analysis of soybean oil based bio-lubricants, *Measurement*, 44, pp. 1337–1341.

103. Tiong, C., I., Azli, Y., Kadir, M. R., A., Syahrullail, S., (2012). Tribological evaluation of refined, bleached and deodorized palm stearin using four-ball tribotester with different normal loads, *Journal of Zhejiang University-SCIENCE A (Applied Physics & Engineering)*, 13(8), pp. 633-640.

104. Wan Nik, W., Ani, F. N., Masjuki, H. H., Eng Giap, S. G. (2005). Rheology of bio-edible oils according to several rheological models and its potential as hydraulic fluid, *Industrial Crops and Products*, 22, pp. 249-255.

105. Wang, M. (2014). *Biolubricants and biolubrication*, PhD, KTH Royal Institute of Technology, Stockholm.

106. Wo, H., Hu, K., Hu, X. G. (2004). Tribological properties of MoS_2 nanoparticles as additive in a machine oil, *Tribology*, 24 pp. 33–37.

107. Wu, H., Zhao, J., Xia W., Cheng X., He A., Yun J. H., Wang L., Huang H., Jiao S., Huang L., Zhang S., Jiang, Z. (2017). A study of the tribological behaviour of TiO_2 nanoadditive water-based lubricants, *Tribology International*, http://dx.doi.org/10.1016/j.triboint.2017.01.013

108. Wu, J. F., Zhai, W. S., Jie, G. F. (2009). Preparation and tribological properties of WS_2 nanoparticles modified by trioctylamine, *Proc Inst Mech Eng J–J Eng Tribol*, 223, 695.

109. Wu, Y. Y., Tsui, W. C., Liu, T. C. (2007). Experimental analysis of tribological properties of lubricating oils with nanoparticle additives, *Wear*, 262, pp. 819-825.

110. Yilmaz, N. (2011). Temperature-dependent viscosity correlations of vegetable oils and biofuel-diesel mixtures, *Biomass and Bioenergy*, 35, pp. 2936-2938.

111. Yu, H., Xu, Y., Shi, P., Xu, B-s, Wang, X., Liu, Q. (2008). Tribological properties and lubricating mechanisms of Cu nanoparticles in lubricant, *T Nonferr Metal Society*, 18, p. 636.

112. ***SPIP The Scanning Probe Image Processor SPIP™, Version 6.7.2 (2017), disponibil on-line: http://www.imagemet.com/WebHelp/spip.htm.

113. *** SR EN ISO 4287 (2003). Specificaţii geometrice pentru produse (GPS). Starea suprafeţei: Metoda profilului. Termeni, definiţii şi parametri de stare ai profilului

114. *** SR EN ISO 4288 (2002). Specificaţii geometrice pentru produse (GPS). Starea suprafeţei. Metoda profilului. Reguli şi proceduri pentru evaluarea stării suprafeţei

115. *** SR EN ISO 25178-2 (2012). Specificaţii geometrice pentru produse (GPS). Starea suprafeţei: Areal. Partea 2: Termeni, definiţii şi parametri de stare a suprafeţei

116. *** ASME B46.1: 2009 Surface Texture (Surface Roughness, Waviness, and Lay)

117. *** NanoFocus AG μScan® – Instruction Manual.

118. *** Soybean oil-based lubricants, September 2012, http://www.soy2020.ca/pdfs/Biobased-Lubricant.pdf

119. *** EN ISO 20623 (2003). Petroleum and related products. Determination of the extreme-pressure and anti-wear properties of fluids. Four ball method (European conditions)

120. *** North America soybean oil-based lubricants market analysis, by application (metalworking fluids, engine oils, hydraulic fluids, process oils), by country, and segment forecasts, 2014 - 2025 (2017). http://www.grandviewresearch.com/industry-analysis/north-america-soybean-oil-based-lubricants-market

121. *** OECD (2014). Lubricants and lubricant additives, Paris, OECD Publishing. http://dx.doi.org/10.1787/9789264221154-en

122. *** ASME B46.1: 2009 Surface Texture (Surface Roughness, Waviness, and Lay)

123. *** ASME B46 Committee – Surface Texture – Panel Discussion

124. *** Oilseeds and protein crops market situation Committee for the Common Organisation of Agricultural Markets. (May 2017), https://ec.europa.eu/agriculture/sites/agriculture/files/cereals/presentations/cereals-oilseeds/market-situation-oilseeds_en.pdf

Papers

eng. George Cătălin Cristea

1. **Cristea G. C.,** Georgescu C., Dima D., Alexandru P., Deleanu L., Tribological Evaluation of Soybean Oil Additivated with Nano Graphene, Mechanical Testing And Diagnosis ISSN 2247 – 9635, 2016 (VI), Vol. 4, pp. 5-11.
2. **Cristea G. C.,** Dima C., Georgescu C., Dima D., Solea L., Deleanu L., Evaluating lubrication capability of soybean oil with nano carbon additive, 15th International Conference on Tribology, Kragujevac, Serbia, 17 – 19 May 2017.
3. **Cristea G.C.**' Dima D., Dima D., Georgescu C., Deleanu L., Nano graphite as additive in soybean oil, 2017, 21st Innovative Manufacturing Engineering & Energy Intern.l Conf. – IManE&E 2017.
4. Georgescu C., **Cristea C.G.,** Dima S., Deleanu L., Evaluating lubricating capacity of vegetal oils using Abbott-Firestone curve, IOP Conf. Ser. Mater. Sci. Eng. 17401205
5. Georgescu C., Solea L. C., **Cristea G.C.,** Deleanu L., On the lubrication capability of rapeseed oil, paper 5533, recent advances in mechanics and materials in design, M2D'2015, 26-30 July 2015, Ponta Delgada, Azores, Portugal
6. Botan M., Georgescu C., **Cristea G. C.,** Deleanu L., Influence of aramid fibers on tribological behavior of pbt, paper 5540, Recent Advances in Mechanics and Materials in Design, M2D'2015, 26-30 July 2015, Ponta Delgada, Azores, Portugal.
7. Georgescu C., Solea L. C., **Cristea C. G.,** Deleanu L., On lubricating characteristics of rapeseed oils, Fist International Conference on Tribology, Turkeytrib'15, 2015, Istanbul, Turkey, 7-9 October, 2015.
8. **Cristea G. C.,** Cazamir D., Dima C., Deleanu L., Georgescu C., Dima D., Influența concentrației de TiO_2 ca nanoaditiv în uleiul de rapiță asupra comportării tribologice pe tribotesterul cu patru bile, Ugal Invent, 19-20 octombrie, 2017, Universitatea Dunărea de Jos, Galați.
9. **Cristea G. C.,** Deleanu L., Georgescu C., Dima D., Alexandru Petrică A. Comportarea tribologică a uleiului de soia aditivat cu nanografit, UgalInvent 2017, 19-20 octombrie, 2017, Universitatea Dunărea de Jos, Galați, **bronze medal.**